THE UNIVERSITY OF QUEENSLAND

AUSTRALIA

Development of vehicle emissions models for Australian conditions

Sicong Zhu

B.Eng., M.Sc.

A thesis submitted for the degree of Doctor of Philosophy at
The University of Queensland in 2014
School of Civil Engineering

Abstract

Microscopic simulation models such as AIMSUN, VISSIM and/or PARAMICS have the ability to output emissions based on default values for emission factors derived mainly from European test data. Emission algorithms in those models are based on overseas vehicle emissions datasets, which do not reflect the different Australian vehicles, fuels, climate and fleet composition. The proposed research provides a set of emission algorithms to be used in conjunction with traffic simulation modelling, to better represent local conditions.

Macro level models based on average vehicle speeds may not be appropriate for use at a more localized and detailed level when vehicle speed profiles may change significantly. Emission rates for a number of vehicles were compared using Australian data based on dynamometer testing. The results show that only CO_2 shows a strong correlation with average speed. All other pollutants show very low levels of correlation. On the other hand, an evaluation of several micro level emissions models has been undertaken by applying them to the results of Australian vehicle emissions measured in the field. A number of models have been analysed and the results compared. Power based models have some significant shortcomings and their use is not consistent with our finding that there are significant variations in emissions for small changes in vehicle power. The results highlight the need to model acceleration, deceleration and cruising stages of the urban cycle separately. A speed based approach, such as that followed in by the AIMSUN traffic simulation model, was found to have merit based on the evaluation results discussed here. The current research investigates the gap between estimated emissions and actual measurements using an Australian emissions dataset and the widely used micro-simulation model AIMSUN. The results indicate that the model adequately predicts CO_2 emissions. However, the likely errors associated with the prediction of other pollutants are significantly greater. As a result, the thesis puts forward improved emissions estimation relationships for use with micro-simulation models. Using Australian emissions data, it was possible to improve the estimation ability of existing micro-simulation models.

The thesis discusses the limitations of existing emissions estimation approaches at the micro level. A methodology to establish emission models for predicting emission pollutants other than CO_2 is proposed. The models adopt a genetic algorithm approach to select the predicting variables. The approach is capable of solving combinatorial optimisation problems. Overall,

the emission prediction results reveal that the proposed new models outperform conventional equations.

There is a need to match emission modelling estimation to the accuracy levels of confidence in the outputs of transport models. In order to quantify the likely level of uncertainty attached to forecasts of emissions, an analysis of errors needs to be undertaken. The two major sources of error are the deficiency inherent in the model structure itself and the uncertainty in the input data used. This thesis deals with both of these error types in relation to CO_2 emissions modelling using a case-study from Brisbane, Australia. To estimate input data uncertainty, an analysis of different traffic conditions using Monte Carlo simulation is shown here. Model structure induced uncertainties are also quantified by statistical analysis for a number of traffic scenarios. To arrive at an optimal overall CO_2 prediction, the interaction between the two components was taken into account. Since a more complex model does not necessarily yield higher overall accuracy, a balanced solution needs to be found. The results obtained suggest that the CO_2 model used in the analysis produces low overall uncertainty under free flow traffic conditions. However, when average traffic speeds approach congested conditions, there are significant errors associated with emissions estimates.

Using different scenarios for different road configurations and traffic conditions, the results of applying the new approach are compared with those obtained by using default emissions parameters commonly found in a simulation package.

The enhancement of emission predictions rests to a large extent on the further improvements to traffic micro-simulation models. The results obtained suggest that the new approach produces low overall errors under several traffic conditions. The accuracy of emissions predictions is, to a large extent, dependent on the errors associated with transport model outputs and on the accuracy of the emissions models themselves.

Declaration by author

This thesis is composed of my original work and contains no material previously published or written by another person, except where due reference has been made in the text. I have clearly stated the contribution by others to jointly-authored works that I have included in my thesis.

I have clearly stated the contribution of others to my thesis as a whole, including statistical assistance, survey design, data analysis, significant technical procedures, professional editorial advice, and any other original research work used or reported in my thesis. The content of my thesis is the result of work I have carried out since the commencement of my research higher degree candidature and does not include a substantial part of work that has been submitted to qualify for the award of any other degree or diploma in any university or other tertiary institution. I have clearly stated which parts of my thesis, if any, have been submitted to qualify for another award.

I acknowledge that an electronic copy of my thesis must be lodged with the University Library and, subject to the General Award Rules of The University of Queensland, immediately made available for research and study in accordance with the Copyright Act 1968.

I acknowledge that copyright of all material contained in my thesis resides with the copyright holder(s) of that material. Where appropriate I have obtained copyright permission from the copyright holder to reproduce material in this thesis.

Sicong Zhu

May 2014

Publications during candidature

Refereed Journal Papers

S. Zhu, L.S. Tey and L. Ferreira. 2014. *modelling vehicle emissions using a genetic algorithm approach*. Transportation Research Part C (Forthcoming)

S. Zhu, I. Kim, and L. Ferreira. 2014. *Analysis of vehicle acceleration profiles for emissions modelling at signalised intersections.* Transportation Research Part C (Forthcoming)

S. Zhu and L. Ferreira. 2013. *Framework to quantify errors in micro-scale emissions models.* Transportation Research Part D, Volume 21, Page 19–25.

S. Zhu and L. Ferreira. 2012. *Evaluation of vehicle emissions models for micro-simulation modelling: using CO_2 as a case study.* Journal of Transport and Road Research, Volume 21, Issue 3, Page 3-18.

P.Bover, S. Zhu and L. Ferreira. 2012. *Modelling vehicle emissions for Australian conditions.* Journal of Transport and Road Research. Volume 22 Issue 4, Page 7-21.

L.Tey, S. Zhu, L. Ferreira and G. Wallis. 2014. *Micro-simulation modelling of driver behaviour towards alternative warning devices at railway level crossings***.** Accident Analysis & Prevention, Volume 71, Page177-182.

L,Tey., G,Wallis., S,Cloete., L, Ferreira., S, Zhu. 2013. *evaluating driver behaviour towards innovative warning devices at railway level crossings using a driving simulator*. Journal of Transportation Safety & Security, Volume 5, Page 118-130.

Z, Ma., L. Ferreira., M. Mesbah and S, Zhu. 2014. *Modelling distributions of travel time variability for bus operations. Jounral of Advanced Transportation.* (Accepted)

Refereed Conference Papers

S. Zhu and L. Ferreira. 2013. *Quantifying traffic related emissions using micro-simulation model outputs*. 36th Australasian Transport Research Forum, Brisbane.

S. Zhu and L. Ferreira. 2012. *Assessing the uncertainty in micro-simulation model outputs*. 35th Australasian Transport Research Forum, Perth.

Publications included in this thesis

No publications included

Contributions by others to the thesis

No contributions by others.

Statement of parts of the thesis submitted to qualify for the award of another degree

None.

Acknowledgements

This research would not have been possible without the advice, encouragement and support of many people. I would like to take this opportunity to extend my sincere gratitude and appreciation to all those who made this PhD thesis possible.

I would like to extend my sincere gratitude to Professor Luis Ferreira, my Principal Advisor, for his endless patience, expert advice, optimistic attitude and critical support during my difficult times. My special words of thanks should also go to Professor Phil Charles, my Associate Advisor. I would also like to acknowledge Professor Mark Hickman for his kind support and Dr Mahmoud Mesbah who has always supported my tutorial work.

I thank my fellow postgraduate students of the transport group at the University of Queensland. My best wishes to them for future career and family life.

Keywords
Traffic simulation, vehicle emission modeling, Genetic Algorithm, uncertainty quantification, Urban drive cycle and Monte Carlo simulation.

Australian and New Zealand Standard Research Classifications (ANZSRC)
090507, Transport Engineering, 100%

Fields of Research (FoR) Classification
0905, Civil Engineering, 100%

TABLE OF CONTENTS

List of Figures

List of Tables

Chapter 1. Introduction

1.1 Background

The concern with air quality standards has prompted road and transport authorities to pay more attention to the development of enhanced traffic management and infrastructure strategies mainly to mitigate the adverse health and other environmental impacts of road traffic. Quantitative travel demand and emissions models are necessary for the evaluation of future transport/land use options, as well as for the management of existing transport systems. The modelling of emissions is seen as an increasingly important tool in transportation planning and management. The application of Intelligent Transport System (ITS) has also been a potential solution to reduce emissions and improve air quality. The combination of traffic simulation and vehicle emissions modelling is increasingly seen as providing the tools to evaluate ITS applications.

Emissions models can be broadly divided into two categories, namely: micro and macro level models. Micro models predict emissions at the individual vehicle level and may involve a complete driving cycle for each vehicle. They require a large amount of data and are often based on instantaneous measurements. Traffic-based micro models predict emissions from vehicles operating in a street network from information such as vehicle speeds, number of stops, idling times, and acceleration and deceleration times. Emission factors are provided for the various vehicle/engine technologies given these network characteristics. Macro models give the average emissions for a group of vehicles. These models use statistics such as vehicle-kilometre travelled (VKT) and average vehicle speed to calculate the overall level of emissions usually at a study area level. The advantages of average speed models include the fact that they can be used with a smaller experimental database than modal modelling or engine mapping approaches. Strategic travel demand models tend to be large and regional in nature whereas micro simulation models are mainly used for detailed tactical or operational testing of options. The accuracy demanded by emissions models is not usually matched in either strategic or detailed simulation models (Ferreira, 2007).

Currently, microscopic simulation models such as AIMSUN, VISSIM and PARAMICS have the ability to output emissions data based on default values for emission factors derived mainly from European test data. Emission algorithms in those models are based on overseas vehicle emissions datasets, which do not reflect the different Australian vehicles, fuels, climate and fleet composition. For example, Australia has:

- A larger proportion of vehicles with six and eight cylinder engines;
- A significantly lower percentage of diesel cars;
- Different composition of fuels;
- Different emission standards;

- Vehicles with different calibration of engine management systems;
- Vehicles with different configuration of emission reduction technologies (e.g. size, location of catalysts, catalyst material)
- Other emission behaviour aspects.

1.2 Research question

The current thesis is concerned with answering the question:

Can emissions models be developed, based on Australian data and conditions, which are suited for use in conjunction with the outputs of existing traffic models?

Predictions of the pollution impacts of mode and route choice decisions need to be considered in conjunction with conventional travel demand modelling outputs. In order to evaluate the environmental impacts generated by the implementation of particular transportation management schemes over a period of time and to make sound policy-related decisions based on such evaluations, environmental emissions models need to be developed as accurate and reliable assessment tools.

In light of the strong relationship between carbon dioxide (CO_2) emissions and fuel consumption (Akcelik and Besley, 2003), fuel consumption and emission estimation can be critical for comprehensive transportation planning. These require more accurate tools to quantify environmental impacts so that project evaluation can adequately address community expectations. There is a need to match emission estimation to accurate levels of confidence in the outputs of transport models.

Given these considerations, the current research develops models to predict vehicle emissions under various traffic conditions using an Australian vehicle fleet emissions inventory database.

1.3 Research significance

There are three main reasons why this research is significant, namely:

(i) There is room for improvement in the field of vehicular traffic environmental impact predictions. Current models fail to take into consideration the differences across vehicles that populate an entire fleet. Current state of-the-art models estimate fuel consumption and emission outputs based on typical driving cycles with most models being based on average speeds that do not consider other changes that occur during the driving cycle, such as vehicle acceleration and deceleration.

(ii) Australia does not currently have standard models for estimating vehicle emissions unlike other countries such as the United States (US). The models developed by other countries are based on their own traffic conditions and vehicle fleet characteristics and are therefore inappropriate for use in Australia.

(iii) There is an absence of a methodology to quantify emission modelling reliability in terms of the uncertainty attached to prediction outcomes. The reliability of any proposed new emissions models should be evaluated using an analysis of the expected errors that are attached to the inputs used.

1.4 Main Thesis contributions

The main areas in which this thesis makes a significant contribution to new knowledge are:

(1) Enhancing the predicted reliability of emissions models using the outputs of traffic simulation models. The modelling of all pollutants has been improved by the application of new models;

(2) A methodology for the quantification of emission predictions is proposed. This is achieved by the use of traffic micro-simulation coupled with new emissions models. The likely uncertainty in the estimation of emissions is related to the error analysis of micro-simulation outputs for several traffic flow scenarios.

1.5 Research objectives

The aim of this study is to develop a new emissions modelling approach at micro level, to deliver reliable estimates of all the main pollutants.

In order to achieve the aim, the following objectives have been defined:

i. To review emissions models at the micro and macro levels and identify advantages and shortcomings of different modelling approaches;
ii. To review traffic models at the micro and macro levels to achieve compatibility with the most appropriate emissions models, in terms of prediction accuracy and modelling scale;
iii. To evaluate driving cycles under varied traffic conditions and validate the emission datasets from the Australian national in-service emissions study (NISE2);
iv. To establish new emissions models by implementing a Genetic Algorithm (GA) approach to optimise the process of selecting explanatory variables;
v. To determine an appropriate level of pollutant modelling complexity by comparing the errors due to the new model specification with those due to input data uncertainty; and
vi. To apply the new emissions models to a Brisbane traffic network, using as input data the outputs from a traffic simulation model.

1.6 Structure of this thesis

The outline of the thesis is shown in Figure 1.1. Chapter 2 outlines all related factors associated with traffic induced emission, including emission introduction, testing method,

driving cycle development. Chapter 3 reviews the existing research regarding emission modelling at macro and micro levels. After the reviews, the research methodology is proposed in Chapter 4. It not only improves emission modelling accuracy but also considers the input uncertainty, in order to deliver an optimised overall prediction. Chapters 5 and 6 describe the two components respectively, namely GA-based modelling development and overall uncertainty quantification using the Monte Carlo method. The proposed new emission model is integrated with micro traffic-simulation in Chapter 7. Finally, Chapter 8 draws the conclusions from the results obtained here and discusses related potential future research topic.

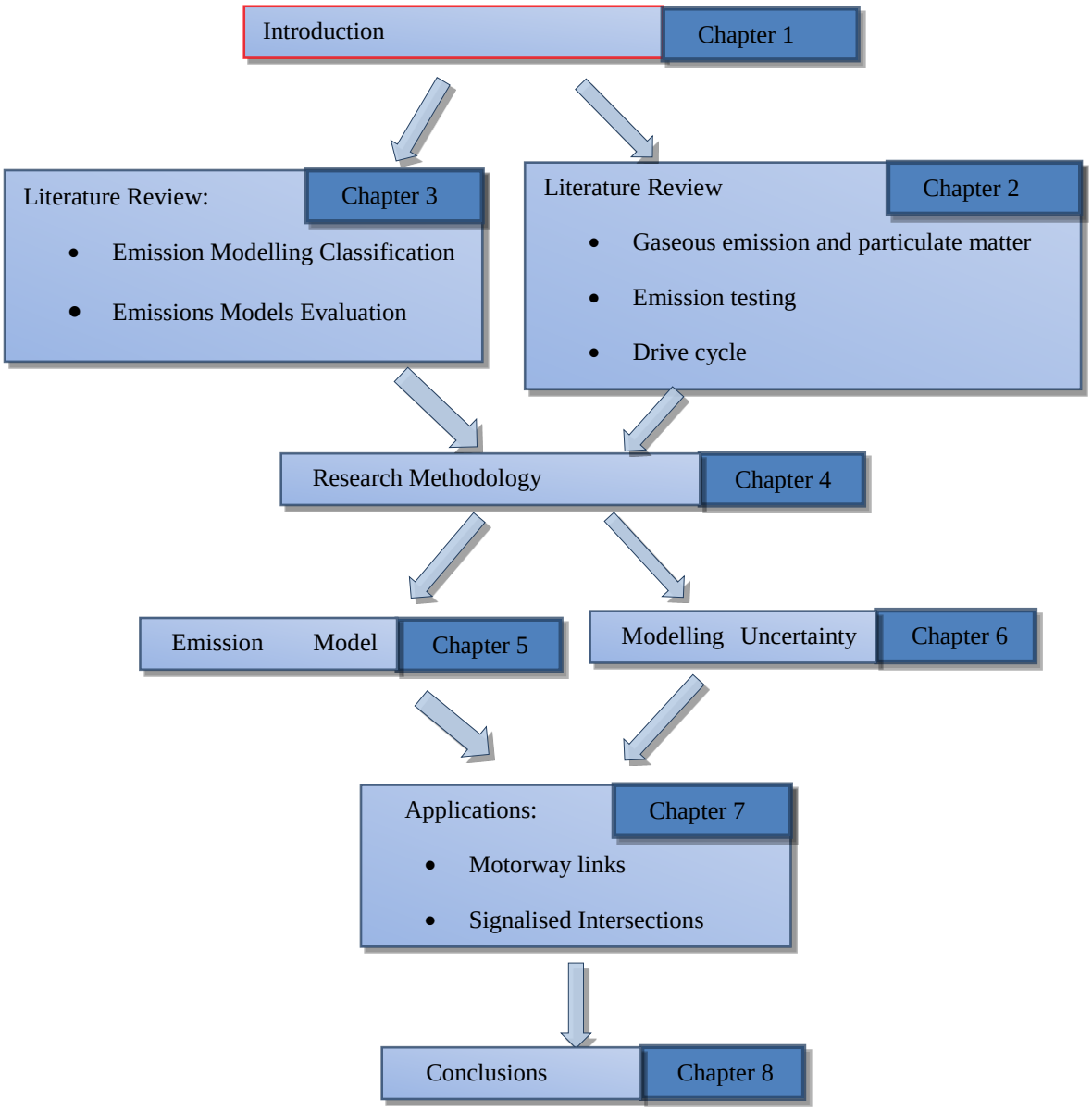

Figure 1.1 Thesis flow chart

Chapter 2. Literature Review

2.1 Introduction

Vehicle induced emissions are a major source of air pollution in metropolitan areas. A large portion of air pollution has adverse human health impacts. It is recognised that road transport is one of the major pollution sources for urban dwellers (Ahrens, 2003). This chapter deals with the following topics: the origin of vehicle emission pollutants and their classification are introduced in the next section; this is followed by a brief description of emission testing methods. Finally, a number of drive cycles currently in use in different countries are reviewed.

2.2 Vehicles emission pollutants

2.2.1 Background

Road transport emits air pollution from the combustion of liquid or gaseous fossil fuels. Although thousands of air pollutants from road traffic can be identified, most of them can be classified in the following major groups according to their origins and formation processes:

- Products of incomplete combustion, including carbon monoxide (CO), particulate matter (PM) and hydrocarbons (HCs);
- Products of high-temperature combustion processes, including nitrogen oxides (NO_x);
- By-products of combustion due to impurities in the fuel, including heavy metals and sulphur oxides (SO_x);
- Non-combustible products, including evaporative hydrocarbons when HC in the fuel escapes into air; diurnal emission from standing vehicle fuel evaporation.

"Road vehicles are the dominant emission source, if not the most important, anthropogenic source of air pollution in urban areas" (Fenger, 1999). Moreover, traffic-induced pollutants are emitted in close proximity to human receptors, which increases exposure levels. By means of an example, Figure 2.1 shows the estimated relative contribution of road traffic to anthropogenic emissions of key primary air pollutants in the South-East Queensland Region, for 2000.

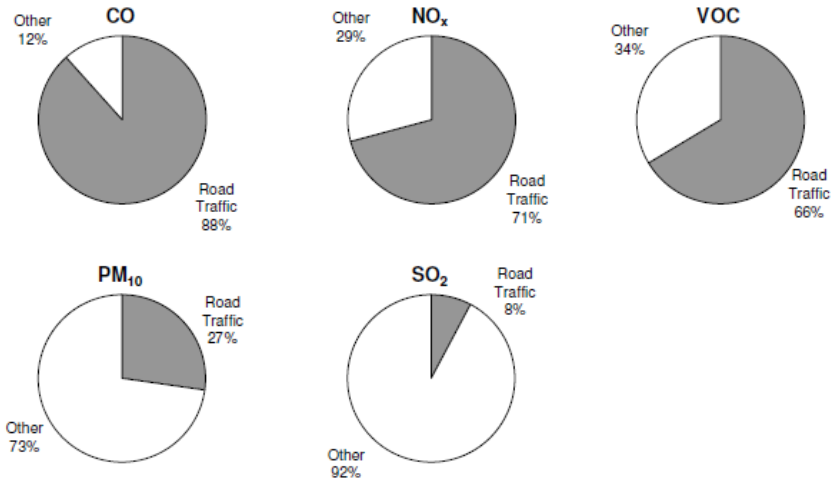

Figure 2.1 Road traffic and air pollution in SEQ (BCC/QGEPA, 2004)

PM can be classified into three categories by particle diameter, namely, PM 1 (diameter <1 μm) is ultra-fine; PM 2.5 (diameter <2.50 μm) is fine; and PM 10 (diameter <10 μm) consists of coarse particles. The majority of ultra-fine PM is emitted by vehicles. Most anthropogenic pollution sources are combustion-related and generate particles with diameters<1 μm (Jamriska and Morawska, 2001). For different engines, the emission properties are slightly different with each other. Particles emitted from diesel engines are in the size range 20-130 nm and from petrol engines in the range 20-60 nm (Morawska et al., 2008a). Therefore, a large proportion of the PM in urban air is found in the ultra-fine size range (Morawska et al., 1998). Overall, "it has been shown that in urban environments the smallest particles make the highest contribution to the total particle number concentrations, while only a small contribution to particle volume or mass" (Morawska et al., 2008a). In contrast, "almost all particles in the coarse particle mode originate from natural and anthropogenic mechanical processes, including grinding, breaking and wear of material and dust re-suspension" (Morawska et al., 2008b).

Several researchers have reported significant health risks associated with exposure to PM, which is common in urban areas (Pope et al., 2002; Pope and Dockery, 2006). Among the PM categories, those small enough to lodge deep in the lungs where they can do serious damage are of the most concern (American Lung Association, 2004).

2.2.2 Factors affecting transportation pollutants

Travel–related Factors

Travel-related factors include vehicle-operating modes, speeds and acceleration (deceleration). Figure 2.2 illustrates four different types of vehicle emission measurements under different accelerations. Panis et al. (2006b) suggest that the emission data plot reveals a clear distinction in the scatter for acceleration and deceleration. Different researchers are divided on the mechanism of emission modelling. Some of them consider that emissions models should be physical, depending on the tractive power of a vehicle. Others think emission is correlated with speed and acceleration. Both points of view will be discussed in detail in Chapter 3.

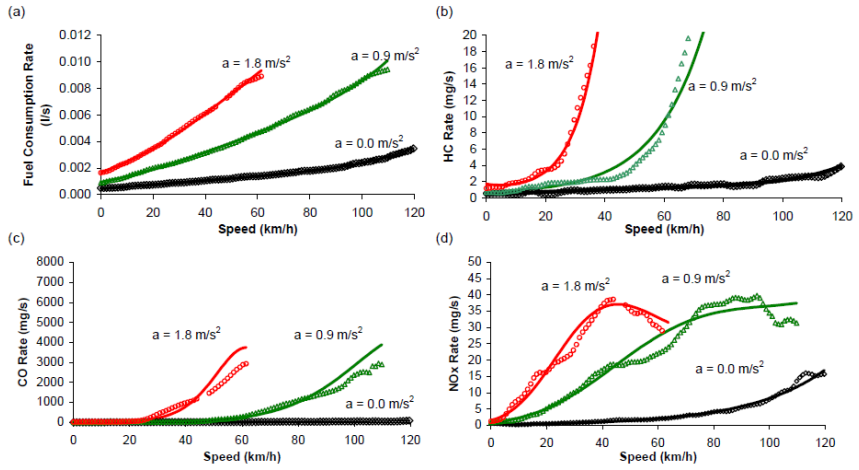

Figure 2.2 Fuel consumption, emissions and acceleration (Rakha et al., 2003)

(a) Fuel consumption, (b) HC, (c) CO, (d) NO_x.

Driver–related factors

Driver behaviour varies greatly with different drivers and traffic conditions. For example, aggressive drivers may exert sharp accelerations more frequently than their less aggressive counterparts in congested conditions. Sharp accelerations impose heavy loads on the engine and thus result in higher emission levels.

Vehicle –related factors

Air pollutant emissions and fuel consumption vary substantially with vehicle design characters, which include; vehicle size and weight, engine type, transmission type, presence and type of emission control technology, auxiliary systems, and aerodynamic characteristics.

The European Climate Change Working Group estimated that the use of air conditioning systems under 'average' European conditions would cause an increase in fuel consumption of between 4% and 8% by 2020 (Rakha et al., 2011) . Ageing is a critical cause of progressive deterioration of emission standards for individual vehicles. During vehicle use, the converter is exposed to heat, which causes the metal particles to agglomerate and grow, and their overall surface area to decrease. As a result, catalytic activity deteriorates. The problem has been exacerbated in recent years by the trend to install catalytic converters closer to the engine, which ensures immediate activation of the catalyst on engine start-up, but also places demanding requirements on the catalyst's heat resistance (Nishihata et al., 2002). Australian vehicle test data show a significant gap between catalytic converted and non-catalytic converted emissions (Orbital, 2009). Vehicle emissions also vary with ambient temperature. At colder temperatures, engine and emission control systems need more time to heat up, increasing cold start emissions.

2.2.3 Vehicle emission standards in Australia

Australia has a commitment to match emissions standards with those developed by the UN Economic Commission for Europe wherever possible. The emission standards now in place reflect that commitment. The codes of emissions have been compliant with the Australia Design Rules since 1970s. Table 2.1 provides details of past and current standards and shows the relationship between Australian standards.

Table 2.1Australian emission standards

Standard	Date Introduced #	Exhaust Emission Limits (petrol vehicles)			Source Standard / Test Method
		HC	CO	NO_x	
ADR26	1/1/72	NA	4.5% by vol	NA	Idle CO test
ADR27	1/1/74	8.0 - 12.8 g/test	100 - 220 g/test & 4.5% by vol	NA	ECE 'Big Bag'
ADR27A	1/7/76	2.1 g/km	24.2 g/km	1.9 g/km	US '72 FTP
ADR27B	1/1/82	2.1 g/km	24.2 g/km	1.9 g/km	US '72 FTP
ADR27C +	1/1/83	2.1 g/km	24.2 g/km	1.9 g/km	US '72 FTP
ADR37/00	1/2/86	0.93 g/km	9.3 g/km	1.93 g/km	US '75 FTP
ADR37/01	1/1/97 - 1/1/99	0.26 g/km	2.1 g/km	0.63 g/km	US '75 FTP
ADR79/00	1/1/03 - 1/1/04	0.25*g/km	2.2 g/km	0.25* g/km	UN ECE R83/04 (Euro 2)
ADR79/01	1/1/05 - 1/1/06	0.2 g/km	2.3 g/km	0.15 g/km	UN ECE R83/05 (Euro 3)
ADR79/02	1/7/08 - 1/7/10	0.1 g/km	1.0 g/km	0.08 g/km	UN ECE R83/05 (Euro 4)

Where:

Two dates specified: first date applies to vehicle models produced on or after that date, with all new vehicles required to comply by the second date.

+ ADR27C introduced a number of administrative changes, based on procedures of ADR37/00.

* ADR 79/00 has a combined $HC+NO_x$ limit of 0.5, so the $HC:NO_x$ split is indicative only "NA" means no limit applies.

United States emission standards (CFR Title 40)

In the US, emission standards are managed by the Environmental Protection Agency (EPA) at national level, except in California where the California Air Resource Board (CARB) has its own standard system. Table 2.2 shows current EPA emission standards for passenger cars and light commercial vehicles (<3.5 tons).

Table 2.2 Light-Duty Vehicle and Light-Duty Truck -- Clean Fuel Fleet Exhaust Emission Standards (EPA, 2005)

Vehicle Type	Emissions Category	Useful Life Standard	Test Weight (lbs)	NMOG (g/mi)	NO_x (g/mi)	CO (g/mi)	Formaldehyde (g/mi)	PM (g/mi)[b]
LDVs	TLEV	Intermediate	All	0.125	0.4	3.4	0.015	-
	LEV			0.075[c]	0.2	3.4[c]	0.015[c]	-
	ULEV			0.04	0.2[c]	1.7	0.008	-
	TLEV	Full		0.156	0.6	4.2	0.018	0.08
	LEV			0.090[c]	0.3	4.2[c]	0.018	0.08[c]
	ULEV			0.055	0.3[c]	2.1	0.011	0.04
LLDTs	TLEV	Intermediate	0-3750 LVW	0.0125	0.4	3.4	0.015	-
	LEV			0.075[c]	0.2	3.4[c]	0.015[c]	-
	ULEV			0.04	0.2[c]	1.7	0.008	-
	TLEV		3751-5750 LVW	0.16	0.7	4.4	0.018[c]	-
	LEV			0.100[c]	0.4	4.4[c]	0.018[c]	-
	ULEV			0.05	0.4[c]	2.2	0.009	-
	TLEV	Full	0-3750 LVW	0.156	0.6	4.2	0.018	0.08
	LEV			0.090[c]	0.3	4.2[c]	0.018[c]	0.08[c]
	ULEV			0.055	0.3[c]	2.1	0.011	0.04
	TLEV		3751-5750 LVW	0.2	0.9	5.5	0.023	0.08
	LEV			0.130[c]	0.5	5.5[c]	0.023[c]	0.08[c]
	ULEV			0.07	0.5[c]	2.8	0.013	0.04

Table 2.3 Light-Duty Vehicle and Light-Duty Truck -- Clean Fuel Fleet Exhaust Emission Standards (Continued)

HLDTs	LEV	Intermediate	0-3750 LVW	0.125[c]	0.4[d]	3.4[c]	0.015[c]	-
	ULEV		ALVW	0.075	0.2[c, d]	1.7	0.008	-
	LEV		3751-5750	0.160[c]	0.7[d]	4.4[c]	0.018[c]	-
	ULEV		ALVW	0.1	0.4[c, d]	2.2	0.009	-
	LEV		5751+	0.195[c]	1.1[d]	5.0[c]	0.022[c]	-
	ULEV		ALVW	0.117	0.6[c, d]	2.5	0.011	-
	LEV	Full	0-3750 LVW	0.180[c]	0.6	5.0[c]	0.022[c]	0.08[c]
	ULEV		ALVW	0.107	0.3[c]	2.5	0.012	0.04
	LEV		3751-5750	0.230[c]	1	6.4[c]	0.027[c]	0.10[c]
	ULEV		ALVW	0.143	0.5[c]	3.2	0.013	0.05
	LEV		5751+	0.280[c]	1.5	7.3[c]	0.032[c]	0.12[c]
	ULEV		ALVW	0.167	0.8[c]	3.7	0.016	0.06

Notes:

a These standards have in effect been superseded by newer, more stringent standards in 40 Code of Federal Regulations (CFR) Part 86. See Manufacturer Guidance Letter CCD-05-12, July 21, 2005.

b Applies to diesel vehicles only.

c Applies to Inherently Low Emission Vehicles.

d Does not apply to diesel vehicles.

European Union emission standards

EU emission regulations for new light duty vehicles (passenger car and light commercial vehicles <3.5 tons) are specified in the Directive 70/220/EEC. The standards have evolved from Euro 1 to Euro 6 in the last two decades, demonstrated in Table 2.3.

- Euro 1 standards (also known as EC 93): Directives 91/441/EEC (passenger cars only) or 93/59/EEC (passenger cars and light trucks)
- Euro 2 standards (EC 96): Directives 94/12/EC or 96/69/EC

- Euro 3/4 standards (2000/2005): Directive 98/69/EC, further amendments in 2002/80/EC
- Euro 5/6 standards (2009/2014): Regulation 715/2007 ("political" legislation) and Regulation 692/2008

Table2.4 European emission standards for passenger cars (Category M), g/km*

Tier	Date	CO	THC	NMHC	NO_x	$HC+NO_x$	PM
Diesel							
Euro 1†	July 1992	2.72 (3.16)	-	-	-	0.97 (1.13)	0.14 (0.18)
Euro 2	January 1996	1.0	-	-	-	0.7	0.08
Euro 3	January 2000	0.64	-	-	0.50	0.56	0.05
Euro 4	January 2005	0.50	-	-	0.25	0.30	0.025
Euro 5	September 2009	0.500	-	-	0.180	0.230	0.005
Euro 6 (future)	September 2014	0.500	-	-	0.080	0.170	0.005
Petrol (Gasoline)							
Euro 1†	July 1992	2.72 (3.16)	-	-	-	0.97 (1.13)	-
Euro 2	January 1996	2.2	-	-	-	0.5	-
Euro 3	January 2000	2.3	0.20	-	0.15	-	-
Euro 4	January 2005	1.0	0.10	-	0.08	-	-
Euro 5	September 2009	1.000	0.100	0.068	0.060	-	0.005**
Euro 6 (future)	September 2014	1.000	0.100	0.068	0.060	-	0.005**

* Before Euro 5, passenger vehicles > 2500 kg were type approved as light commercial vehicles N_1-I
** Applies only to vehicles with direct injection engines
*** A number standard is to be defined as soon as possible and at the latest upon entry into force of Euro 6

2.3 **Vehicle emissions data testing**

The most common method of emissions testing uses dynamometers. During the test, the vehicle runs on a roller according to a specific driving cycle, while a set of instruments record real-time emissions from the tailpipe. Pre-catalyst results are recorded as "modal" data, this being a second-by-second recording of instantaneous emissions. Likewise modal data is recorded for tailpipe (post-catalyst) emissions. The emissions are typically sampled raw using

exhaust gas analysers with high range detectors. No compensation is made for ambient levels for these raw readings. In addition, "bagged" results are obtained for the tailpipe sample. "Bag" sampling of emissions is typically used for certification tests and relies upon "bagging" a dilute proportion of the tailpipe emission sample for subsequent measurement. The sample bag usually measures the emissions for a complete phase of the test. The bagging process requires specialised sampling equipment and this makes the process expensive compared to the modal integration method. Figure 2.3 illustrates the process.

Another testing method, an on-board diagnostic, can be conducted under actual road conditions. For example, the OEM-2100 system, a Portable Emissions Measurement System, can be set up in approximately 15 minutes on most motor vehicles. It interfaces with the vehicle in two ways: (1) it obtains engine data from an on-board diagnostic link found on most vehicles manufactured since the early 1990s; and (2) it obtains a small sample of engine exhaust using a sampling probe. The device simultaneously records engine data and measures the concentration of several gases in the vehicle's exhaust, including carbon monoxide, hydrocarbons, nitric oxide, carbon dioxide, and oxygen. Figures 2.4 and 2.5 demonstrate how an on-board system connects with a vehicle. The instrument reports engine and emissions data every second and the data are retrieved for later analysis (Unal et al., 2003)

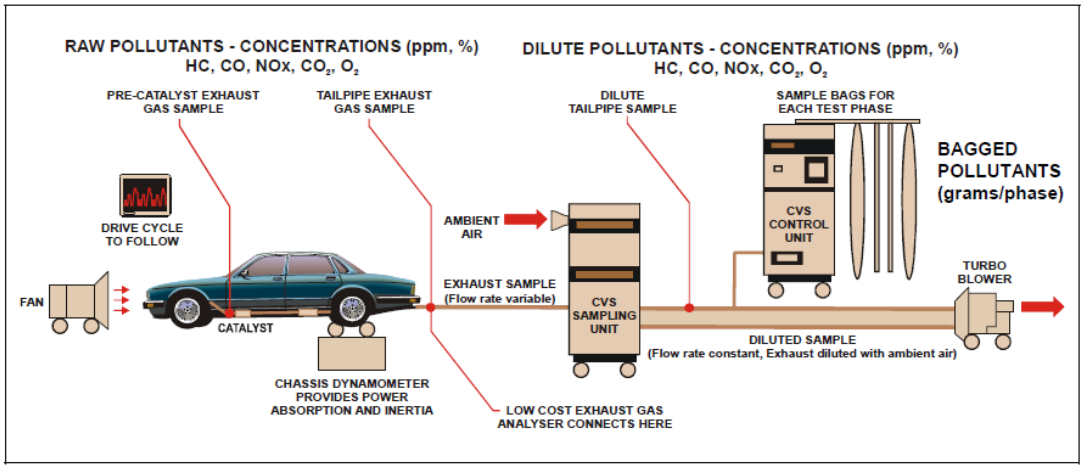

Figure 2.3 Overview of Vehicle Emissions Measurement Facility (Orbital, 2009)

Figure2.4 Portable Emissions Measurement System setup (on-board diagnostic)

Figure2.5 Portable Emissions Measurement System setup

2.4 Vehicle driving cycles

To simulate real vehicle driving conditions, different agencies have developed various speed-time profiles to represent real driving behaviour under dynamometer testing conditions.

European ECE driving cycle

The emission test procedure for European passenger cars was defined by ECE regulation 15. The ECE+EUDC test cycle is performed on a chassis dynamometer. The whole cycle is used for emission certification of light duty vehicles in Europe, consisting of four ECE 15 segments and one Extra Urban Driving Cycle. The ECE 15 cycle is an urban driving cycle (UDC). It was devised to represent city driving conditions. It is characterised by low vehicle speed, low engine load, and low exhaust gas temperature, shown in Figure 2.6(a). The Extra Urban Driving Cycle (EUDC) segment has been added after the fourth ECE15 cycle to account for more aggressive, high speed driving modes, as shown in Figure 2.6(b). The maximum speed of the EUDC cycle is 120 km/h. An alternative EUDC cycle for low-powered vehicles has been also defined with a maximum speed limited to 90 km/h. The entire cycle is illustrated in Figure 2.7.

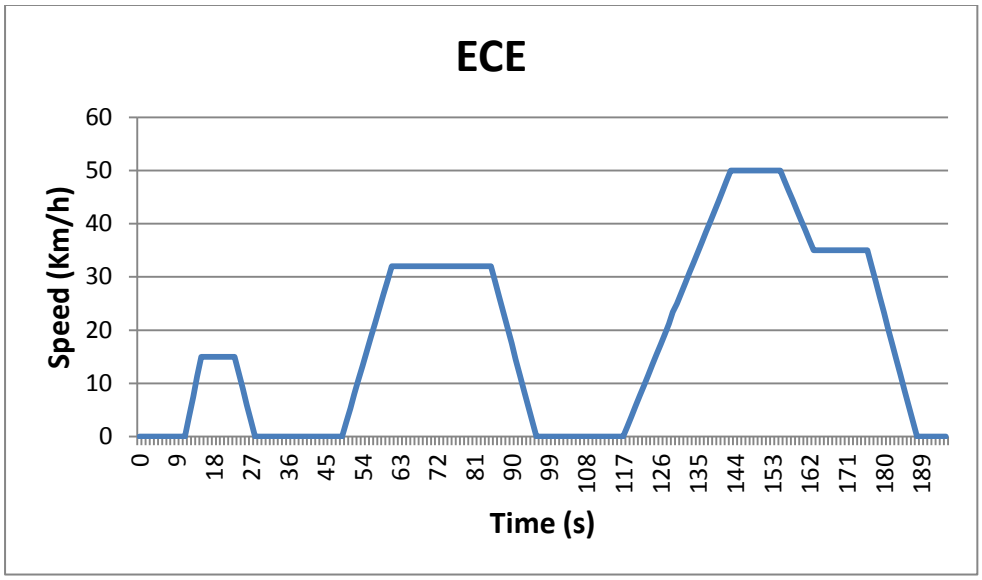

Figure 2.6 (a) ECE 15 Cycle (Samuel et al., 2002)

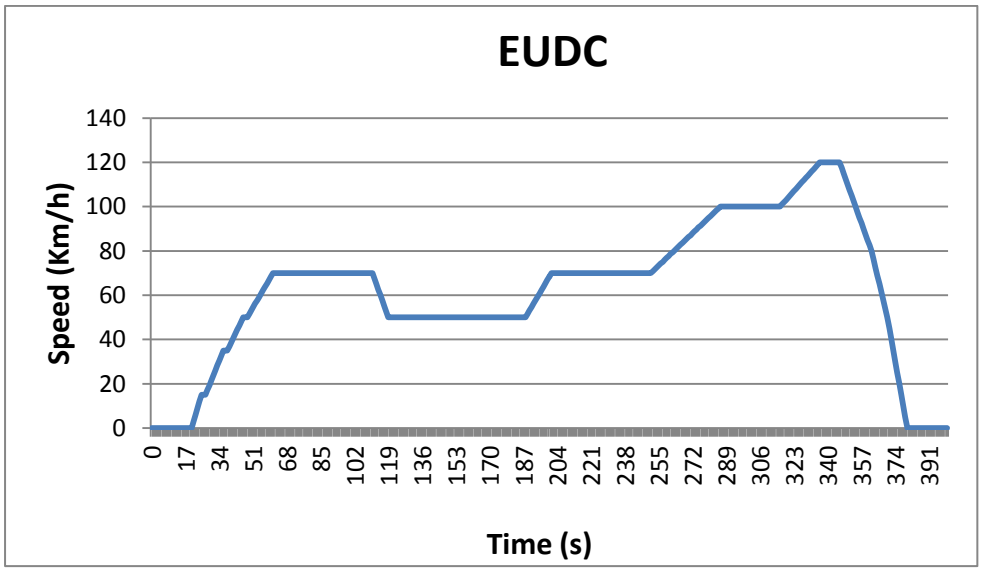

Figure 2.6 (b) The EUDC Cycle (Samuel et al., 2002)

Figure 2.6 The European drive cycle: ECE and EUDC

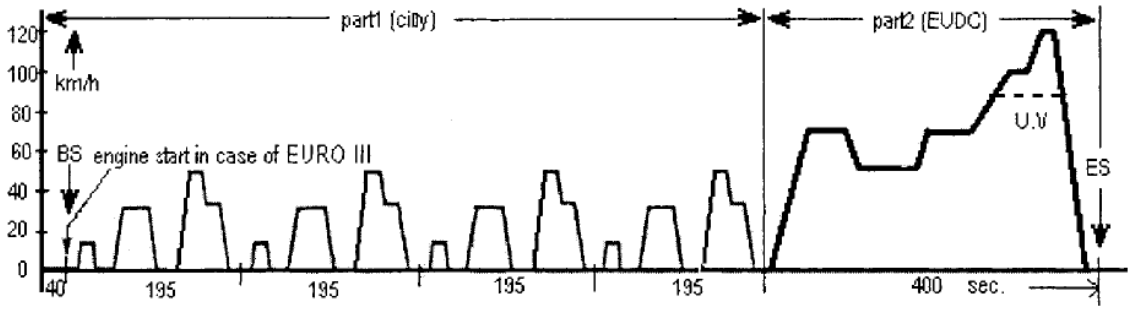

Note: BS, beginning of cycle; ES, end of cycle

Figure 2.7 The entire ECE test drive cycle (Samuel et al., 2002)

European ARTEMIS cycle(André, 2004)

Firstly, observations of vehicle uses and operating conditions are obtained by the instrumentation and monitoring of a representative and relatively large sample of private cars. A simple approach is based mainly on the visualisation of the driving cycles as a function of instantaneous speed and acceleration. A vehicle trip dataset is classified into typical segments according to their speed-acceleration distribution. In order to describe the class through overall parameters, central segments are selected as representative of varied classes. As a result, 12 typical and contrasted driving situations were identified with their respective share. The next step is based on the analysis of the kinematical content of the cycles, through the 2-dimensional distribution of the instantaneous speed and acceleration. Finally, the cycle is established by juxtaposing representative kinematic segments of driving classes. Figure 2.8 (a), (b) and (c) demonstrate the ARTEMIS drive cycles under different scenarios.

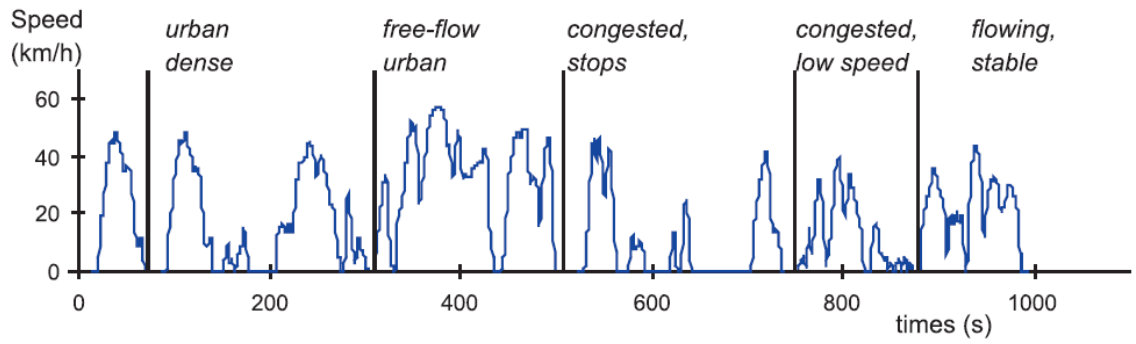

Figure 2.8(a) ARTEMIS urban driving cycles(Andr é, 2004)

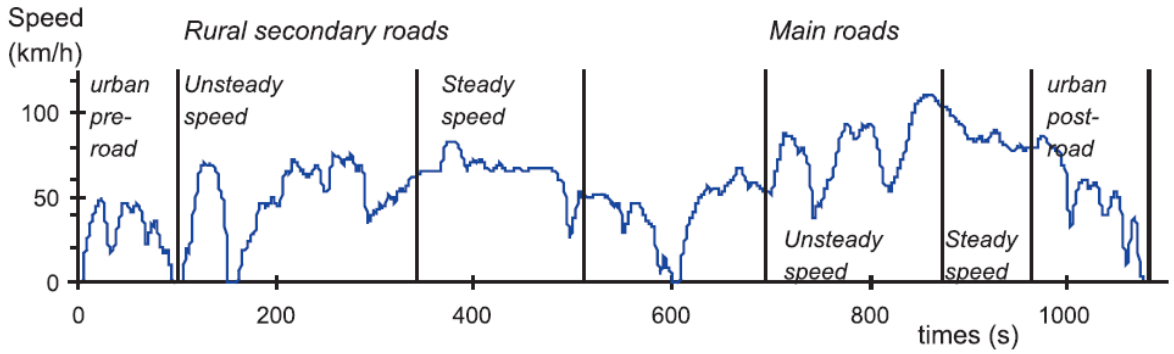

Figure 2.8(b) ARTEMIS rural-road driving cycles (Andr é, 2004)

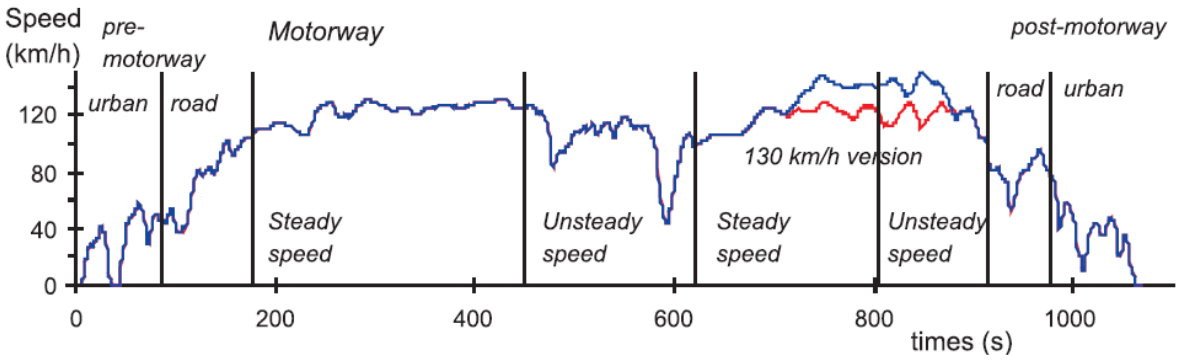

Figure 2.8(c) ARTEMIS motorway driving cycles (Andr é, 2004)[1]

[1] The red line represents 130 km/hr speed version

Figure 2.8 ARTEMIS driving cycle

US drive cycles

The Federal Test Procedure 75 (FTP-75) has been used for emission certification of light duty vehicles in the US. From 2000, vehicles have to be additionally tested on two Supplemental Federal Test Procedures (SFTP) designed to address shortcomings with the FTP-75 in the representation of aggressive, high speed driving and the use of air conditioning. The FTP-75 cycle is derived from the FTP-72 cycle by adding a third phase of 505 seconds, identical to the first phase of FTP-72 but with a hot start. The third phase starts after the engine has been stopped for 10 minutes. Thus, the entire FTP-75 cycle consists of the following phases: cold start; transient; and hot start, as shown in Figure 2.9.

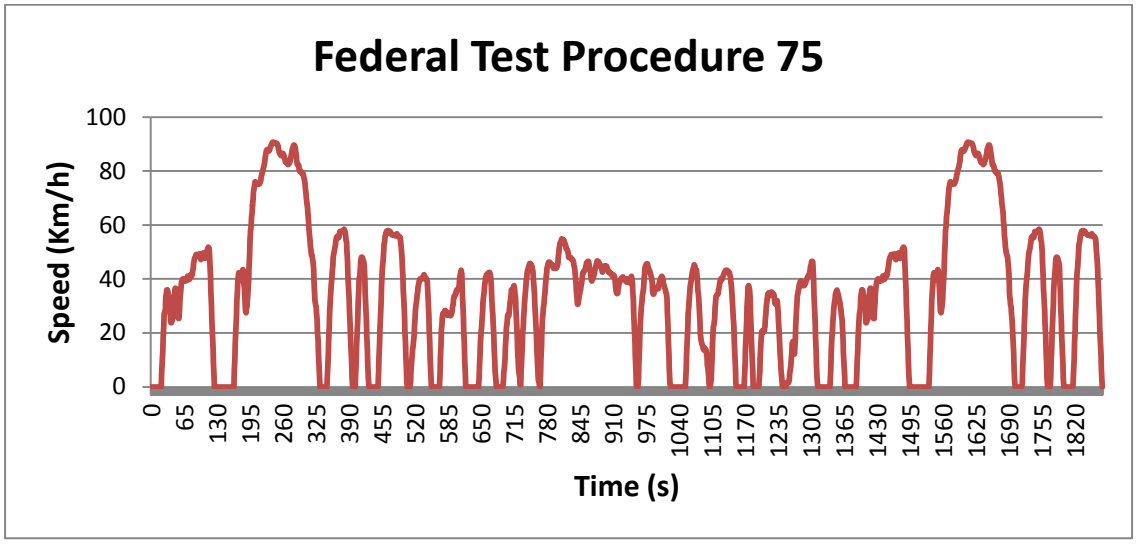

Figure 2.9 TP-75 Cycle (Samuel et al., 2002)

Japanese drive cycles

In 2010, Japan introduced a new test cycle, the JC10. Compared with the previous test cycle, the length of JC10 cycle is longer. The cycle accounts for more aggressive driving behaviours, with higher average and maximum speeds. The cycle is illustrated in Figure 2.10.

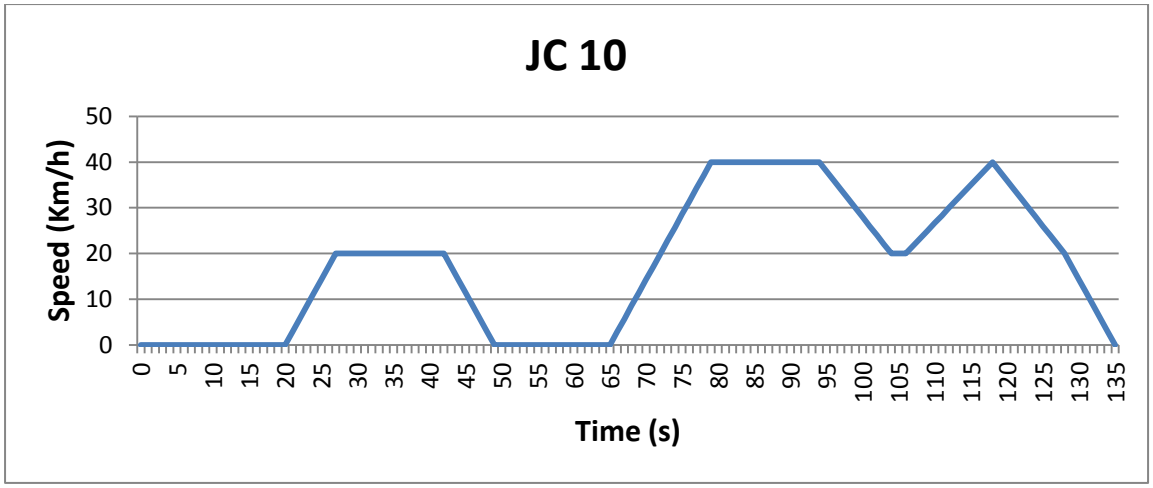

Figure 2.10 JC08 drive cycle (Walsh, 2011)

Australian drive cycles

Australian Design Rules (ADR) 37/xx Drive Cycle

An FTP cycle can be split into a transient portion and a stabilised portion. It is set to test a series of mechanical performances (EPA, 1989). Phase 1 consists of 505 seconds transient phase, which includes a brief high speed highway component; phase 2 is start-stop slower speed transient phase meant to replicate congested traffic; and phase 3 is a repeat of phase 1 but initiated with a hot start. The ADR37 time-speed profile is shown in Figure 2.11.

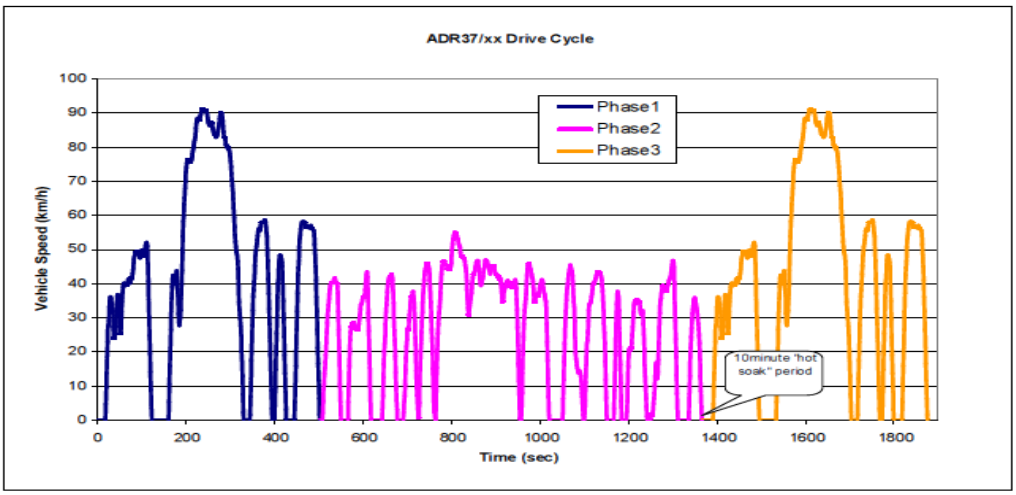

Figure 2.11 ADR 37 profile (Zito and Primerano, 2005)

ADR 79/01

ADR 79/01 adopts the ECE 83/04 drive cycle. The prototype was introduced in the early 1990s to test light duty vehicles with catalytic converters. It has two phases: phase 1 consists of four duplicated urban modes of driving; and phase 2 is an extra-urban driving cycle to account for more aggressive high speed driving modes. The maximum velocity of this phase reaches 120 km/h. The ADR79 time-speed profile is shown in Figure 2.12.

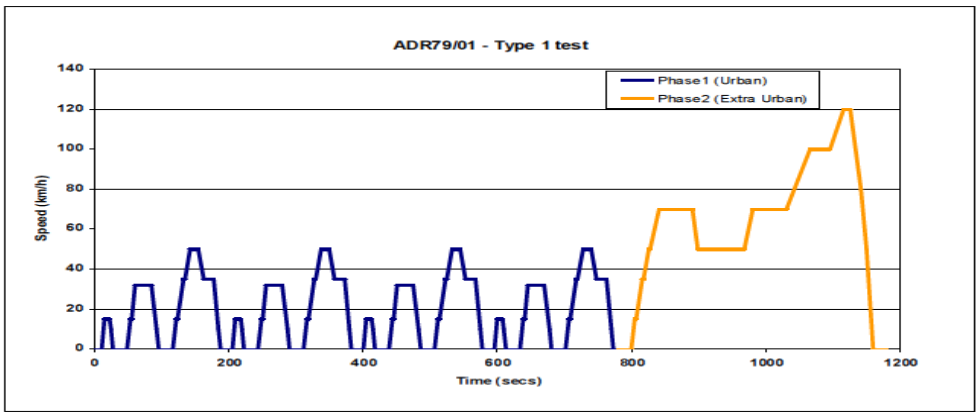

Figure 2.12 ADR 79/01 profile (Zito and Primerano, 2005)

Composite urban emissions drive cycle (CUEDC, NISE2, 2009)

To obtain a truly representative national driving cycle, data were collected from the Brisbane, Sydney, Melbourne, Adelaide and Perth metropolitan areas. The methodology was proposed by Lin and Niemeier (2003), and adopted and used in several applications (Biona and Culaba, 2006; Hung et al., 2007). The first step of drive cycle development is the composite urban emissions drive cycle (CUEDC) categorised into six phases by driving pattern. The Markov-chain approach is used to construct the stochastic cycle based on the transition probability from one modal event to another.

The drive cycle is built to represent a comprehensive drive cycle in Australia on varied road conditions; this cycle consists of four components, including residential road, arterial road, freeway and congested conditions. Due to the time gap between consecutive phases, each one can be taken as an independent distinct cycle. The flow chart of the methodology is shown in Figure 2.13. From GPS measurements and GIS processing, instantaneous speed, acceleration,

position, and road flow category can be derived. After the data acquisition, the dataset is disaggregated into six phases. To establish a national drive cycle, parameters of each phase are weighted by the estimated number of trips in each state. The CUEDC time-speed profile is shown in Figure 2.14.

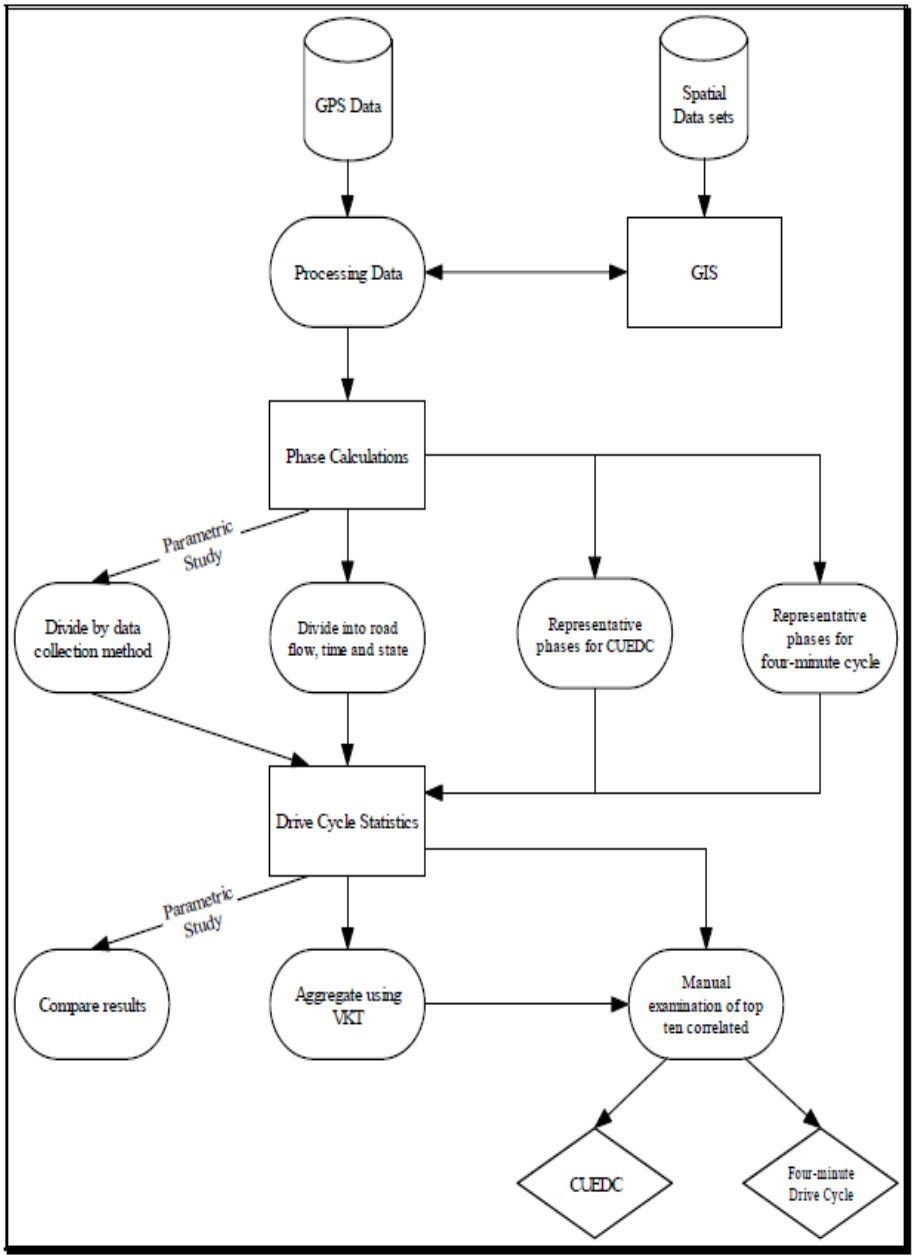

Figure 2.13 Flow Chart for developing CUEDC (NISE 2, 2009)

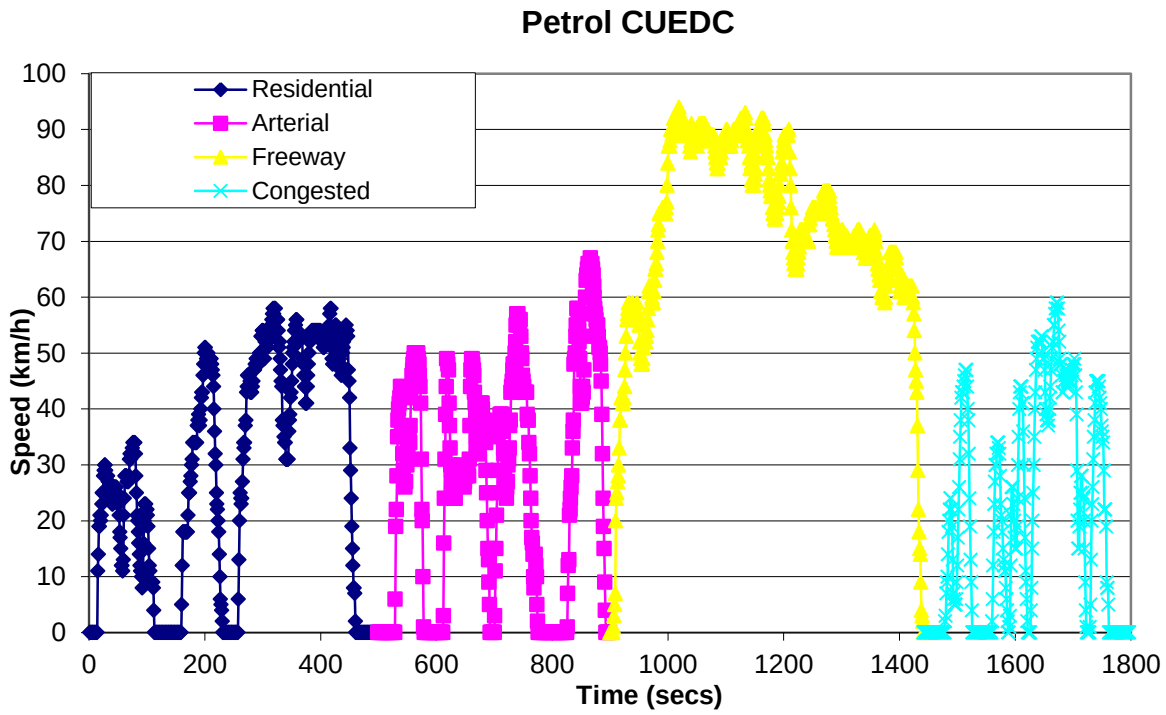

Figure 2.14 CUEDC for light duty gasoline vehicles (NISE 2, 2009)

2.5 Review of development methods for drive cycles

The drive cycle, which is a key building block for emissions modelling, should be representative of vehicle daily travel patterns. For emission modelling at the macro-scale, the emission/fuel consumption rate is determined by the average value of measurements when driving through a cycle. At the micro level, the cycle links the instantaneous emissions with vehicle operational variables (i.e. speed and acceleration). As a result, different countries have developed various cycles based on the results of large travel surveys. The methodologies can be classified as follows:

(1) Stochastic: instantaneous speed data is deconstructed into operational components (i.e. acceleration, deceleration, cruising), then the cycle is constructed by Markov Chain (Lin and Niemeier, 2003).

(2) Semi-Stochastic: According to André (2004), the instantaneous speed data is also deconstructed into components. However, the average sub-cycle is selected in each component, and those selected are combined into a drive cycle.

(3) Empirical: Based on the statistical results of the vehicle's travel, the cycle consists of polygon-like blocks to describe the relationship between speed and time (Samuel et al., 2002).

The Markov Chain represents well the stochastic nature of driver behaviours. The stochastic method, which the CUEDC has adopted, has been applied successfully in different countries(Biona and Culaba, 2006) . The four different components of the cycle enable it to represent urban traffic patterns in Australia. All of these features indicate that the CUEDC is a promising drive cycle for Australian conditions.

2.6 Summary

Generally, gaseous emissions, namely HC, CO, NO_x and particulate matter in various sizes are the major hazardous pollutants. Vehicle emissions vary subject to vehicle loading, driver behaviour, vehicle specification and other factors. The vehicle emission's intensity can be measured by indoor dynamometer testing or mobile on-board equipment. As they closely correlate with emission modelling at either the macro or micro levels, the drive cycles that represent daily travel have been reviewed and compared here. This chapter has presented the main findings of a state-of-the-art literature review conducted on vehicle emissions and their testing methods. The main aim of appraising the literature was to set up the working scope and reveal the collection method of emission data for further emission modelling.

Chapter 3. Data Source and Emissions Modelling Evaluation

3.1 Introduction

Historically, car-following and traffic flow models have been developed using different theoretical bases. This has given rise to two main kinds of models of traffic dynamics, namely: microscopic representations, based on the description of the individual behaviour of each vehicle; and macroscopic representations describing traffic as a continuous flow obeying global rules (Bourrel and Lesort, 2003). Strategic travel demand models tend to be large and regional in nature, whereas micro simulation models are used for detailed tactical or operational testing of options. Taking the highest macroscopic level as an example, the total vehicle flow and the average speed over an entire network may be all that is provided (Barth and Scora, 2006). At the lowest level of the hierarchy, high-resolution microscopic transportation models typically produce second-by-second vehicle trajectories (e.g. location, speed and acceleration). Hence, traffic modelling and emission modelling should be compatible in terms of accuracy and aggregation levels. For instance, driving cycles used for vehicle emission testing are specified on a second-by-second speed-time profile. Microscopic traffic models should integrate real time emission prediction models, which are able to utilise high-resolution transportation modelling results, thereby generating potentially more precise emission estimates. This chapter provides a detailed review and evaluation of emissions models at both the micro and the macro levels.

3.2 Emissions models review

Emissions models range from elemental approaches, which cater for the main elements of an urban movement (acceleration, deceleration, cruising and idling), to aggregate models based on average speed as the only variable. The former are suitable for use in conjunction with micro-simulation of traffic flow and for single intersection deterministic models. Strategic transport models output vehicle flows and average link speeds on road and public transport network links. Flows are categorised by vehicle type, typically passenger cars; and commercial vehicles (disaggregated by light, medium and heavy commercial vehicles), as well as bus flows and bus speeds. Thereby, Smit et al. (2009) proposed a classification of emissions models based on the way driving behaviour is incorporated, namely:

- Models which incorporate speed-time profiles in their development phase (Type 1);
- Models that generate speed-time profiles as part of the emission modelling process (Type 2); and
- Models that require speed-time profiles data as input (Type 3).

Several emissions models, at micro and macro scales, are reviewed in section 3.2.1 and section 3.2.2, respectively, in order to find a promising approach to address the research question.

3.2.1 Macro emissions modelling

Typical relationships are of the type shown in Equation 3.1.

$F = A + (B/V) + C*V + D*V^2$ Equation 3.1

Where:

V=average speed (km/h);

F=fuel (l/100 km); and

A, B, C and D are coefficients which depend on vehicle type and road link type.

According to Akcelik and Besley (2003) the fuel consumption is highly correlated with CO_2 emissions. In contrast, other pollutants, including HC CO NO_x have weak correlation with fuel consumption.

There are several reasons to predict fuel consumption and air quality impacts of transport/land use, namely: to estimate the total energy impact of projects or strategies; to estimate the changes in transport modal energy efficiency levels; and to estimate the greenhouse gas impacts either at the total study area aggregation or at more disaggregated levels (in both time and space). Some environmental impacts have local, regional and global effects, as well as short- and long-term effects (e.g. air pollution with its impact on local residents' health and on global warming). The macro-level of emissions models is suitable to provide large scale area (regional or corridor) impacts.

US MOBILE6 (EPA, 2003)

The MOBILE6 model was developed by the US EPA and is the latest of the MOBILE models. MOBILE6 was developed using recent vehicle-emission testing data collected by the EPA, CARB, and automobile manufacturers, as well as inspection and maintenance tests conducted in various states. The emissions for specific classes of vehicle are a product of traffic volume and emission factors.The latter, which are, at the core of macro emissions models, can be adjusted for different facility types and different average speeds based on vehicle testing over a series of facility cycles. A methodology, known as named running exhaust factor, quantifies emission rate by using a serial of adjustment factors, which are influenced by surrounding environment, vehicle usage and fleet status.

Mobile 6 running exhaust factor methodology:

$[\text{Fleet} - \text{ave emission Rate}]\ \text{vehicle class} = \sum_{\text{Age}=1}^{25}[\text{Travel fraction}]$ * [LA4 emission rate+ Tampering offset + Aggressive Driving +Air Conditioning]*[Temperature Adjustment]*[Speed Adjustment]*[Fuel adjustment]

VISUM (PTV, 2005)

In the strategic transport demand modelling package, VISUM, emissions are determined on the basis of emission factors from the Swiss Federal Office for the Environment. The calculation of the pollution emission values is carried out internally by the program on the basis of direction; volume values for both directions are later added. The emissions are calculated for every car and every truck (HGV), with every value multiplied by the number of vehicles (link volume for HGVs or cars). For every pollutant a regression curve is used of the form:

$$Emission = A + B * \mathrm{V} + C * \mathrm{V}^2 + D * V^3 + E * V^4 + F * \mathrm{V}^5 \qquad \text{Equation 3.2}$$

Where:

V: Speed (km/h)

The parameters A, B, C, D, E and F were determined separately for different pollutants for cars and HGVs for the reference years 1990, 1992, and 2000.

COPERT 4 (Andréand Rapone, 2009)

This model provides the methodology, emission factors and relevant activity data to enable exhaust emissions to be calculated for the following categories of road vehicles:

- Passenger cars
- Light-duty vehicles (1) (< 3.5 t)
- Heavy-duty vehicles (2) (> 3.5 t) and buses
- Mopeds and motorcycles

The summation approach for exhaust emissions uses the following general equation:

$$E_i = \sum_j (\sum_m (FC_{j,m} * EF_{i,j,m})) \qquad \text{Equation 3.3}$$

Where:

E_i = emission of pollutant i [g],

$FC_{j,m}$ = fuel consumption of vehicle category j using fuel m [kg],

$EF_{i,j,m}$ = fuel consumption-specific emission factor of pollutant i for vehicle category j and fuel m [g/kg].

The fuels to be considered include gasoline, diesel, LPG and natural gas. This equation requires the fuel consumption/sales statistics to be split by vehicle category, as national statistics do not provide vehicle category details.

Artemis emission model - European Union (Cantú-Paz, 1998)

Essentially, this model measures total emissions of a given pollutant from a road traffic source as the product of a specific emission factor and a quantity of traffic activity. Compared with other emissions models, the emission factor is determined by the vehicle's kinematic content in modelling area. An approach based on kinematic similarity is developed. The approach consists of three main steps:

(i) Identify cycles by kinematic content through the construction of a classification scheme.
(ii) Select of appropriate cycles to represent each group; determine the appropriate emission factor for specified traffic activities.
(iii) Determine the corrections to develop reference emission factors.

Macro-level models: summary

The common macro-level modelling approach used to produce a mobile source emission inventory is based on two processing steps. The first step consists of determining a set of emission factors that specify the rate at which emissions are generated, and the second step is to produce an estimate of vehicle activity. The emission inventory is then calculated by multiplying the results of these two steps together. This methodology has two major shortcomings:

(1) Inaccurate characterisation of actual driving behaviour

The current methods used for determining emission factors are based on average driving characteristics embodied in a pre-determined driving cycle which is used to certify vehicles for compliance of emission standards and from which most of the emissions' data are based. This drive cycle does not represent Australian driving behaviour.

(2) The emissions factor methodology does not represent properly actual conditions

The non-representative nature of the US FTP driving cycle tests is exacerbated by the procedure used for collecting and analysing emissions (Barth et al., 1996). Dynamometer tail-pipe measurements are used as base values to reconstruct statistically the relationship between emission rates and average vehicle speeds. These "averaged speeds" are at variance with the vehicle operation at the micro level, under Australian conditions. For example,

frequent and sharp accelerations (or decelerations) can be found in the urban phase of the CUEDC drive cycle.

Hence, the relationship between vehicle use and each individual pollutant is, for the most part, complex and difficult to quantify using average emission factors. Whilst greenhouse gases are directly related to fuel consumption, other pollutants show no such direct correlation. Typical Australian based macro emission factors for particle and gaseous pollutants, by vehicle class, road type and average speed have been summarised by Ferreira (2007). Keogh et al.(2010) have undertaken an analysis of over 600 particle emission factors in the international literature. This has resulted in the development of statistical models that can estimate average particle emission factors for light duty vehicles (mainly passenger cars), heavy vehicles and buses. Having obtained estimates of total pollutants for each road link, it is possible to use detailed estimates of exposure by linking emission estimates with dispersion models and land use adjacent to transport links, to arrive at exposure impacts on the local population. As an intermediate stage, it may be worthwhile to arrive at measures of environmental impact by weighting link-based emissions according to the likely population exposure.

3.2.2 Micro emission modelling

Type 3 (micro-level) models typically simulate traffic systems on a vehicle-by-vehicle basis, updating speed, acceleration and other variables on a second-by-second basis. These models require a large amount of data and are often based on instantaneous measurements. Macro models (Type 1) give the average emissions for a group of vehicles. Typically, these models use vehicle-kilometres travelled (VKT) and average vehicle speed to calculate the overall level of emissions. The matching between traffic modelling outputs and emission modelling means making sure there is compatibility between the levels of uncertainty attached to the inputs (and outputs) of both types of models.

There have been a number of modelling approaches proposed to estimate future vehicle emissions in conjunction with the outputs of transport models. One such approach is the use of engine power as the main predictive basis. Another is the use of vehicle speed and acceleration as predictive variables. Three main modelling approaches were reviewed, namely: power-based; speed-based; and hybrid models. A review of microscopic emissions models has been undertaken using the results of Australian vehicle emissions measured in the field. As shown in Table 3.1, those three approaches were covered by seven different models which have been analysed by the same dataset from NISE2 and the emission prediction results compared.

Table 3.1 Emissions models assessed

Model	General approach	Reference
	Power-based	
1: CSIRO		(Leung and Williams, 2000)
2: CMEM		(Barth and Scora, 2006)
3:VT-CPFM		(Rakha et al., 2011)
	Speed-based	
4: Energy and emissions model (VT)		(Ahn et al., 2002)
5: Instantaneous traffic emissions		(Int Panis et al., 2006b)
	Hybrid	
6: Micro-scale modelling		(Qi et al., 2004)
7: Micro-scale modelling		(Smit and McBroom, 2009)

3.2.2.1 Power-based models

Model 1: CSIRO, (Leung and Williams, 2000)

The performance of a power-based fuel consumption and exhaust emissions model has been evaluated. The model was found to predict fuel consumption well when compared with on-road and dynamometer tests. Average exhaust emissions including HC and CO were also well predicted.

The tractive power equation has the form shown in Equation 3.4.

$$Zt = Zd + Zr + Za + Ze + Zm$$

Equation 3.4

Where:

Zt : Tractive power

Zd: Power of overcoming vehicle drive − train resistance

$$Zd = 2.36 * 10^{-7} V^2 M$$

Zr : Power to overcome tyre rolling resistance

$$Zr = (3.72 * 10^{-5} V + 3.09 * 10^{-8} V^2) M$$

Za : Power to overcome aerodynamic drag

$$Za = 1.29 * 10^{-5} Cd AV^3$$

Ze: Power to overcome inertial and gravitational resistance

$$Ze = 2.78 * 10^{-4} (a + g \sin\theta) MV$$

Zm: Power for accessories

M (kg) is the inertia mass of vehicle; V (km/h) the vehicle speed; a (m/s^2) the vehicle acceleration, Cd the aerodynamic drag coefficient; A (m2) the vehicle frontal area; and θ the road gradient.

The emission rate equation is given by:

$$\text{Pollutant Emission rate} = \alpha' + \beta' Z_t = \gamma' EC + \beta' Z_t \qquad \text{Equation 3.5}$$

Where :

α'represents the idle emission rate

β' represents the emission rate per unit power output.

As the emission rate increases with the fuel consumption rate, α' is expected to be a function of engine capacity and thus can be expressed as a product of $\gamma'$and EC.

The intersect of Equation 3.5 reflects idling emission (or fuel consumption) when power equals zero. This model shows a theoretical link between emissions and instantaneous power. For macro-scale emission modelling, this approach can provide an adequate estimate of emissions. However, the results are based on statistical average values for power, fuel consumption and emissions. For micro-scale modelling, it is important to be able to account for variations in vehicle characteristics, such as age and the use of catalytic converters.

Some parameters, such as vehicle aerodynamic drag coefficient, were not available to estimate Equation 3.4. Therefore, instead of instantaneous power, vehicle specific power (VSP) was used, which is defined as the engine power output per vehicle unit mass expressed as a function of vehicle speed, road grade, and acceleration (Frey et al., 2006). Model 1 was evaluated using Equation 3.6.

$$\text{VSP} = V\left[a + 9.81 * \left(A\ tan(\sin(grade))\right) + 0.092\right] + 0.00021V^3$$

Equation 3.6

Where:

VSP = vehicle specific power (kW/ ton)

A and V are as defined in Equation 3.4.

Model 2: Comprehensive Modal Emissions Model (CMEM), (Barth and Scora, 2006) .

Model 2 is a physical, power-demand model based on a parameterised analytical representation of emissions production. The emission process is divided into different components that correspond to physical phenomena associated with vehicle operation and emissions. Each component is modelled as an analytical representation consisting of various parameters that are characteristic of the process (Barth et al., 1996). In developing these models, both engine-out and tailpipe emissions of over 300 vehicles were measured in a laboratory at a second-by-second level of resolution along three drive cycles (Barth et al., 1996). However, the establishment of this type of model is data intensive. To compute the real-time emission rate, a large number of physical variables need to be collected or measured and a second-by-second vehicle speed-time profile is required as input.

Model 3: Virginia Tech Comprehensive Power-Based Fuel Consumption Model (Barth and Scora, 2006)

The Virginia Tech Comprehensive Power-Based Fuel Consumption Model-1 and Model -2 (VT-CPFM-1 and VT-CPFM-2) address the two deficiencies in existing models, namely: the ability to result in a non-bang–bang control (on–off controller) and the ability to calibrate the model parameters using publicly available fuel consumption and vehicle driveline data. The use of a second-order model with a positive second order parameter is used to ensure that a bang–bang control does not result from the application of the model. Addition of higher than second-order parameters would add to the complexity of the model and thus not allow for model calibration using the US EPA city and highway cycles. Consequently, a second-order model provides a good compromise between model accuracy and applicability.

VT-CPFM-1:

$$FC(t) = \alpha_0 + \alpha_1 P(t) + \alpha_2 P(t)^2 \qquad P(t) \geq 0$$

$$FC(t) = \alpha_0 \qquad P(t) < 0$$

VT-CPFM-2:

$$FC(t) = \beta_0 w_e(t) + \beta_1 P(t) + \beta_2 P(t)^2 \qquad P(t) \geq 0$$

$$FC(t) = \beta_0 w_{idle} \qquad P(t) < 0$$

Equation 3.7

Where:

α_0, α_1, a2 and β_0, β_1, and β_2 are vehicle-specific model constants that are calibrated for each vehicle

w_{idle} is the engine idling speed (rpm)

$P(t)$ is the instantaneous engine output power.

3.2.2.2 Speed-based models

Model 4: Microscopic energy and emissions model (Virginia Tech) (Ahn et al., 2002)

Model 4 is based on the relationship between emissions and vehicle speed established by Ahn et al.(2002).The results indicate that vehicle emissions and fuel consumption rate increase as speed increases, and occur even when the vehicle is in deceleration mode. This phenomenon cannot be explained by power-based models which assume idling conditions for negative tractive effort (Biggs and Akcelik, 1986). For Model 4, the final regression includes linear quadratic and cubic speed and acceleration terms. As Rakha et al. (2003) have pointed out, the model provides the least number of terms with a relatively good fit to the original data (R^2> 0.92) for all measures of effectiveness (MOE). However, the regression equation includes a high number of terms (16). The regression results are sensitive to the testing method used, namely the driving cycle and the sample of vehicles chosen to represent the fleet composition.

Model 4 has a set of equations produced for each MOE, as shown in Equation 3.8.

$$\text{MOE} = \sum_{i=0}^{3} \sum_{j=0}^{3} k_{i,j}^{e} * V^{i} * A^{j} \qquad \text{Equation 3.8}$$

Where:

MOE = Instantaneous fuel consumption and other pollutants;

$k_{i,j}^{e}$ Model regression coefficient for MOE e at speed power i and acceleration power j

V^i Speed (m/s)

A^j Acceleration (m/s^2)

Model 5: Instantaneous traffic emissions (Int Panis et al., 2006b)

Model 5 is a simplification of Model 4 consisting of only six variables. Emission functions for each vehicle are derived with instantaneous speed and acceleration as parameters use non-linear multiple regression techniques. The model has been calibrated using data from 25 vehicles (6 buses, 2 trucks and 17cars). Since the data revealed a clear distinction in emissions for acceleration and deceleration phases, the entire dataset was categorised into three components, namely: acceleration greater than 0.5 m/s^2; deceleration less than -0.5 m/s^2; *and* cruising and idling within 0.5 m/s^2 and -0.5 m/s^2, respectively. The model can be used to estimate NO_x, volatile organic compounds (VOC), CO_2 and PM. Model 3 has the form shown in Equation 3.9

$$E_n(t) = \max[E_0, f_1 + f_2 V_n(t) + f_3 V_n(t)^2 + f_4 A_n(t) + f_5 A_n(t)^2 + f_6 V_n(t) A_n(t)]$$

Equation 3.9

Where:

$V_n(t)$ and $A_n(t)$ are the instantaneous speed and acceleration of vehicle n at time t; $E_0(t)$ is a lower limit of emission (g/s) specified for each vehicle and pollutant type; and f_1 to f_6 are emission constants specific for each vehicle and pollutant type determined by the regression analysis.

3.2.2.3 Hybrid models

Model 6: Micro-scale modelling (Qi et al., 2004)

Model 6 incorporates acceleration and deceleration into a single vehicle emission model. The calibration was based on a testing program of 327 vehicles over three cycles. This model adopts lagged acceleration (or deceleration) variables. Nine terms in the equation represent acceleration (or deceleration) of one to nine seconds before current time. Two variables, T' and T", are introduced to represent the duration of acceleration and deceleration since its inception, respectively. The model takes the form shown in Equation 3.10.

$$E(t) = \beta_0 + \beta_v V(t) + \beta_{v^2} V^2(t) + \beta_{v^3} V^3(t) + \beta_{T'} T'(t) + \beta_{T''} T''(t) + \beta_{A_t} A(t) \ldots\ldots + \beta_{A_{t-9}} A(t-9) + \beta_w W(t)$$

Equation 3.10

Where:

$E(t)$: Emission rate

$W(t)$: Kinetic powe

$A(t)$: Acceleration at time t seconds

$A(t-9)$: Acceleration at time (t-9) seconds

$T'(t)$: Duration that deceleration has been continuously executed since inception

$T''(t)$: Duration that acceleration has been continuously executed since inception

Model 7: Micro-scale model (Smit and McBroom, 2009)

This recently developed model is similar in principle to model 6 Australian emissions measurement data (Orbital, 2009) was used to calibrate the model which consists of two parts, namely: (1) relating emissions to the instantaneous speed, acceleration and instantaneous power; and (2) relating historic power change to the current emission rate. Model 7 has the form shown in Equation 3.11.

$$E_m(t) = \beta_0 + \beta_1 V(t) + \beta_2 A(t) + \beta_3 A(t)V(t) + \beta_4 P(t) + \beta_5 P(t)^2 + \beta_6 P(t)v(t) + \beta_7 \Delta P3 + \beta_8 \Delta P9 + \beta_9 oP9 + \beta_{10} \log TAD_t^N + \varepsilon$$

Equation 3.11

Where:

The definition of terms for this model are shown below

Instantaneous speed at time: V(t)

Acceleration at time: A(t)=V(t)-V(t-1)

Instantaneous power at the wheels: P(t)

Delta power over last three seconds

$$\Delta P3(t) = P(t) - P(t-2)$$

Delta power over last nine seconds

$$\Delta P9(t) = P(t) - P(t-8)$$

Oscillation power over last nine seconds

$$oP9(t) = |P(t) - P(t-1)| + \ldots + |P(t-7) - |P(t-8)|$$

Logarithm of distance normalised total absolute difference in speed (TAD) over last 9 seconds at time

$$\log TAD9_t^n = \log(1 + \frac{1000(|V(t) - V(t-1)| + .. + |V(t-7) - V(t-8)|)}{\sum_t^{t-8} x_t})$$

Error term or Residual : ε

3.2.3 Micro-scale model comparison results

These models are applied to the NISE2 dataset, which covers a range of vehicle sizes and ages. Eight average-aged passenger vehicles (which had travelled approximately 50,000-100,000km each), as listed in Table 3.2, were used here for model assessment.

Table 3.2 Selected vehicles for model comparisons

Vehicle(1)	Odometer (km)	Engine Displacement (L)	Transmission	Mass (kg)
Mazda 323	75,615	1.6	Manual	1215
Echo	53,859	1.5	Manual	921
Vectra	81,666	2.0	Auto	1317
Mazda 323	62,229	1.8	Manual	1142
Camry	81,783	2.2	Auto	1395
Tarago	90,749	2.4	Auto	1615
Pulsar	65,120	1.6	Manual	1067
Commodore	95,979	3.8	Auto	1654

Note: (1) All vehicles have 4 cylinders except the Commodore (V6).

Each chosen vehicle was ‘driven’ through the speed profile of the CUEDC, which is simulated using a purpose specific program and is presented in Figure 2.14. Gaseous emission rates for CO_2, CO, HC and NO_x were recorded second-by-second in addition to instantaneous speed. The CUEDCs were developed to represent typical vehicle journeys in a given study area. To obtain a representative Australian driving cycle, data were collected from the Brisbane, Sydney, Melbourne, Adelaide and Perth metropolitan areas (Orbital, 2009).

This cycle consists of four components, representing conditions on residential roads, arterial roads, freeways, as well as highly congested conditions. Due to the time gap between consecutive phases, each component can be taken as an independent distinct cycle. The emissions data described above was validated and verified before further analysis. Cold start and abnormal emissions were separated since they represent significant characteristics to hot stabilised conditions (Weilenmann et al., 2009). Figures 3.1 and 3.2 demonstrate the significant differences between the two datasets of the same vehicle. The integrity of the data was validated by a series of comparisons (Favez et al., 2009), namely: comparisons between two ways of collecting emission data; comparison between emission rates for different vehicles of the same category; and comparisons with European emission standards for new vehicles. The instantaneous emission measurements were averaged over those vehicles.

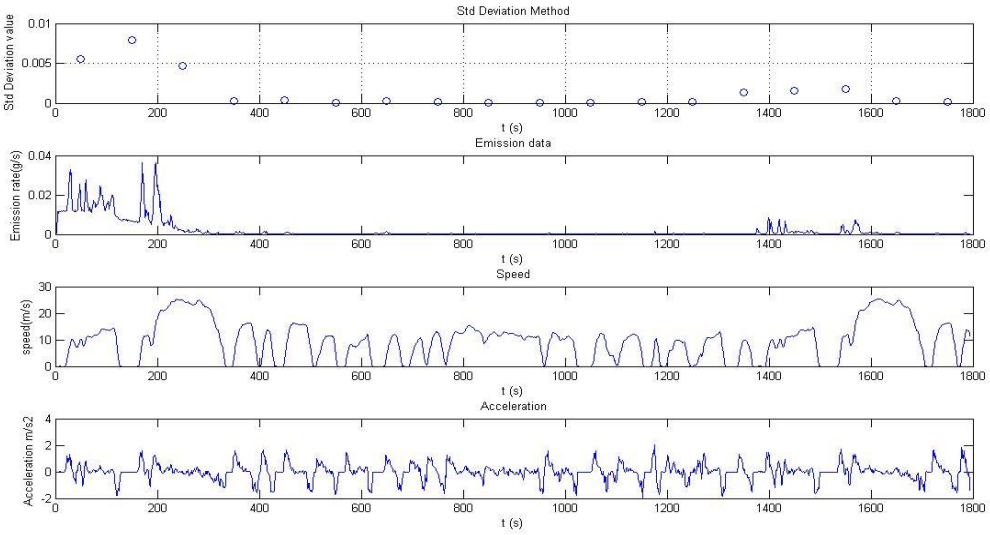

Figure3.1 Hydrocarbon emission dataset of the cold start condition

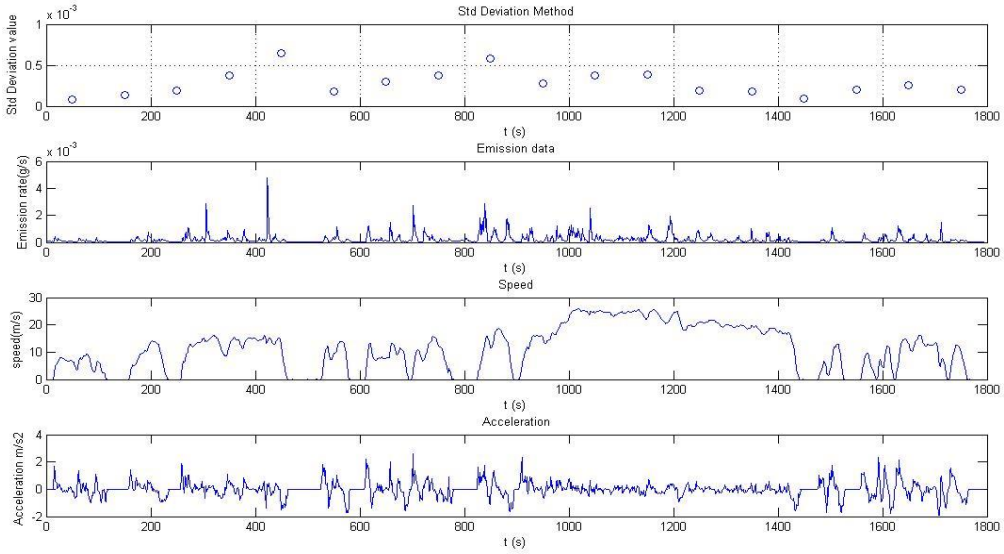

Figure 3.2 Hydrocarbon emission dataset under hot stabilised conditions An evaluation of the reviewed models included the analysis of a number of statistical measures comparing modelled with measured values for CO_2. The measures used include: the coefficient of correlation, R^2, an indicator of overall fitting; the root mean square error (RMSE); and the number of instances of negative emissions estimates. RMSE is given by:

$$RMSE_m = \sqrt{\frac{\sum_t [\hat{e}_m(t) - e_m(t)]^2}{T}}$$ Equation 3.12

Where:

$\hat{e}_m(t)$: emission estimation for time t

$e_m(t)$: emission measurement for time t

m : Emission type

T : No of measurements

Table 3.3 Overall model results

Model	R^2	RMSE	No of negative predictions	Make-up method
Model 1	0.76	0.69	91	N/A
Model 2	0.64	0.85	0	N/A
Model 4: Acceleration	0.92	0.44	0	
Model 4: Deceleration	0.86	0.28	0	
Model 4: Whole	0.93	0.38	0	Logarithm of emission data before regression analysis
Model 5: Acceleration	0.86	0.57	0	
Model 5: Cruising & idling	0.89	0.39	0	
Model 5: Deceleration	0.10	0.10	0	
Model 5: Whole	0.92	0.40	0	Assign a specific value to minus estimation
Model 6	0.91	0.43	51	N/A
Model 7	0.91	0.42	44	Square root of emission data before regression analysis

Table 3.3 shows the overall evaluation results. Speed-based models are more efficient in estimating emissions. In general, power-based models underperform, whilst hybrid models

produce more satisfying results. Between the two speed-based approaches, model 3 yields the highest values of statistical performance. However, this model has high levels of multicolinearity. In addition, its complex structure is a limiting factor for practical application.

The 'instantaneous traffic emissions' model (model 5) has been adopted by the AIMSUN traffic simulation model. The latter adopts European fleet derived coefficients to calculate instantaneous emission for specified types of vehicles (TSS, 2010). In the current paper, the AIMSUN emission methodology was adopted and each vehicle was 'driven' through the speed profile of the CUEDC drive cycle. A purpose specific program was developed to simulate the CUEDC in AIMSUN. Figures 3.3 (a) and (b) show the simulated and the actual cycles, respectively. The AIMSUN default settings are derived from European vehicle emission tests. To have a considerate evaluation of AIMSUN emission module, the pollutant emission predictions using the AIMSUN default settings were compared with the average of observed emissions from the NISE2 database (Orbital, 2009), using eight vehicles as representative of the current Australian passenger vehicle fleet. Figure 3.4 shows the goodness of fit obtained (R^2=0.8).

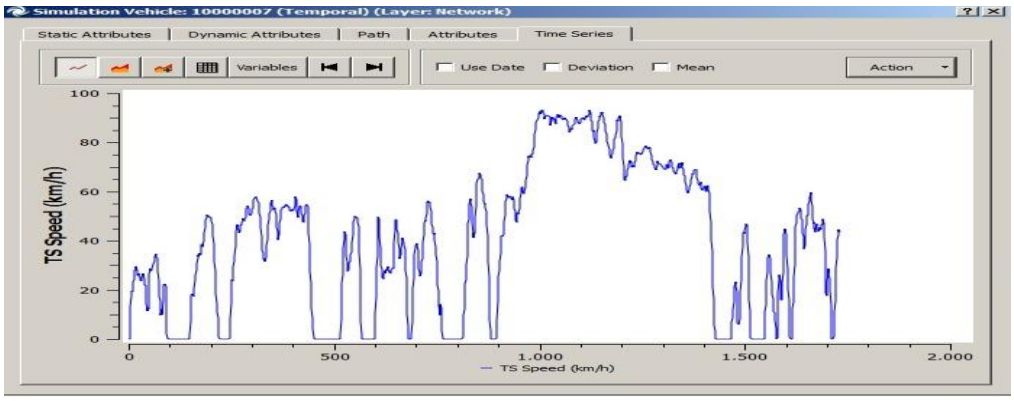

a.Simulated AIMSUN instantaneous speed profile

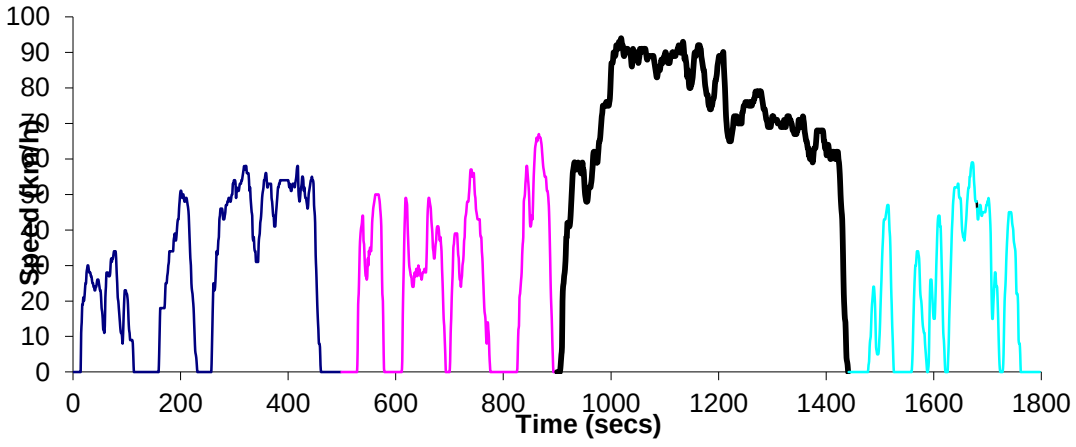

b. Australian Composite Urban Emissions Drive Cycle (petrol CUEDC)

Figure 3.3 Matching the simulated AIMSUN speed profile to CUEDC

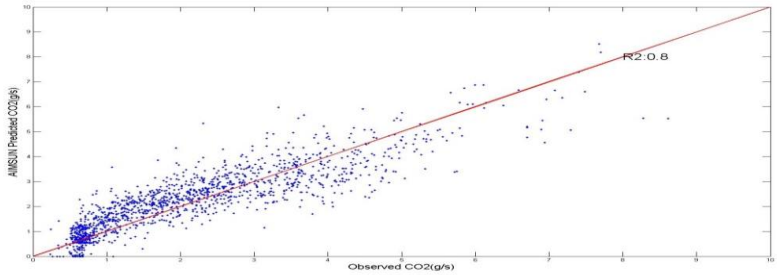

Figure 3.4 Comparison of CO2 AIMSUN predictions with averaged observed data

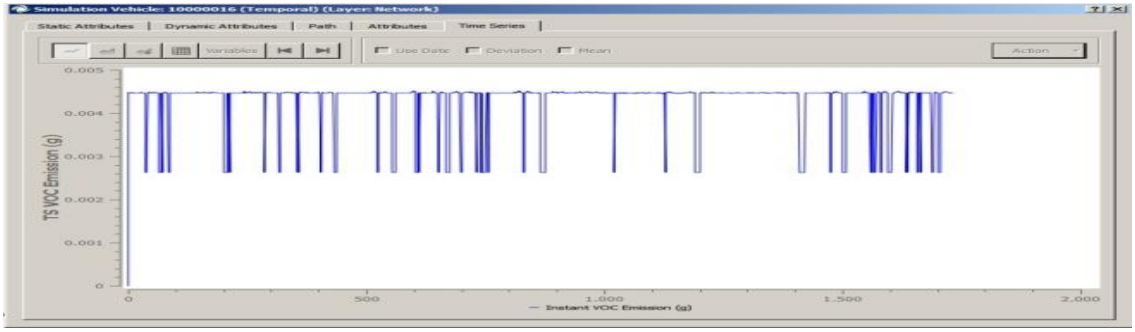

(a) Secondly CUEDC HC emissions prediction using AIMSUN

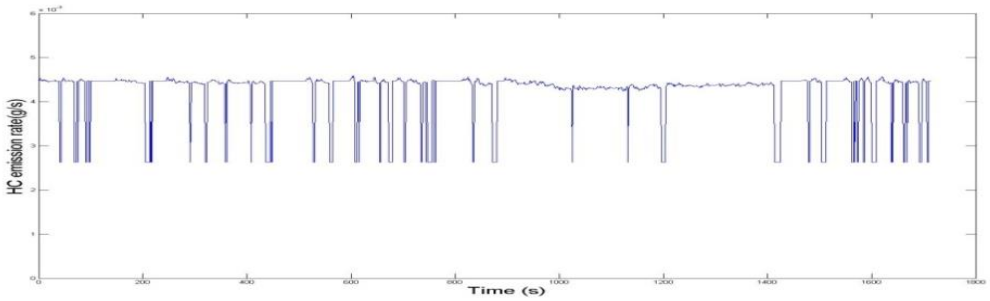

(b) Estimated emissions using AIMSUN default coefficients

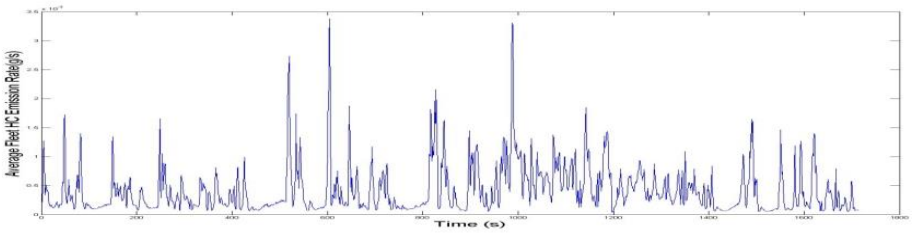

(c) Averaged Observed data (NISE2 dataset)

Figure 3.5 HC emission prediction comparisons

For other pollutants, such as HC, PM and NO_x, AIMSUN does not display second-by-second emission predictions properly. It was therefore necessary to calculate emissions manually using the instantaneous emissions model equation. Further investigation of pollutants other than CO_2 reveals that emission predictions are rather less robust. For instance, Figure 3.5 demonstrates that the HC emission prediction using AIMSUN (Figure 3.5 (a) and (b)) varies significantly from the average of observed HC emissions for the eight selected vehicles (Figure 3.5 (c)).The gap between NISE2 data observations and predictions by the current transportation simulation emissions module shows the European vehicle emission dataset derived coefficients are not applicable to the Australian fleet.

3.3 Summary

This chapter reviewed the macro and micro level emissions models, which are integrated with corresponding traffic models. The micro level models were classified and evaluated in terms of the modelling approach, accuracy and robustness. The initial results for CO_2 show that the speed-based model of Panis et al. (2006b) is a promising approach with several advantages. However, the modelling of other pollutants remains a challenge for current emissions models. To deliver a reliable solution of emission estimation, Chapter 4 introduces the research methodology and Chapter 5 proposes a new set of models for other pollutants.

Chapter 4. Research Methodology

Based the review of the relevant literature (Chapter 2) and on the results of the evaluation of existing models (Chapter 3), this chapter presents the research methodology and introduces the contributions of this thesis.

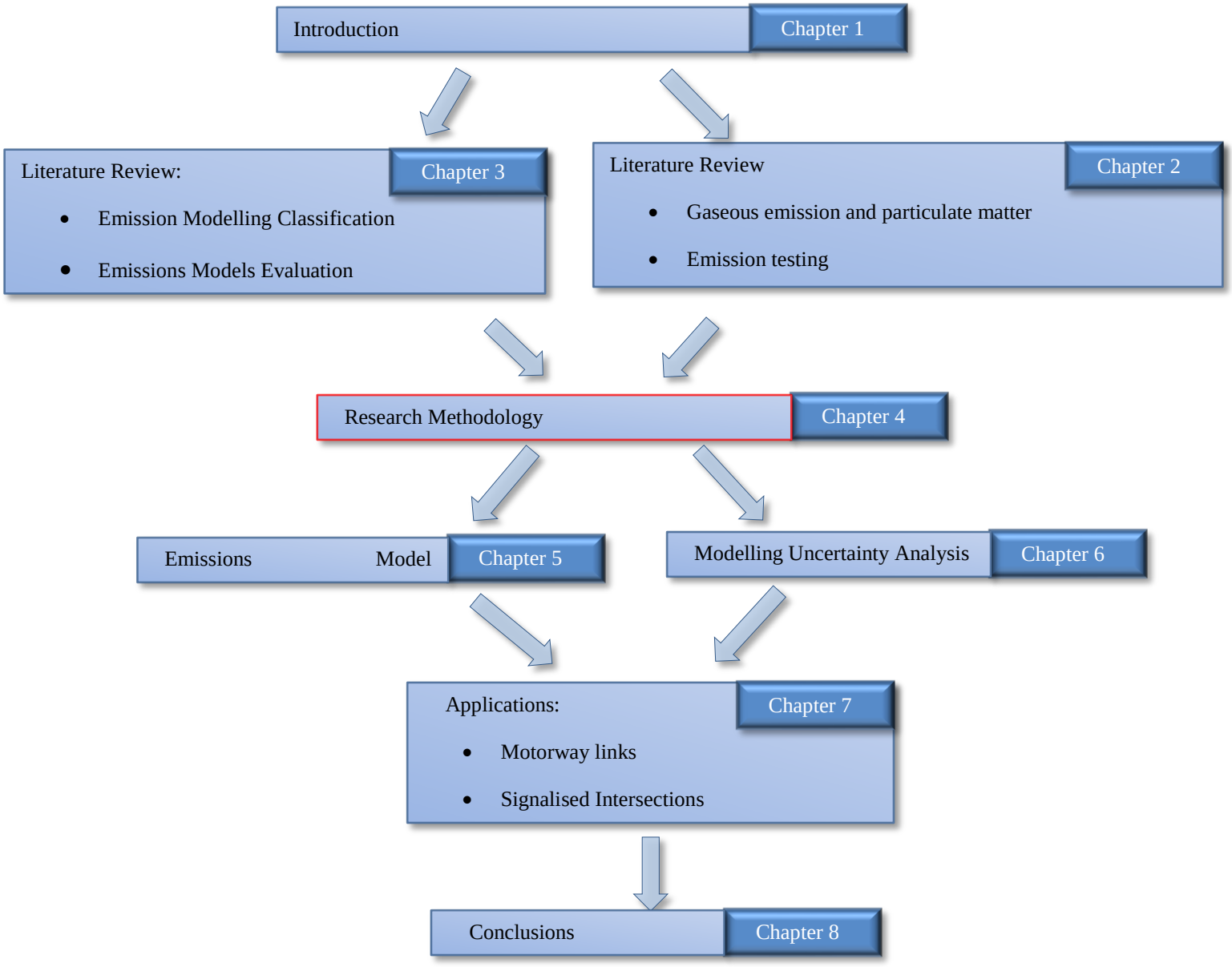

Figure 4.1 Thesis flow chart

4.1 Background: Overview on research methodology

The methodology was designed to achieve the stated research objects. The process is outlined in Figure 4.2. The main research tasks include the development of new emissions models, as well as the analysis of uncertainties presented in the outcomes of those models. The current chapter also deals with the way in which model development and uncertainty analysis influence each other.

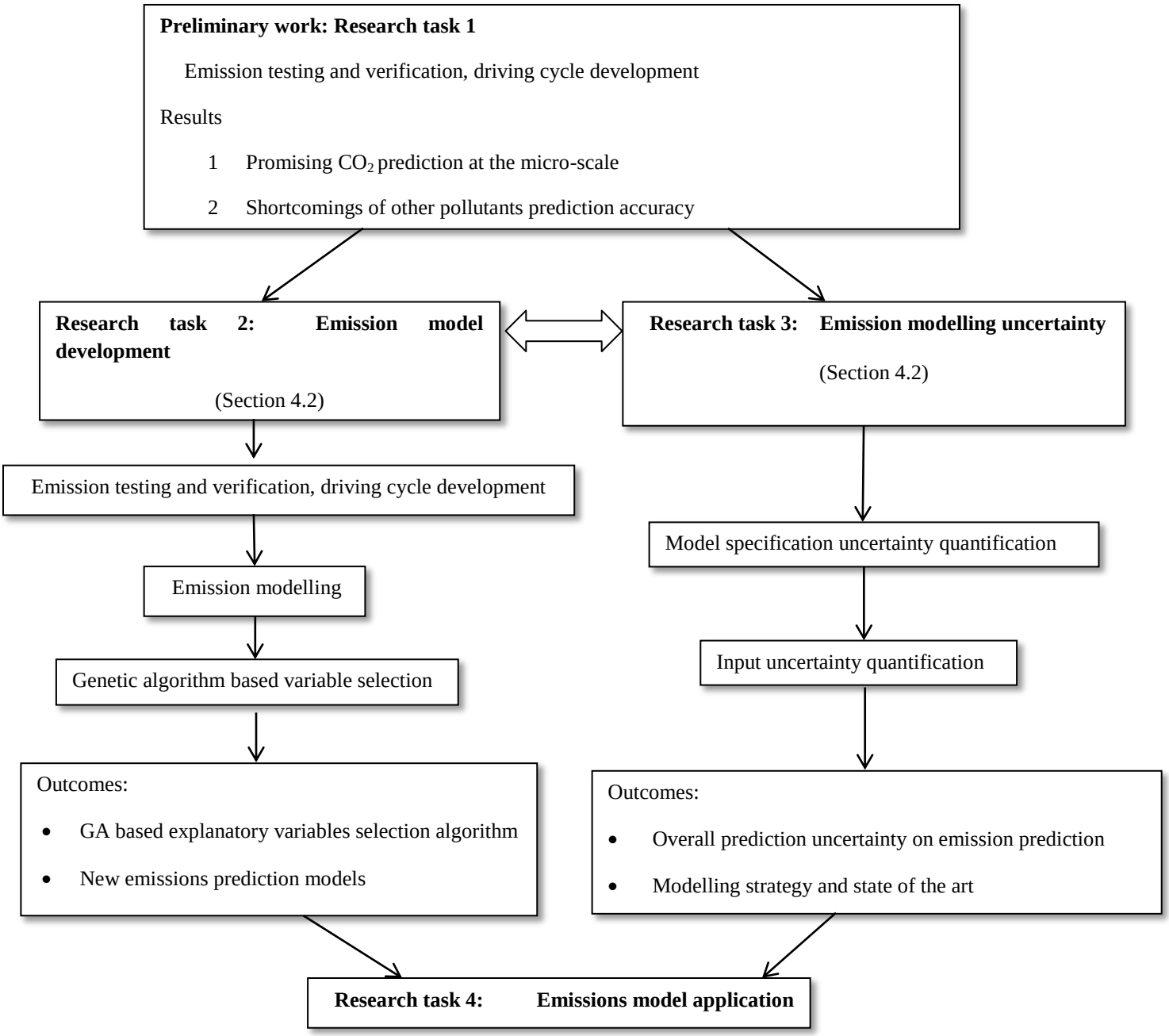

Figure 4.2 Research methodology outline

4.2 Model development

Historically, traffic flow models have been developed using different theoretical basis. “This has given rise to two main kinds of models of traffic dynamics, namely: microscopic representations, based on the description of the individual behaviour of each vehicle; and macroscopic representations describing traffic as a continuous flow obeying global rules” (Toledo, 2007). Taking the highest macroscopic level as an example, the total vehicle flow over an entire network may provide the average speed only (Barth et al., 1996) . Correspondingly, a number of emissions models deliver the predictions based on the aggregated traffic model outputs, for example the ARTEMIS in Europe and MOBILE6 from the US.(Andr éand Rapone, 2009; EPA, 2003). The common macro-level modelling approach used to produce a mobile source emission inventory is based on two processing steps. The first step consists of determining a set of emission factors that specify the rate at which emissions are generated, and the second step is to produce an estimate of vehicle activity. The emission inventory is then calculated by multiplying the results of these two steps together. This methodology has two major shortcomings, namely:

- ***Inaccurate characterisation of traffic activities; and***
- ***Emissions factors which may not represent actual conditions adequately.***

At the lowest level of the hierarchy, microscopic transportation models typically produce second-by-second vehicle trajectories (location, speed and acceleration). Driving cycles used for vehicle emission testing are also specified on a second-by-second speed-time profile. Microscopic models should be integrated with real time emission prediction models which are able to utilise high resolution transportation modelling results, thereby generating potentially more precise emission estimates. Several commercial micro-simulation traffic packages are widely used to estimate emissions (TSS, 2010).There have been a number of modelling approaches at the micro-level proposed to estimate future vehicle emissions in conjunction with the outputs of transport models. One such approach is the use of engine power as the main predictive basis. Another is the use of vehicle speed and acceleration as predictive variables. There are three main types of modelling approaches, namely: power-based, speed-based, and hybrid models, shown in Table 3.1 (Zhu and Ferreira, 2012b). The instantaneous traffic emissions model, a speed-based approach which utilises the micro-simulation result as an input, was found to have merit based on the evaluation results. New models are put forward in Chapter 5, based on the structure of existing models reviewed earlier. The new approach uses a GA to optimise the combination of explanatory variables, in terms of accuracy and robustness.

4.3 Uncertainty analysis

The degree of confidence obtained from model results is the conventional definition for modelling uncertainty by Klauer and Brown, (2004). According to Walker et al (2003), the main uncertainty sources for environmental modelling can be characterized as:

- Input uncertainty: In terms of external driving factors and system data that are input into the model, such as predicted speeds and accelerations in the case of emission modelling.
- Model structure errors: the conceptual uncertainty due to incomplete understanding and simplified descriptions of modelled processes as compared to observed data.
- Parameter uncertainty: the inaccurate parameters calibration leads to a downgrade of output solution.

In the current research, parameter uncertainty has been minimised by the use of locally derived data to calibrate the model. Hence, to quantify the overall modelling uncertainty, the analysis focuses on the effects of model structure errors; input data errors; and the interaction between the two. The modelling structure or specification errors can be estimated using residual analysis, by quantifying the differences between modelled results and measured emissions. Traffic micro-simulation consists of two distinct scenarios, namely, un-signalised traffic flow on motorway sections and at signalised intersections. The difficulty of motorway traffic simulation is due to the speed break-down, when vehicle numbers approach capacity. In contrast, there are two challenges posed by the simulation of queues at the micro-scale level for signalised intersections, namely: the acceleration profile of the leading vehicle in the queue (Li et al., 2004); and the headway of the following vehicles (Jin et al., 2009). The quantification of input data errors is presented in detail in Appendix A and an overview of the approach is presented in Chapter 6.

4.3.1 Uncertainty of un-signalised traffic flow

Limited research has been undertaken on the validation of motorway traffic flow simulation, in terms of the gap between prediction and measurement for vehicle speeds for each modelled time period. The performance of these types of models, with respect to their ability to predict average speeds and traffic volumes, is dependent on several external and internal factors. This chapter focuses on uncertainty induced by internal factors in the form of the driver behaviour model used. Theoretically, micro-simulation has two core algorithms, namely: car-following and lane-changing, which are the main drivers of overall model accuracy. Panwai and Dia (2005) undertook a comparative evaluation of car-following behaviour in a number of traffic simulation models to validate their reliability. The results point to similar performance for the psychophysical spacing models used in VISSIM and PARAMICS with better performance reported for the Gipps-based models implemented. Hidas (2006) confirms the findings and points out that lane-changing behaviour is a challenge for prediction accuracy. In most models, lane-changing behaviour requires two stages, namely: consideration of lane-changing and execution. The improvement of lane-changing may be facilitated in two major directions: an increase in the level of detail in the specification of models to better capture the complexity and sophistication of human decision-making processes; and an improvement in the quality of data used to calibrate these models (Toledo,

2007). Zhu and Ferreira (2012a) have assessed model output uncertainty for varied traffic flow conditions. Chapter 6 provides a detailed account of that analysis.

4.3.2 Signalised traffic flow at intersection

Insufficient research has been documented on the leading vehicle acceleration behaviour at intersections. Generally, an assumption of constant acceleration is implemented by most micro-simulation packages. The deceleration and acceleration behaviour at intersections affects the emission intensity significantly (Minoura et al., 2009). On the other hand, Wang et al. (2004) have assumed that drivers normally accelerate with a polynomial decreasing relationship with speed. Long (2000) has concluded that linearly decreasing acceleration rates better represent both maximum vehicle acceleration capabilities and actual motorist behaviour.

The initial and primary challenge is data collection, since high-resolution and accurate-positioned vehicle trajectory datasets are difficult to obtain in practice. Currently, there are two ways to collect trajectory data, namely, vehicle-mounted GPS and feature-capture camera (Gordon et al., 2012). The data accuracy of both methods is subject to weather and surrounding environments, with downgrading reliability of the leading vehicle's acceleration behaviour. The issue is significant for both traffic simulation and modelling of vehicle fuel consumption and emissions, which rely on the acceleration characteristics of vehicles starting from idling. The major proportion of vehicle emissions occurs at the intersection approaches, due to the final acceleration to cruising speed and to the stop-and-go cycles (EPA, 2003). Through the evaluation of a driving simulator dataset, an analysis of the acceleration profile of the leading vehicle was undertaken to improve the vehicle trajectory prediction. The results of that analysis are shown in Appendix B.

4.4 Interactions between model development and uncertainty analysis

This thesis defines the modelling robustness as the degree of modelling accuracy able to withstand input uncertainties. There are two main types of errors associated with emission forecasts which rely on transport models outputs, namely input data errors and emission model specification errors. The former have to do with uncertainty in forecasts of vehicle movement data, such as instantaneous speed and acceleration. Input data related uncertainty shows very different characteristics for different traffic flow conditions (Zhu and Ferreira, 2012a). Specification errors are due to the fact that the models cannot account for emission behaviour in a precise manner. An important issue is the trade-off between model specification accuracy and input data accuracy. As model complexity increases, more variables are needed and the input related errors increases. "The latter may negate the increased accuracy derived from an improved model specification" (Smit et al., 2009). Therefore, there is an optimum level of modelling detail for a certain application. This optimum is highlighted in Figure 4.3, which shows graphically the relationship between model complexity, input data errors and model specification errors. Besides CO_2, current modelling of gaseous pollutants (CO HC NO_x) is to the left of the optimum level, with more

significant modelling specification errors, while CO_2 modelling is to the right of the optimum level.

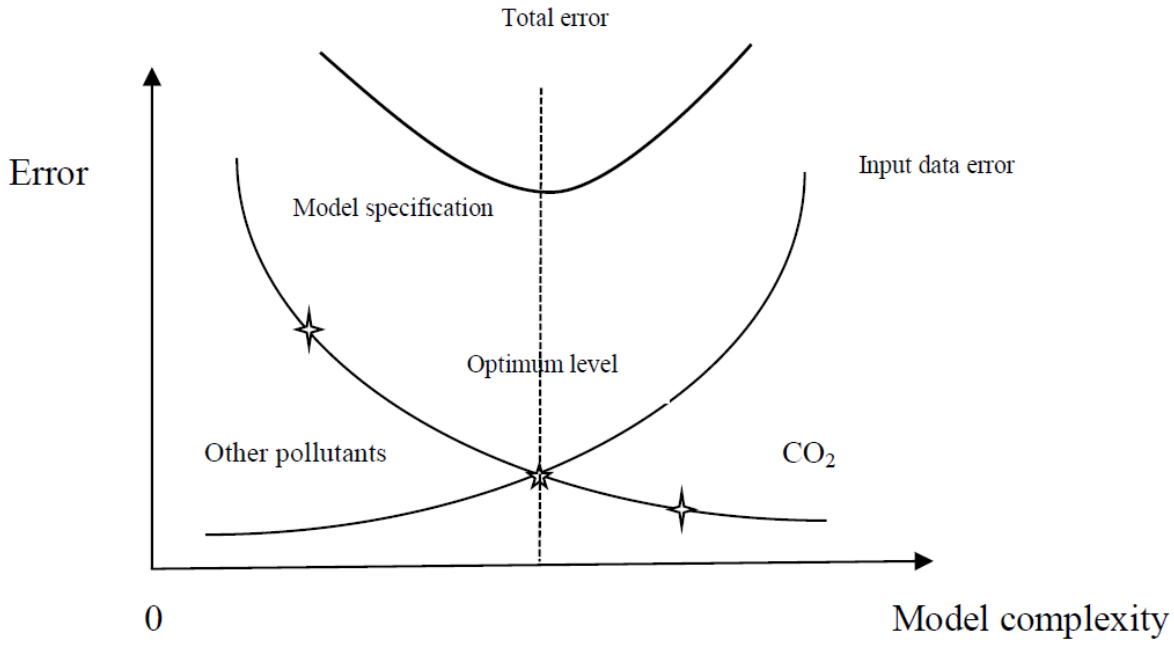

Figure 4.3 Model complexity and errors

The reliability of emission prediction relies on two factors, namely accuracy and robustness. On one hand, the modelling accuracy can be improved by more complex modelling formulations. On the other hand, the robustness of model complexity tends to be negated by the increasing input errors. The analysis of emission uncertainties will be introduced in Chapter 6. The results of uncertainty analysis evaluate the overall performance with regard to input errors and specification errors. Specifically, Figure 4.4 demonstrates how model development and uncertainty analysis interact as both cause and effect.

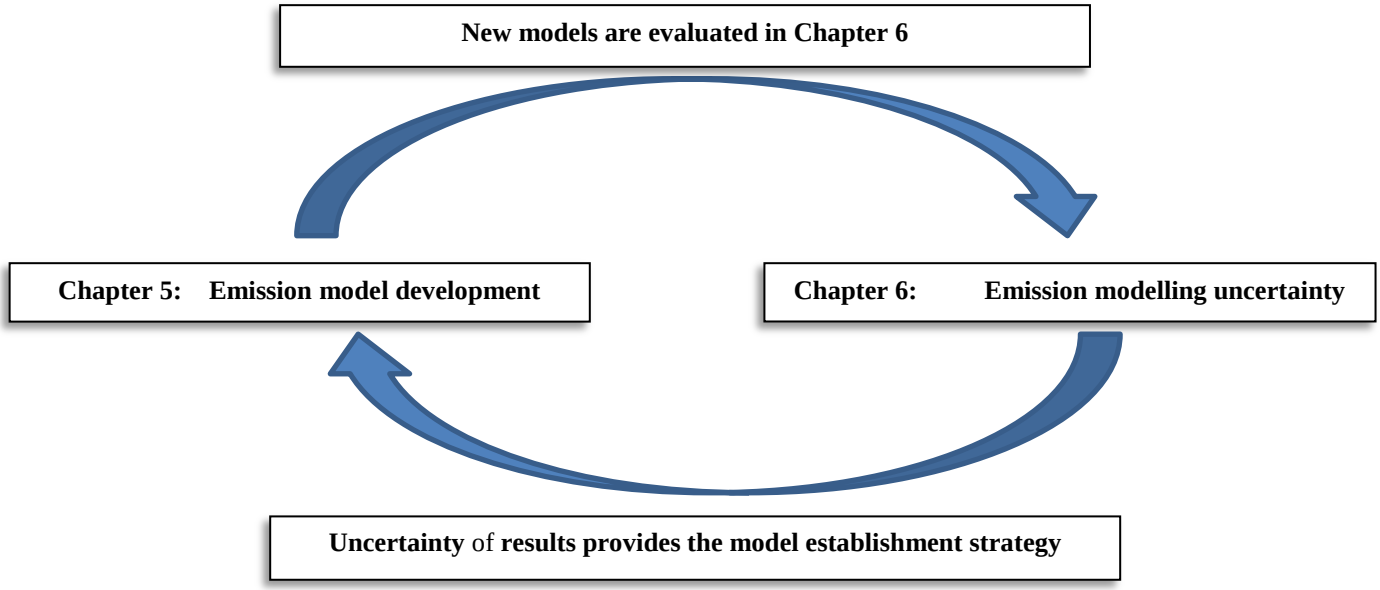

Figure 4.4 Interactions between modelling development and uncertainty analysis

4.5 Summary

To minimise the overall modelling uncertainty, emission modelling has to take the input uncertainties into consideration. This is especially so for the case of CO_2 modelling. For the other gaseous pollutants, namely, CO, HC and NO_x, the priority is to improve the modelling accuracy. Therefore, Chapters 5 and 6 address the two main areas, namely:

(1) Model development

A new emission model using GA to select its main variables will be discussed in detail in Chapter 5.

(2) Uncertainty analysis

Both existing emissions models and the proposed new models were evaluated using a new methodology based on the Monte Carlo simulation. Chapter 6 puts forward an evaluation, which deals with both data inputs and specification errors.

Chapter 5. A Proposed New Emissions Model

5.1 Introduction

There is a need to match emission estimations accuracy with the outputs of transport models. The overall error rate in long-term traffic forecasts resulting from strategic transport models is likely to be significant. Micro-simulation models, whilst of high-resolution in nature, may have similar measurement errors if they use the outputs of strategic models to obtain traffic demand predictions. This chapter discusses the limitations of existing emissions micro-level estimation approaches. Emissions models for predicting emission pollutants other than CO_2 are proposed. A GA approach is adopted to select the predicting variables for the new model. The approach is capable of solving combinatorial optimisation problems. Overall, the emission prediction results reveal that the proposed new models outperform conventional equations in terms of accuracy and robustness.

There are three main types of modelling approaches, namely; power-based, speed-based, and hybrid models. Two models from each category, as shown in Chapter 3, have been analysed (Zhu and Ferreira, 2012b). It was found that power-based models have some significant shortcomings and their use is not consistent with the finding that there are significant variations in emissions for small changes in vehicle power. The results from speed-based models highlight the need to model acceleration, deceleration and cruising stages of the urban cycle separately. The instantaneous traffic emissions model, a speed-based approach which utilises the micro-transportation simulation result as an input, was found to have merits based on the evaluation results. More complex models, whilst theoretically more desirable, may mean additional input measurement errors, such that the overall effect may not yield more accurate estimates (Smit et al., 2009).

The instantaneous traffic emissions model developed by Int Panis et al. (2006b) has been adopted by the AIMSUN traffic simulation model (TSS, 2010). The model, shown in Equation 5.1, has been reviewed and its merits mentioned in Chapter 3.

$$E_n(t) = \max\left[E_o, f_1 + f_2V_n(\mathrm{i}) + f_3V_n(i)^2 + f_4A_n(i) + f_5A_n(i)^2 + f_6V_n(i)A_n(i)\right]$$-----Equation 5.1

Where:

$E_0\ (i)$ = a lower limit of emission (g/s) specified for each vehicle and pollutant type;

$V_n\ (i)$ = instantaneous speed of vehicle n at time i;

$A_n\ (i)$ = acceleration of vehicle n at time i;

f_1 *to* f_6 = emission constants specific for each vehicle and pollutant type determined by regression analysis.

5.2 Data sources, selection and validation

The data used for analysis in the current chapter were extracted from the NISE2 dataset (Orbital, 2009), which was developed using a petrol CUEDC. The cycle is established to represent daily driving behaviours by the Markov process. The emission rates for CO_2, CO, HC and NO_x of the test-bed vehicles from the NISE2 fleet, which travels on the composite urban driving cycle (CUEDC), were recorded second-by-second in addition to the instantaneous speed. Prior to analysis, the integrity of the emission measurements from NISE2 was reconfirmed and corrected to enhance the reliability of the instantaneous emissions using the method followed by Smit et al. (2010). In addition, cold start affected datasets were filtered prior to analysis by adopting an approach recommended by Favez et al. (2009). Table 3.2 demonstrates a composite car, consisting of eight average-aged passenger vehicles shortlisted from the NISE database (which had travelled approximately 50,000-100,000 km each).

5.3 Development of emissions models

The current chapter proposes a methodology to improve those results. The concept is briefly described below. Based on the reviews in Chapter 3, microscopic models use a combination of instantaneous velocity and acceleration to predict various gaseous pollutants including HC and CO. The latter are primarily formed during in-cylinder combustion processes depending on many factors such as air-fuel ratio, cylinder temperature and pressure, and engine speed (Heywood, 1988). The formation of HC and CO rises in a rich fuel environment. Thus, the fact of high correlation between CO_2 emission rate and fuel consumption was taken into account in the modelling of these gaseous pollutants. In addition, vehicle acceleration or deceleration leads to substantial change in fuel injection per combustion cycle. The change in air-fuel ratio forces the engine to adapt to a new equilibrium and tends to lead to a transient variation in pollutant formation (North et al., 2006). This effect may be compounded by dynamic effects in the catalyst and exhaust system, such as catalyst malfunctioning, which can cause a sudden increase of the pollutant emissions. For these reasons, modelling of HC and CO, as the products of incomplete fuel combustion, should take the time-lag effect described above into consideration. Hence, several lag variables (i.e., variables at previous time steps of *i-1*, *i-2*, *i-3* or *i-4* seconds) of the time-lag effect are introduced into the models as predicting variables.

A range of variables for the instantaneous and lag velocity, acceleration and CO_2 emission rate were selected and tested:

$$[B_0 \quad V_i \quad A_i \quad V_i^2 \quad A_i^2 \quad V_iA_i \quad V_i^3 \quad A_i^3 \quad V_iA_i^2 \quad V_i^2A_i$$
$$V_{i-1} \quad V_{i-2} \quad V_{i-3} \quad V_{i-4} \quad A_{i-1} \quad A_{i-2} \quad A_{i-3} \quad A_{i-4} \quad Rate\_CO2_i$$
$$Rate\_CO2_{i-1} \quad Rate\_CO2_{i-2} \quad Rate\_CO2_{i-3} \quad Rate\_CO2_{i-4}\ ]$$

Where:

B_0 = constant;

V_i = velocity at time i;

A_i = acceleration at time i;

$Rate\_CO2_i$ = CO_2 emission rate at time i.

A total of 23 candidate variables were identified. An exhaustive enumeration method is not a practical alternative, while step-wise and stage-wise regression procedures produce only local optimum solutions (Chatterjee et al., 1996). The solution to such a combinatorial optimisation problem can be obtained by using an enumerative technique such as GA. GA is a stochastic search process that mimics the natural process of 'survival of the fittest' through the manipulation of a population of chromosomes (possible solutions) (Vladisavljevic et al., 2007). As a result, the elite individual solution is a balanced one with high accuracy and consisting of strong statistically related variables. The GA programme was compiled using Matlab 7.9. A selective weighted fitness for the GA, Equation 5.2, was used to implement an automated variables selection procedure to build the calibration models based on least-square regression.

$$Fitness_i = \frac{1}{\sqrt{\frac{\sum_1^N (P_i - O_i)^2}{N}}} \qquad \text{-------Equation5. 2}$$

Where

$$P_i = \sum \alpha_i \beta_i Variable_i$$

P_i = estimated instantaneous emission rate at time i;

O_i = observed instantaneous emission rate at time i;

α_i = binary logic control parameter after regression analysis;

$$\alpha_i = \begin{cases} 1 \quad if \quad P - value < 0.05 \quad this\ variable\ is\ included \\ 0 \quad Otherwise \end{cases}$$

β_i = coefficient derived from regression analysis;

N = number of observations.

P_i is the prediction of emission rate as a product of selected coefficients and the corresponding candidate variables whose *p-value* of the t-statistical analysis is lower than 0.05. The reciprocal relationship of root-mean-square error enables the accurate prediction of solutions with high fitness values.

Figure 5.1 shows the flow chart of the GA application. Firstly, chromosomes that represent feasible solutions of a non-linear optimisation problem are randomly generated to form the initial population following the fitness test (Equation 5.2). Each chromosome symbolises a potential solution to the emission modelling problem. Figure 5.2 demonstrates an example of an individual chromosome consisting of 23 bits. Each bit represents a corresponding variable in the list of all potential variables. The dichotomous data on each bit are either 'included in the model' valued 1 or 'not included in the model' valued 0. The size of the solution is therefore 2^{23}. In determining the fitness value, the chromosome tends to take more variables for better prediction accuracy. This may include irrelevant candidate variables that undermine the robustness of the model. To avoid this happening, the calculation of the emission rate prediction, P_i, was limited to those statistically significant variables ($p < .05$). In order to achieve acceptable solutions, the calculations of the fitness values and selection of chromosomes continued. This procedure evolves through many generations by a natural genetic process. The genetic process includes three types of operation, namely, crossover, selection, and mutation (Mitchell, 1998). It repeats until the number of iterations exceeds a predefined limit. The number of chromosomes in a population and the number of iterations are set to 600 and 100, respectively.

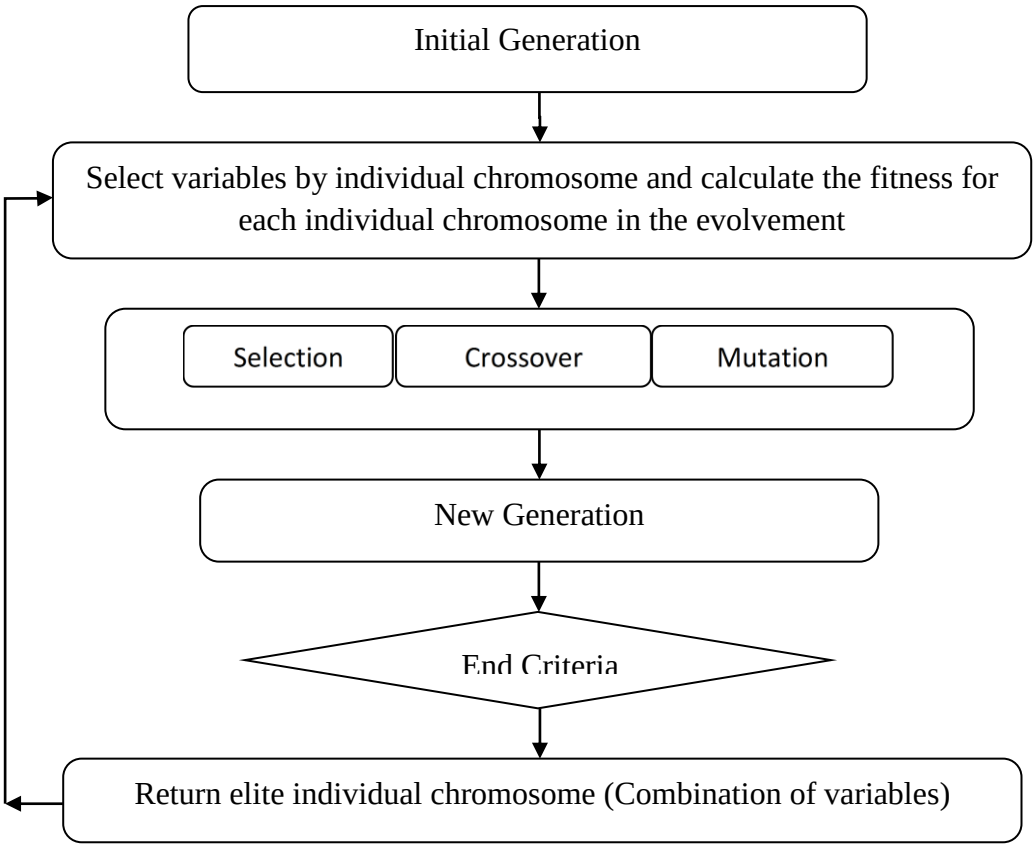

Figure 5.1 Flowchart of genetic algorithm

Figure 5.2 An individual chromosome

Figure 5.3 shows the maximum and averaged fitness reached over the iterations. The averaged fitness for each generation increases substantially at the beginning and reaches stability towards the end. These results indicate that the evolving chromosomes improve the accuracy of the solution until eventually a saturated condition is reached. Hence the elite chromosome can be justified as the optimal solution.

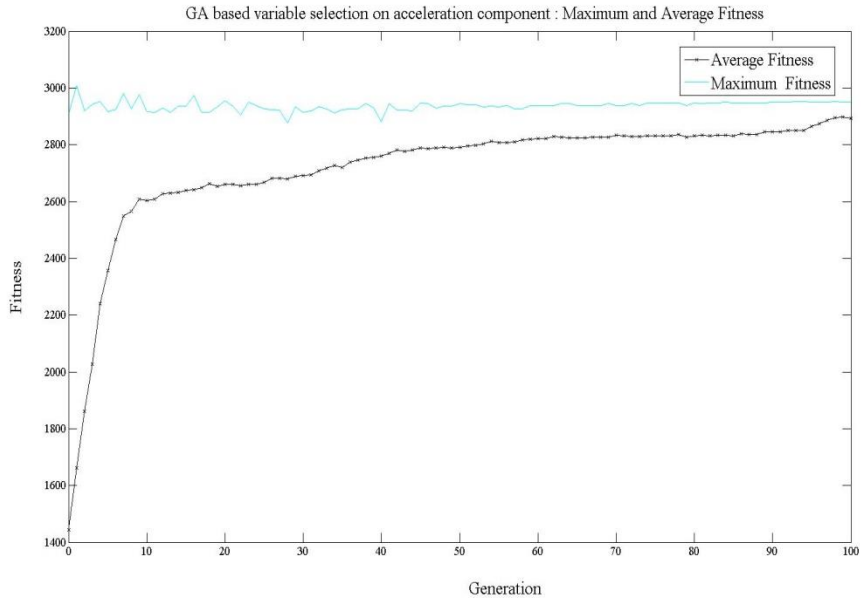

Figure 5.3 Maximum and averaged fitness over generations

5.4 Model development outcomes

5.4.1 General

The proposed GA approach was applied to the HC pollutant for different driving modes: namely, acceleration, cruising, and deceleration. The models for the emission rate, *Y*, from the ultimate chromosome are presented in Equations 5.3, 5.4 and 5.5, respectively. All the predicting variables selected are statistically significant at $p < .05$. Both the instantaneous traffic emissions model (Equation 5.1) and the newly modified equation parameters were calibrated by least square regression on the same test-bed dataset that was used to develop the new model. To conduct meaningful comparisons of modelling-induced error, the goodness of fit, R^2, for the three driving modes, between the newly modified model and the model (Equation 5.1) are shown in Table 5.1.

The proposed new approach significantly improved the modelling results for HC, although the prediction accuracy for the deceleration component was relatively low. The deceleration component accounts for 42% of total driving cycle duration, but the summation of HC deceleration component only takes up 25% of total cycle measurements. As a result, the deceleration component does not play an important role as a percentage of total emissions. Due to the multidimensionality of the solution search space, the GA method is not necessary to lead to a global optimum when formulated as an optimisation problem. Because size of chromes is limited, GA has a tendency to converge towards local optima rather than the global optimum. This means that it is not wise to sacrifice short-term fitness in order to gain longer-term fitness. To tackle this issue, the proposed GA methodology relies on the fitness function, which enables quantification of individual solution appropriateness in terms of the statistical significance of both model accuracy and shortlisted variables.

To test the fitness function, the size of the population was increased to 2,000 in order to enable more potential solutions to search in the multidimensional space; the results being similar to those previously presented. Moreover, taking the HC acceleration component as an example, the proposed new equation R^2 is slightly lower than the theoretical maximum value by which an individual chromosome includes all candidature variables. Hence, the new equation selected by the new algorithm is a close approximation to the global optimum.

Table 5.1: Results of model development – Goodness of fit, R^2

R^2	Driving Mode			
	Overall	Acceleration	Cruising	Deceleration
GA-based model	0.80	0.65	0.75	0.15
Equation5.1 model	0.69	0.47	0.60	0.08

$$Y = B_0 + B_1 A_i + B_2 V_i A_i + B_3 V_i^3 + B_4 V_i^2 A_i + B_5 V_{i-1} + B_6 Rate\_CO2_i + B_7 Rate\_CO2_{i-3}$$

------- Equation 5.3 (Acceleration component)

$$Y = B_0 + B_1 A_i + B_2 V_i^2 + B_3 V_i A_i + B_4 V_i^3 + B_5 V_i^2 A_i + B_6 V_{i-2} + B_7 V_{i-4} + B_8 Rate\_CO2_i + B_9 Rate\_CO2_{i-1} + B_{10} Rate\_CO2_{i-3}$$

------- Equation 5.4 (Cruising component)

$$Y = B_0 + B_1 V_i + B_2 V_i^2 + B_3 V_i^3 + B_4 V_i A_i^2 + B_5 A_{i-3}$$

------- Equation 5.5 (Deceleration component)

Where:

Y = emission rate (g/s) for each vehicle and pollutant type;

V_i = velocity at time i;

A_i = acceleration at time i;

$Rate\_CO2_i$ = CO_2 emission rate at time i;

B_1 *to* B_n = emission coefficients for each vehicle and pollutant type.

The same experimental dataset was used to test the prediction accuracy of the model. Figure 5.4 shows the correlation between modelling predictions and HC measurements, and Figure 5.5 illustrates the corresponding residuals plots.

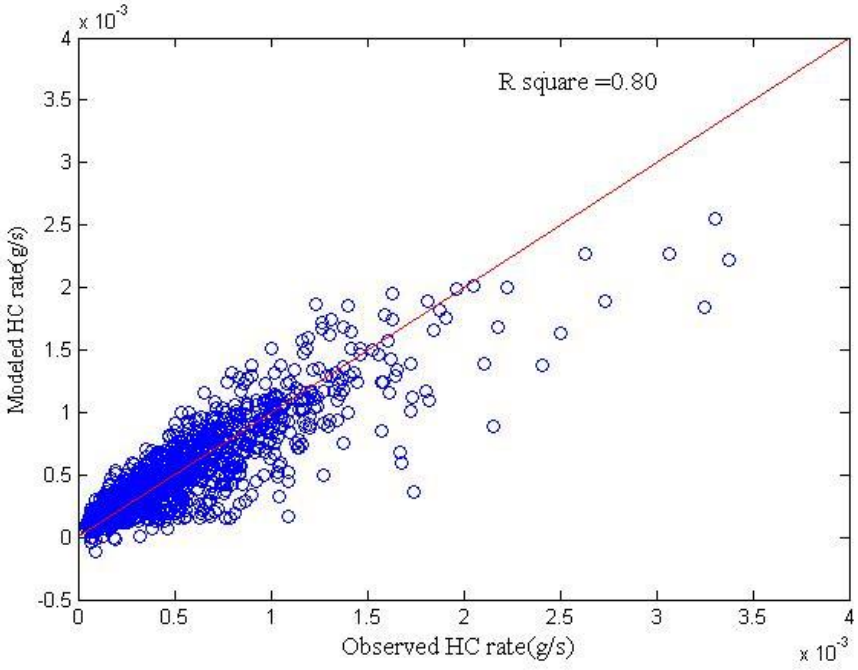

Figure 5.4 New model predicted vs. measured HC

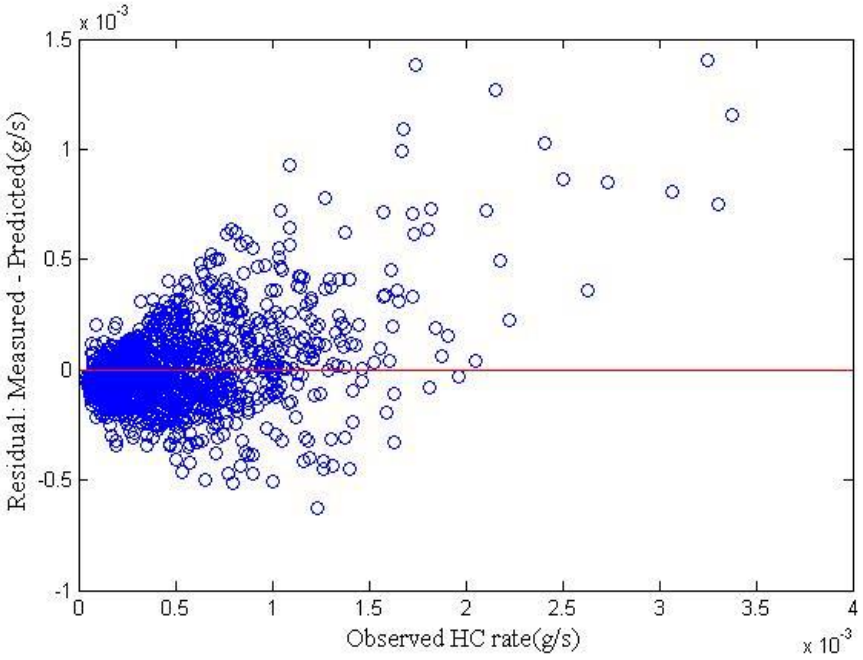

Figure 5.5 New model residuals

5.4.2 Validating the proposed models

The proposed new models were validated on different sets of data with various vehicle size and make for different age ranges, namely: new vehicles with mileages from 1,000-11,000km; middle-aged vehicles with mileages from 75,000-95,000km; and older vehicles with mileages from 130,000-140,000km.

Comparisons of the goodness of fit, R^2, of the overall modelling results for the three vehicle age ranges, between the proposed new models (summation of Equations 5.3 to 5.5) and the instantaneous traffic emissions model (Equation 5.1) are shown in Tables 5.2 (a) to (c), respectively. Overall, the emission prediction results show that the proposed new models provide improved results. The new models are more robust and accurate for HC prediction.

Table 5.2 HC Modelling validation, R^2

Table 5.2 (a): HC Modelling validation, R^2: (New vehicles)

	Vehicles				
	Civic	Getz	Yaris	Tiida	Corolla
GA-based model	0.37	0.77	0.54	0.45	0.41
Equation5.1 model	0.28	0.70	0.45	0.34	0.31

Table 5.2 (b): HC Modelling validation, R^2 (Middle-aged vehicles)

	Vehicles							
	323	Echo	Vectra	323	Camry	Tarago	Pulsar	Commodore
GA-based model	0.68	0.59	0.84	0.51	0.82	0.80	0.41	0.84
Equation 5.1 model	0.61	0.55	0.79	0.44	0.80	0.72	0.38	0.80

Table 5.2 (c): HC Modelling validation, R^2 (Older vehicles)

	Vehicles						
	Festiva	Lancer	Astra	Civic	Astra	Lancer	Pulsar
GA-based model	0.69	0.74	0.61	0.23	0.79	0.85	0.62
Equation5.1 model	0.56	0.69	0.53	0.16	0.67	0.82	0.27

The proposed methodology was also applied to other pollutants, including CO and NO_x. The new CO emission prediction equations for acceleration, cruising, and deceleration components, are shown in Equations 5.6, 5.7 and 5.8, respectively. The overall R^2 for the entire test-bed dataset is 0.70. In Table 5.3, the modelling results using the proposed new models (summation of Equations 5.6 to 5.8) and the instantaneous traffic emissions model (Equation 5.1) are compared for the same vehicle fleet demonstrated in Table 3.2.

$$Y = B_0 + B_1 V_i^2 + B_2 V_i^3 + B_3 V_i\ A_i^2\ + B_4 V_i^2 A_i\ + B_5 V_{i-2} + B_6 Rate\_CO2_i + B_7 Rate\_CO2_{i-4}$$

------- Equation 5.6 （Acceleration）

$$Y = B_0 + B_1 A_i\ + B_2 V_i^2 + B_3 V_i\ A_i\ + B_4 V_i^3 + B_5 V_i^2 A_i\ + B_6 V_{i-1} + B_7 A_{i-2} +$$

$$B_8 Rate\_CO2_i + B_9 Rate\_CO2_{i-1} + B_{10} Rate\_CO2_{i-3}$$

------ Equation 5.7 （Cruising）

$$Y = B_0 + B_1 V_i^2 A_i + B_2 Rate\_CO2_{i-4}$$

------- Equation 5.8 （Deceleration）

Table 5.3 CO Modelling validation, R^2

Table 5.3 (a): CO Modelling validation, R^2: (New vehicles)

Vehicles					
	Civic	Getz	Yaris	Tiida	Corolla
Modified model	0.39	0.77	0.54	0.43	0.41
Original model	0.21	0.39	0.36	0.20	0.18

Table 5.3 (b): CO Modelling validation, R^2 (Middle-aged vehicles)

Vehicles								
	323	Echo	Vectra	323	Camry	Tarago	Pulsar	Commodore
Modified model	0.68	0.60	0.84	0.53	0.82	0.80	0.41	0.84
Original model	0.44	0.36	0.43	0.28	0.58	0.24	0.37	0.51

Table 5.3 (c): CO Modelling validation, R^2 (Older vehicles)

Vehicles							
	Festiva	Lancer	Astra	Civic	Astra	Lancer	Pulsar
Modified model	0.66	0.74	0.60	0.22	0.79	0.85	0.61
Original model	0.58	0.28	0.16	0.13	0.27	0.29	0.13

New NO_x emission prediction equations for acceleration, cruising, and deceleration components are shown in Equations 5.9, 5.10 and 5.11, respectively. The overall R^2 for the entire test-bed dataset is 0.82. Table 5.4 shows the modelling results using the proposed new models (summation of Equations 5.9 to 5.11) and the instantaneous traffic emissions model (*Equation 5.1*) are compared for the same fleet, demonstrated in Table 3.2.

$$Y = B_0 + B_1 V_i^2 + B_2 V_i^3 + B_3 A_i^3 + B_4 V_i\ A_i^2 + B_5 V_i^2 A_i + B_6 A_{i-2} +$$

$$B_7 Rate\_CO2_i + B_8 Rate\_CO2_{i-2} + B_9 Rate\_CO2_{i-3}$$

------- Equation 5.9

$$Y = B_0 + B_1 V_i + B_2 A_i + B_3 A_i^2 + B_4 V_i A_i + B_5 A_i^3 + B_6 V_i A_i^2 + B_7 V_i^2 A_i + B_8 V_{i-4} + B_9 A_{i-4}$$
$$+ B_{10} Rate\_CO2_i + B_{11} Rate\_CO2_{i-1} + B_{12} Rate\_CO2_{i-2} + B_{13} Rate\_CO2_{i-3}$$

------- Equation 5.10

$$Y = B_0 + B_1 V_i A_i\ + B_2 A_{i-4} + B_3 Rate\_CO2_{i-4}$$

------- Equation 5.11

Table 5.4 NO_x Modelling validation, R^2

Table 5.4 (a): NO_x Modelling validation, R^2: (New vehicles)

Vehicles					
	Civic	Getz	Yaris	Tiida	Corolla
Modified model	0.39	0.71	0.51	0.43	0.36
Original model	0.11	0.31	0.18	0.20	0.08

Table 5.4 (b): NO_x Modelling validation, R^2 (Middle-aged vehicles)

Vehicles								
	323	Echo	Vectra	323	Camry	Tarago	Pulsar	Commodore
Modified model	0.66	0.54	0.84	0.53	0.82	0.80	0.41	0.83
Original model	0.52	0.14	0.55	0.26	0.34	0.26	0.41	0.56

Table 5.4 (c): NO_x Modelling validation, R^2 (Older vehicles)

Vehicles							
	Festiva	Lancer	Astra	Civic	Astra	Lancer	Pulsar
Modified model	0.70	0.74	0.61	0.29	0.79	0.83	0.58
Original model	0.71	0.44	0.15	0.44	0.15	0.76	0.32

5.5 Paralleled genetic algorithm

Cantú-Paz (1998)classified parallel GAs into three main types, namely:

- Global single-population master-slave GA
- Single-population fine-grained GA
- Multiple-population coarse grained GA

Single-population fine-grained GAs and multiple-population coarse grained GAs are suitable to tackle dynamic function optimisation problems (Luque, 2011). That approach has an important role in optimising complex functions whose optima vary in time (learning-like process). In a master-slave GA there is a single population, but the evaluation of fitness is distributed among several processors. Matlab enables the full functionality of the parallel language features by creating a special job on a pool of workers, and connecting the pool to the Matlab client (MathWorks, 2012). Distributed synchronous GA is based on distribution of the workload among processors during the fitness function evaluation phase followed by single central population regeneration. Hence, the massive fitness computations are assigned to workers in order to improve the computation efficiency.

5.6 Summary

Past research on modelling vehicle emissions other than CO_2 reveal relatively weak prediction results. The proposed methodology was applied to all NISE2 pollutants, including HC CO and NO_x. The current chapter proposes a GA-based methodology to determine the contributing variables, including lag ones, for predicting vehicle emissions. Except deceleration mode, the GA-based methodology deliver accurate modelling equation for each operation mode and each pollution. This method provides a new approach to the selection of a combination of variables among a large potential set. The applications of the new models show enhanced results for modelling vehicle emissions, supporting the new variable selection methodology using GA. The modified fitness function for the proposed GA demonstrates the ability to establish a balanced multivariate model. In addition, the improved HC prediction results – obtained by introducing 'historical' CO_2 emission rates – support the time-lag effect hypothesis. Compared with the theoretical maximum value of modelling fitness, the new modelling equation can deliver a goodness of fit result which is close to the global optimum. The proposed GA methodology offers a solution for a combinatorial optimisation problem, providing high modelling accuracy with statistically significant relationships between the selected predicting variables and the dependant variable.

Chapter 6. Framework to Quantify Errors in Micro-Scale Emissions Models

6.1 Introduction

Quantitative travel demand and emissions models are necessary for the environmental evaluation of future transport and land use options, as well as for the management of existing transport systems. This requires more accurate tools to quantify CO_2 and fuel consumption prediction uncertainty so that project evaluation can adequately address community expectations of prediction reliability. Moreover, there is a need to match the levels of uncertainty attached to estimates of emissions models with the uncertainties which are likely to be present in transport model outputs. The error analysis framework put forward in this chapter is aimed at the use of micro-simulation traffic flow models in conjunction with compatible emissions predictive relationships. Although the pollutant chosen to exemplify the framework is CO_2, the methodology may be applied to other pollutants.

There are two main types of errors associated with emission forecasts which rely on transport models outputs, namely input data errors and emission model specification errors. The former have to do with uncertainty in forecasts of vehicle travelling data, such as instantaneous speed and acceleration. Specification errors are due to the fact that the models cannot account for emission behaviour in a precise manner. An important issue is the trade-off between model specification accuracy and input data accuracy. Therefore, there is an optimum level of modelling detail for a certain application. This optimum is highlighted in Figure 4.2 Research methodology outline, which shows graphically the relationship between model complexity, input data errors and model specification errors.

This chapter is organised as follows. The next section outlines the Australian emissions dataset used in this analysis. This is followed by a discussion of the uncertainty quantification methodology. The subsequent sections provide the uncertainty analysis results; and final conclusions based on the results highlighted in the chapter.

6.2 Data sources and validation

6.2.1 Emission data and modelling

The data used for the analysis presented in this chapter were extracted from the NISE2 (Orbital, 2009) dataset. The instantaneous emission observations used the same composite vehicle as described in Chapters 3 and 5 and listed in Tables 3.3 and 5.1, which are similar to Australian vehicle fleet characteristics, in terms of mileage and age (ABS, 2009).

The instantaneous traffic emissions model has been adopted by the AIMSUN traffic simulation model (TSS, 2010). The model 5 is reviewed in Section 3.2.2.As discussed in section 4.5, in order to lower overall model error in the case of CO_2 modelling, it is necessary to focus on reducing input data errors, since the model is already well specified. In contrast,

the results point to more effort being needed to improve model specification for other pollutants.

$$E_n(t) = \max[E_0, f_1 + f_2 v_n(t) + f_3 v_n(t)^2 + f_4 a_n(t) + f_5 a_n(t)^2 + f_6 v_n(t) a_n(t)]$$

---Equation 6.1

Where:

$v_n(t)$ and $a_n(t)$ are the instantaneous speed and acceleration of vehicle n at time t; $E_0(t)$ is a lower limit of emission (g/s) specified for each vehicle and pollutant type; and f_1 to f_6 are emission constants specific for each vehicle and pollutant type determined by the regression analysis.

6.2.2 Traffic micro-simulation data

The uncertainty in the outputs of motorway micro-simulation was analysed by Zhu and Ferreira (2012a) (see the details in Appendix A). This was done by comparing predicted results with field average speed data obtained from motorway loop detectors at the 1-minute disaggregated level. The Queensland based traffic operations system records real time data by using 1-minute average speed measurements and other road section performance indicators, such as flow count and density (DTMR, 2010). In order to extract the speed information covering several traffic conditions, the datasets were collected in different sections in terms of distance to Brisbane CBD, in March 2012. They are shown in Figure 6.1. A detailed AIMSUN traffic micro-simulation model has recently been calibrated using data obtained from those loop detectors (Chung et al., 2011).

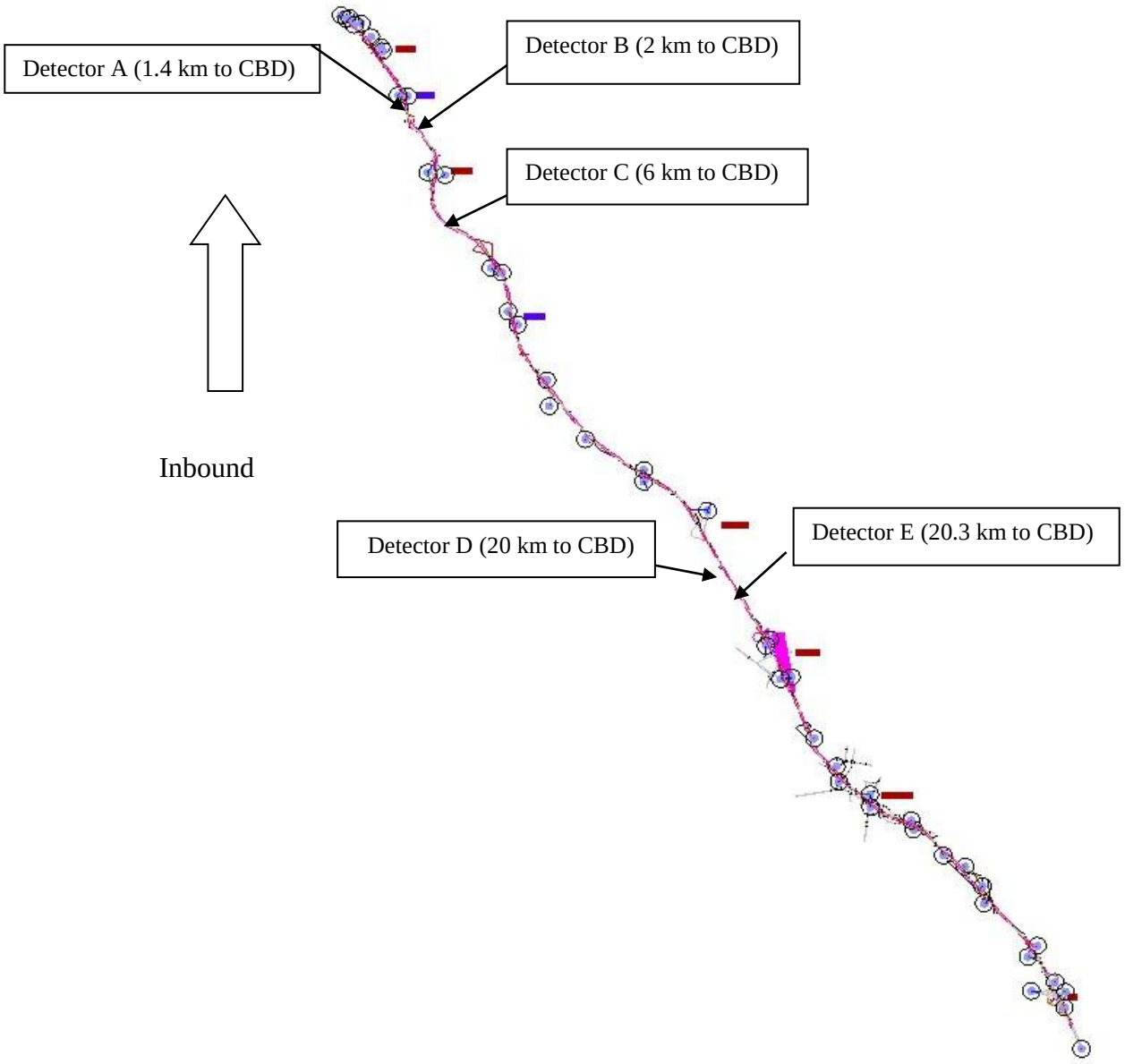

Figure 6.1 Pacific highway network map and selected detectors.

The Taguchi statistical method(Logothetis, 1988) was applied to three traffic flow stages to establish the relationships between modelled vehicle speeds and measured speeds, on a minute-by-minute basis. The results show close agreement between modelled and actual speeds under free flow conditions. In contrast, the transitional stage between free flow speeds and queuing shows a higher level of error. As traffic volumes increase, the quality of model outputs shows statistically significant negative correlation with average speeds and a negative exponential equation has been fitted. When volumes reach saturation levels, the flow break-down phenomenon leads to large model errors.

6.3 Uncertainty quantification methodology

6.3.1 Uncertainty definition

The degree of confidence obtained from model results is the conventional definition for modelling uncertainty Klauer and Brown (2004). According to Walker et al (2003), the main uncertainty sources for environmental modelling are:

- Input uncertainty: in terms of external driving factors and system data that are input into the model, such as predicted speeds and accelerations in case of CO_2 modelling.
- Model structure errors: the conceptual uncertainty due to incomplete understanding and simplified descriptions of modelled processes as compared to observed data.
- Parameter uncertainty: the inaccurate parameter calibration leads to a downgrade of output solution.

In the current analysis, parameter uncertainty has been minimised by the use of locally derived data to calibrate the model. Hence, to quantify the overall modelling uncertainty, the analysis focuses on the effects of model structure errors; input data errors; and the interaction between the two. The modelling structure or specification errors can be estimated using residual analysis, by quantifying the differences between modelled results and measured emissions. The quantification of input data errors is presented in a later section (see Appendix A).

Selection of Uncertainty assessment methodology

A review of environmental modelling uncertainty by Refsgaard et al. (2007), points to the use of error propagation relationships and Monte Carlo simulation as potential methodologies to quantify input data uncertainties for CO_2 modelling. Propagation equations are valid only if the following conditions are met:

(1) The uncertainties have Gaussian (normal) distributions;

(2) The uncertainties for non-linear models are relatively small; and

(3) The uncertainties have no significant covariance;

As will be demonstrated in this chapter, these requirements are not satisfied in the present investigation. In contrast, Monte Carlo simulation is a more robust approach, as it can simulate the structure of the distributions of model outputs. In its simplest form, this distribution is mapped by calculating the deterministic results for a large number of random

draws from the individual distribution functions of input data and parameters of the model (Gentle, 2003). The quality of Monte Carlo analysis relies on random number generator quality. The random samples used here in the Monte Carlo simulation were generated by Matlab functions. The reliability of the random number generator approach has been confirmed by Kroese et al., (2011). According to Muthén and Muthén (2002), the random sample size, another critical factor, should be no less than 10,000. Finally, the CO_2 uncertainties distribution, generated by the Monte Carlo method, should be able to be reproduced strictly in different simulation runs.

6.3.2 Input variables assumptions

In Equation 6.1, speed (v) and acceleration (a) are critical input variables for instantaneous emission modelling. Theoretically, the errors in each input variable need to be quantified by comparison between simulation outputs and field measurements at the disaggregated level. Such speed and acceleration data requires high-resolution instantaneous measurements at the individual vehicle level, which are too data-intensive to be available. High-resolution average speed errors can be considered as approximation to instantaneous values. Field surveys from a motorway in Brisbane, show that the errors between micro-simulation estimations and measured data, in terms of minute-by-minute average vehicle speed, follow a normal distribution for different traffic conditions. Based on data observed in a Brisbane section of motorway, the speeds estimated by a micro-simulation model (AIMSUN) show differences when compared to measured data for all but free flow traffic conditions. However, the trend of simulated average speeds is broadly consistent with loop detector measurements in the transition stage from free flow to queuing. Therefore, the simulated accelerations are assumed to be an unbiased estimation following a normal distribution with zero mean.

Sub-sets of data from the CUEDC were used to investigate driving behaviour under several scenarios. Table 6.1 shows the standard deviations and the correlation coefficients between speed and acceleration for each scenario. In order to undertake Monte Carlo simulation, it is important to evaluate the covariance among the input variables (EPA, 1997). Generally, disregarding the correlation between variables in a Monte Carlo simulation results in a dispersion of simulation output standard variance (Touran and Wiser, 1992). Hence, the correlation between acceleration and speed must be taken into considerations when evaluating different traffic conditions. In the CUEDC, the correlation coefficients between speed and acceleration show distinct differences for each level of acceleration, as shown in Table 6.1.

Table 6.1 Correlation Coefficient between Speed and Acceleration (CUEDC)

	Acceleration standard deviation (m/s^2)	Correlation coefficient
Acceleration component ($A>0.5m/s^2$)	0.41	-0.414
Cruising component ($-0.5m/s^2<A<0.5m/s^2$)	0.20	0.015
Deceleration component ($A<-0.5m/s^2$)	0.42	0.233
Congested phase (fourth phase of CUEDC)	0.70	0.10

In the case of correlated variables, random samples may be generated by the algorithm proposed by Touran and Wiser (1992) and shown below.

Generate Z ~ Normal distribution

Compute the Cholesky decomposition C such that $C^TC = \sum$

Set $X = C^TZ$

Where:

$\sum$: Covariance matrix of speed and acceleration

$Z = (Z_a\ Z_v)^T$. Z_v and Z_a are speed and acceleration vectors.

C is the lower triangle matrix of Cholesky decomposition.

X consists of correlated speed and acceleration vectors, following respective normal distribution.

In order to investigate the CO_2 modelling uncertainties under several vehicle speed conditions, the following four emissions scenarios were considered:

- Scenario 1: Free flow stage – speed error follows a normal distribution with zero mean; acceleration is assumed to be zero.

- Scenario 2(a): Acceleration stage – simulated speed has systematic error following a normal distribution, acceleration has significant correlation with speed.

- Scenario 2(b): Acceleration stage – simulated speed has systematic error following a normal distribution; the samples of acceleration are generated regardless of the correlation between speed and acceleration.

- Scenario 3: Congestion stage – simulated speed error follows a normal distribution; acceleration has some correlation with speed.

To quantify the input-induced uncertainties, two random samples have been generated, representing speed and acceleration as the inputs to Equation 6.1. The following Monte Carlo simulation method was used:

For i=1 to n

Generate X_i

Set $\delta_n = h(X_i) - \varphi$

Where:

X_i: Random samples;

$h(X_i)$: CO_2 model estimations using Equation 6.1, based on simulated traffic model outputs;

φ: CO_2 model estimations using Equation 6.1, based on predetermined traffic conditions;

δ: Input induced uncertainties.

6.4 Uncertainty quantification

6.4.1 Model input errors

Table 6.2 shows a summary of the data assumed for the error analysis presented here. This data, which is based on the results of field surveys (see Appendix A for details), includes assumptions about measured vehicle speeds and standard deviations, as well as the corresponding acceleration results, for each scenario modelled. The correlation between speed and acceleration is taken into consideration in Scenarios 2(a) and 3.

Table 6.2 Simulation Parameters for Different Stages

Variables	Scenario 1	Scenario 2(a)	Scenario 2(b)	Scenario 3
Vehicle speed	21 m/s	16 m/s	16 m/s	10 m/s
Speed standard deviation	1.31 m/s	2 m/s	2 m/s	1.47 m/s
Acceleration	0 m/s^2	1 m/s^2	1 m/s^2	0 m/s^2
Acceleration standard deviation	0 m/s^2	0.3 m/s^2	0.3 m/s^2	0 m/s^2
Simulated speed biases	0 m/s	4 m/s	4 m/s	0.7 m/s
Correlation coefficient (speed/acceleration)	NA	-0.414	NA	0.10

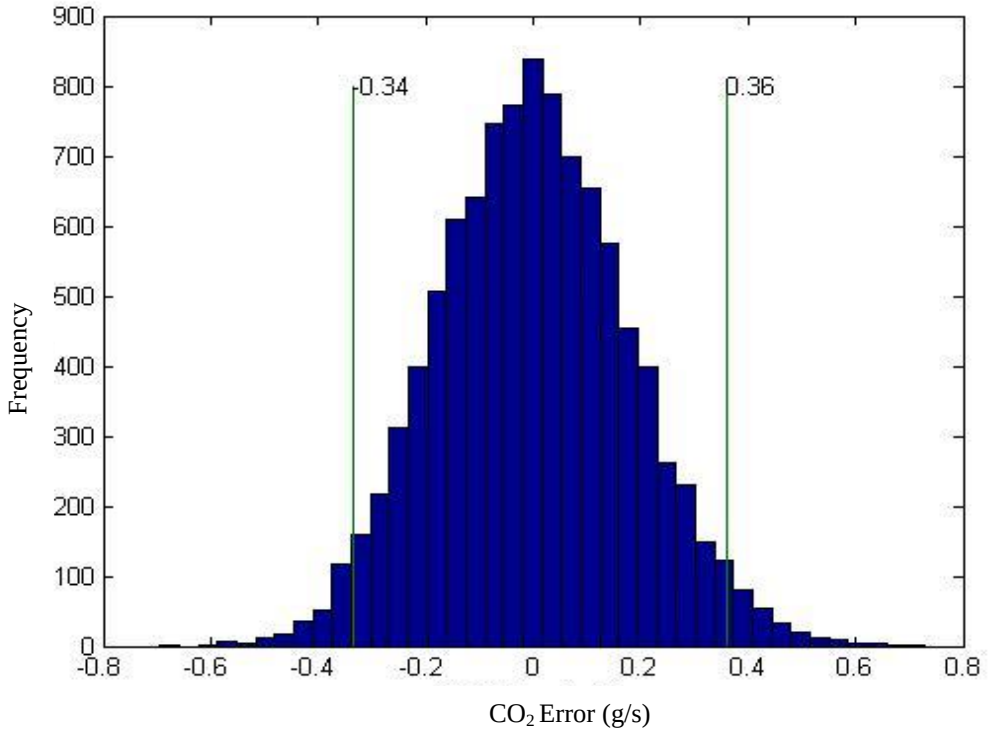

Figure 6.2 Error distributions – Free flow stage

Figure 6.2 shows a histogram of input data-induced uncertainties for the free flow stage. The range between the two vertical lines represents the 95% confidence area. The results confirm that the CO_2 estimation errors follow a normal distribution with zero mean, according to the Kolmogorov–Smirnov test.

Figure 6.3 (a) shows a histogram of input data-induced uncertainties in the acceleration stage, when there is correlation between speed and acceleration. The errors associated with the modelled speed and acceleration estimations lead to a distribution of CO_2 uncertainties, where the mean value is 1.3 g/s. The systematic errors from speed estimation result in higher values of uncertainty, compared with the results of free flow condition. The dataset of uncertainties follows a normal distribution, according to the *Kolmogorov–Smirnov test*. Figure 6.3 (b) shows a histogram of input induced uncertainties, when the correlation between speed and acceleration is ignored. The results highlight the difference between Scenario 2(a) and Scenario 2(b). The negative correlation between speed and acceleration reduces the occurrence of extreme estimation values, hence decreasing the overall error variation.

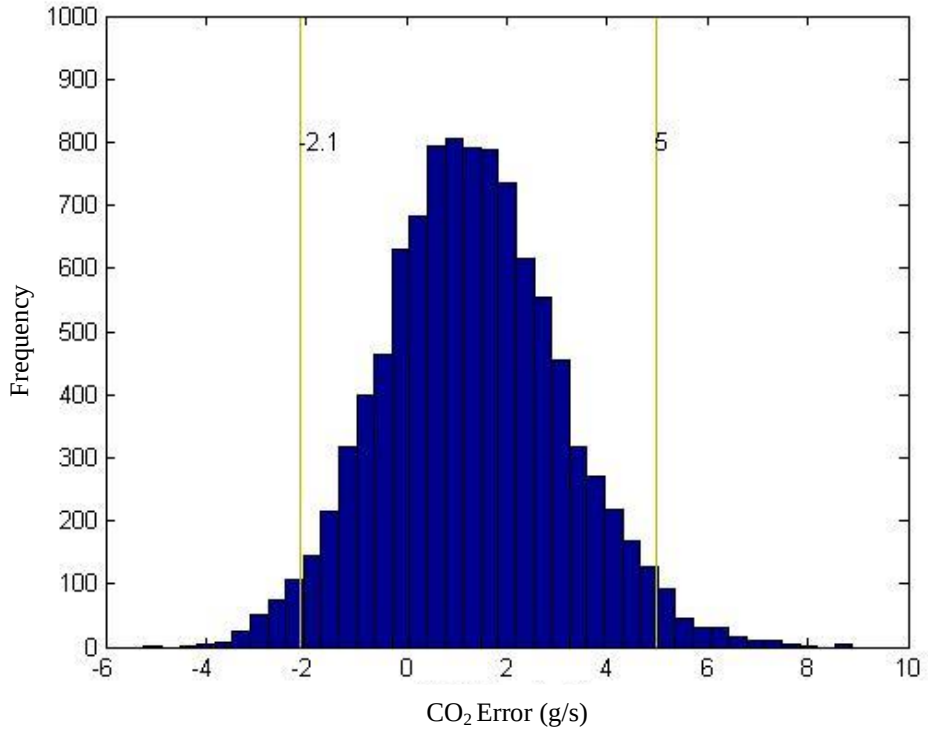

Figure 6.3 [a] Correlated variables,

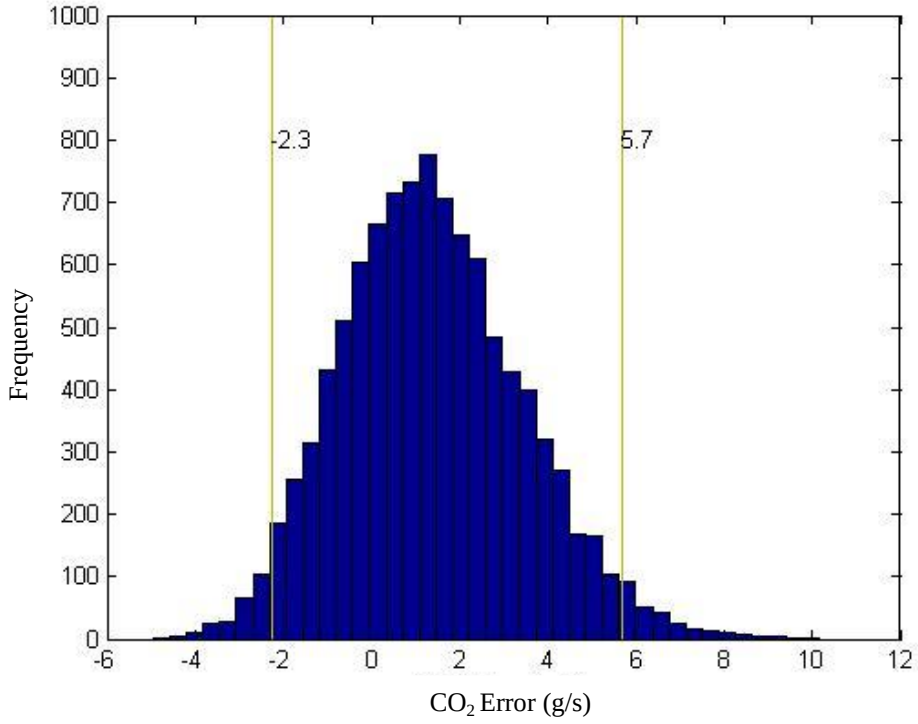

Figure 6.3 [b] uncorrelated variables

Figure6.3 Acceleration transitional stage error distribution

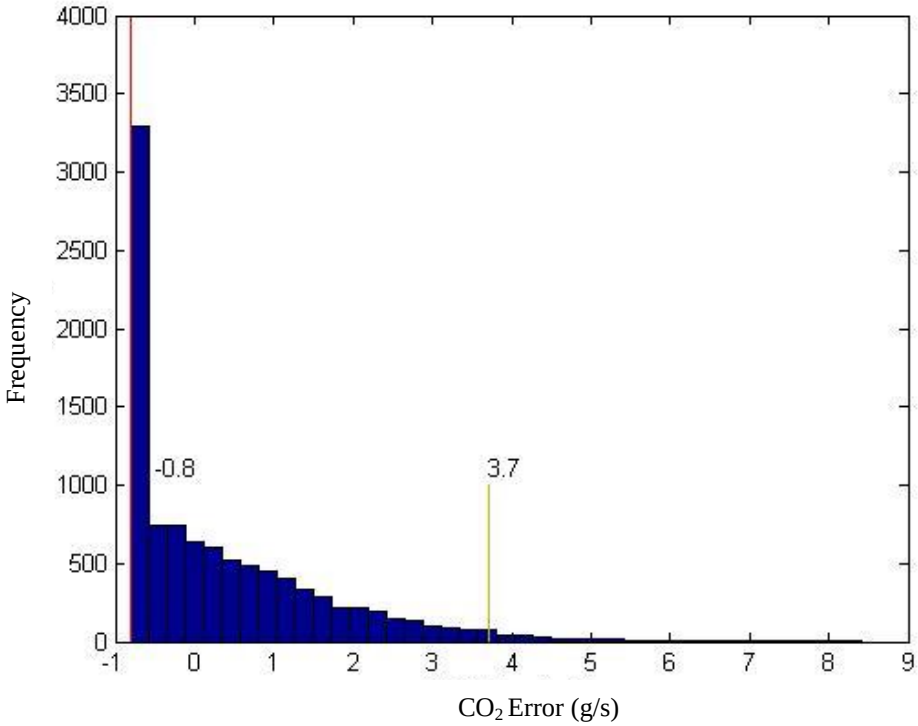

Figure6.4 Congested stage error distribution

Figure 6.4 shows a histogram of uncertainties for the congested stage. As discussed earlier, Equation 6.1 yields a low value of CO_2 estimates under congested traffic flow conditions. This leads to a large number of instances where the CO_2 estimation is set by Equation 6.1 to the minimum value. Hence, a large number of errors occur at low values, as shown in Figure 6.4. The latter also shows that the error distribution has a long tail due to the fact that the acceleration is assumed to have a higher standard deviation for congested conditions.

6.4.2 Quantifying model specification errors

The use of locally derived data using Australian vehicles in combination with Equation 6.1, has led to an improvement in the overall CO_2 model estimates. As a result, errors due to parameter estimation were reduced. The modelling residuals between estimations and observed data were assumed to be model induced errors. Several residual sub-sets were selected from the entire CUEDC, for each traffic scenario. The distributions of these residual sub-sets were difficult to test, due to the limited size of the sub-sample. The statistical properties of model specification error, as well as the corresponding input data errors, are shown in Table 6.3. The latter shows that the two types of errors are closely aligned for the case of free flow traffic conditions. This highlights that the combination of model specification and data input is close to optimal for those traffic conditions. On the other hand, other traffic flow conditions show that input data errors are significantly more important that model specification errors.

Table 6.3 Uncertainties Quantification Summary

	Input-induced		Model-induced	
	Mean (g/s)	Standard Deviation (g/s)	Mean (g/s)	Standard Deviation (g/s)
Free flow Stage	<0.01	0.18	0.08	0.34
Transitional Stage	1.30	1.80	-0.09	0.65
Congested Stage	0.38	1.32	<0.01	0.46

6.5 Summary

Vehicle CO_2 emissions have significant economic and environmental implications for transportation planning and policy, mainly through their impact on greenhouse gases. Sophisticated micro-level CO_2 emissions models have been developed with the aim of producing predictions with higher levels of accuracy. In order to quantify the likely level of uncertainty attached to such forecasts, an analysis of errors, which is seldom done in practice, needs to be undertaken. The two major sources of error are the deficiency inherent in the model structure itself and the uncertainty in the input data used. This chapter deals with both of these error types in relation to CO_2 emissions modelling.

Appendix A concludes that model uncertainty shows very different characteristics for different traffic flow conditions. Model output uncertainty shows distinctly different characteristics for different traffic flow conditions. The results show the close agreement between modelled and actual speeds under free flow conditions, the speed prediction uncertainties can be considered to follow zero-mean normal distribution (white noise). In contrast, the transitional stage between free flow and queuing shows a higher level of discrepancy. As traffic volumes increase, the quality of model outputs shows statistically significant negative correlation with average speeds. When volumes reach saturation levels, the flow break-down phenomenon leads to large model errors.

To estimate input data uncertainty effects, the chapter quantifies such effects for different traffic conditions using Monte Carlo simulation. Model structure induced uncertainties are also quantified by statistical analysis for a number of traffic scenarios. To arrive at an optimal CO_2 emission modelling outcome, the interaction between two components was taken into account. Since a more complex model does not necessarily yield higher overall accuracy, a compromise solution needed to be found. The results obtained here suggest that the CO_2 model used in the analysis, produces low overall uncertainty under free flow traffic conditions. However, when average traffic speeds approach congested conditions, there are significant errors associated with emission estimates.

This chapter focused on the quantification of errors associated with the outputs of un-signalised models on a micro-scale. In particular, the estimation of CO_2 emissions by such models was used as an example. The uncertainties likely to be present in the input data needed to calibrate the models, as well as the specification errors inherent in the models, have been discussed here. It was demonstrated that Monte Carlo simulation analysis could be used successfully to quantify model uncertainties for the outputs of the widely used AIMSUN micro-simulation model. For the signalised traffic, the feature of uncertainties associated with the outputs of micro-simulation model is fundamentally different, when compared with the un-signalised counterpart.

The common assumption in traffic simulation models is that of constant acceleration for the leading vehicle moving from a stationary position at an intersection. In contrast, Appendix B shows that assumption to be unrealistic, following the results of 40 drivers in a driving simulator experiment. The high-resolution data from the driving simulator show significant differences for acceleration behaviour between participants. Hence, typical acceleration profiles are necessary to replace the current constant acceleration assumption for micro-simulation models. The randomness of acceleration behaviour can be simulated by the Markov process. Therefore, the acceleration profile can be reconstructed using a Markov process and the corresponding statistical features of the acceleration operation. The new acceleration profile can play a pivotal role in emission estimation. The instantaneous emission modelling at an intersection is highly dependent on acceleration behaviours (Minocha, 2005; Pandian et al., 2009). Compared with other data collection methods used to establish the driving cycle (Lin and Niemeier, 2003), the high-resolution driving simulator data, including detailed acceleration/brake pedal movements, provides a more certain

operational state classification. This would deliver a more reliable simulation of vehicle trajectory and emissions profile. Appendix B provides a new methodology to build the speed/acceleration profile by 3-Dimension simulator data.

Chapter 7. Proposed New Model: Applications

The prediction of environmental impacts of local traffic management and transport planning measures is usually undertaken using the outputs of transport and traffic models, either at the strategic or the micro-level of detail. The accuracy of emissions predictions is, to a large extent, dependent on the errors associated with transport model outputs and on the accuracy of the emissions models themselves.

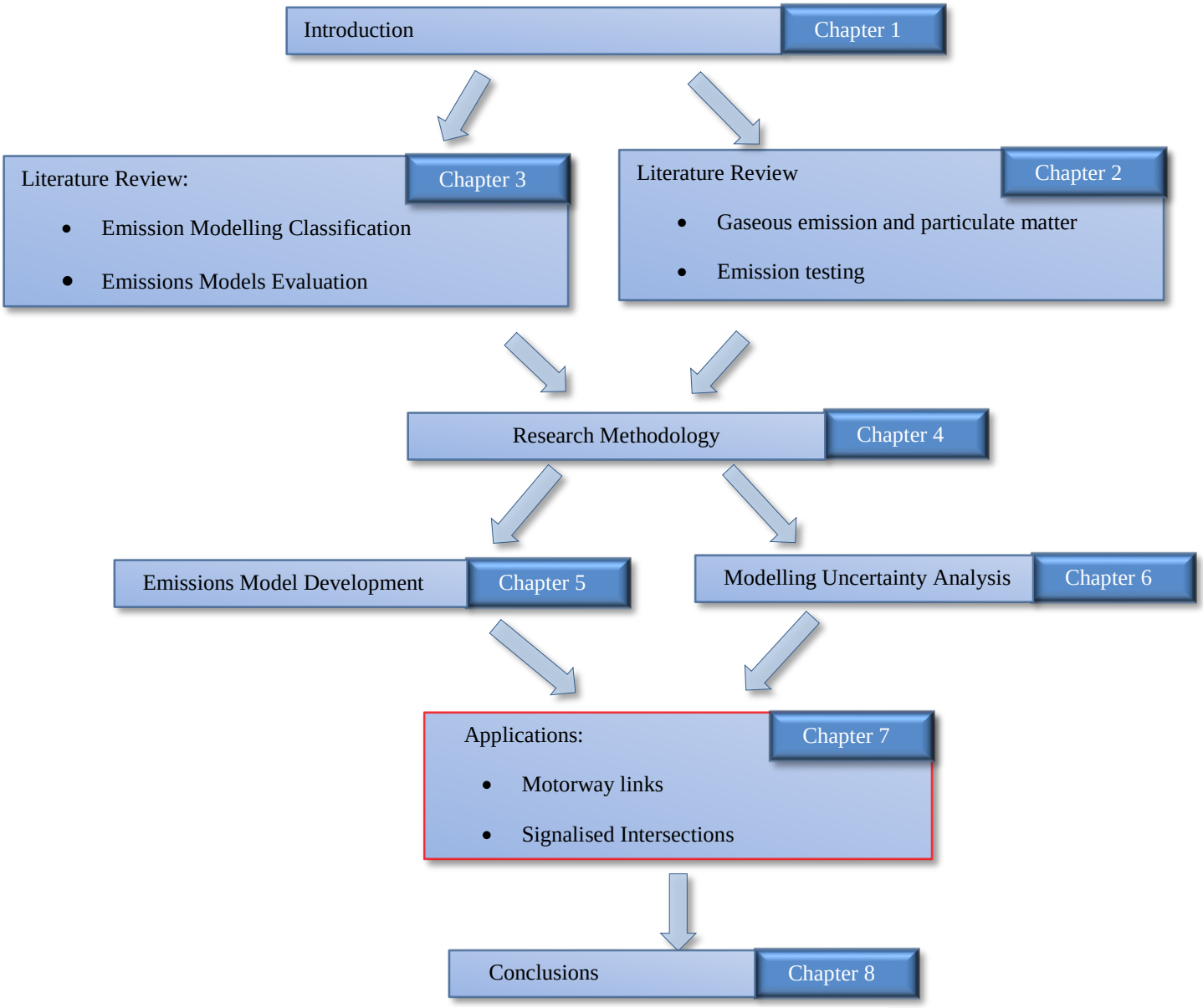

Figure 7.1 Thesis flow chart

Chapter 5 put forward a new approach to forecasting vehicle emissions using the outputs of micro-simulation traffic models and a set of emission equations based on the analysis of an Australian test dataset. In the current chapter the new model is applied to a case study in Brisbane. Using different scenarios for different road configurations and traffic conditions, the results of applying the new approach are compared with those obtained by using default emissions parameters commonly found in a simulation package. The results obtained suggest that the new approach produces low overall errors under several traffic conditions.

7.1 Introduction

Vehicle emissions have become a major source of gaseous emissions and fine particles (PM2.5) in major cities due to a rapid growth in the vehicle population. PM2.5 is responsible for harmful effects on human health. NO_x is another important pollutant which is also well known as a major precursor to photochemical formation of ozone (O_3).

Historically, car-following and traffic flow models have been developed using different theoretical bases. "This has given rise to two main kinds of models of traffic dynamics, namely: microscopic representations, based on the description of the individual behaviour of each vehicle; and macroscopic representations describing traffic as a continuous flow obeying global rules"(Toledo, 2007). Driving cycles used for vehicle emission testing are also specified on a second-by-second speed-time profile. Microscopic models should be integrated with real time emission prediction models which are able to utilise high resolution transportation modelling results, thereby generating potentially more precise emission estimates. Several commercial micro-simulation traffic packages are widely used to estimate the emissions (TSS, 2010). There have been a number of proposed modelling approaches at the micro-level to estimate future vehicle emissions in conjunction with the outputs of transport models.

Furthermore, an integration of emission modelling and dispersion can deliver an estimation of pollutant concentration, a more meaningful result for environmental protection. For example, a modelling system for predicting urban air pollution in the Helsinki metropolitan area integrates the EMME/2 strategic modelling package with a more comprehensive population activities model, which covers spatial and time distribution of population (Kousa et al., 2002).

To apply any emission model in a given area, the population exposures to air pollutants relies on the modelling of emission intensity and population activities. According to Kousa et al. (2002), exposure models have been classified by the modelling methodology of traffic emission and dispersion, namely, statistical, mathematical and stochastic. The stochastic approach attempts to include a treatment of the inherent uncertainties in the model, for

example, those caused by the turbulent nature of atmospheric flow, passengers and pedestrians' spatial distribution.

This chapter focuses on the emission modelling by using the outputs of traffic micro-simulation which can deliver more precise vehicle trajectory predictions than their strategic level counterparts (Zhu and Ferreira, 2012b). The chapter is organised as follows: Section 7.2 outlines the methodology used. Section 7.3 sets out the data used in the research reported here and shows the results obtained when using the emissions model proposed here.

7.2 Methodology

For a given road section, total emissions equals the summation of emissions by individual vehicles. The simulated network adopts the instantaneous emission model(Int Panis et al., 2006a) and the proposed model in Chapter 5. The traffic flow is assumed to consist of passenger car only. The vehicle trajectories, extracted by micro-simulation (AIMSUN 6.2), are exhibited in Table 7.1 for each vehicle and for each simulation step (0.45s).

Table 7.1 Sample outputs of micro-simulation outputs

Vehicle ID	Speed(km/h)	Time(s)	Vehicle Type
6169	88.9	3600.45	1
5431	93.4	3600.45	1
4602	95.5	3600.45	1
6101	95.9	3600.45	1
4516	85.3	3600.45	1
4552	86.8	3600.45	1
6082	86.8	3600.45	1
4575	101.2	3600.45	1

Note: 1 under vehicle type symbolises the passenger car

To identify the acceleration and time based variables, the output dataset was divided into cells and sorted by vehicle ID. After estimating the accelerations by differentiating instantaneous speeds, the dataset was realigned by time sequence to calculate the different categories of instantaneous emission profiles, using Equations 5.3 to 5.11(Chapter 5 Section 5.4). A Matlab program was developed to produce instantaneous emission profiles. Figure 7.2 shows the program in flow chart form.

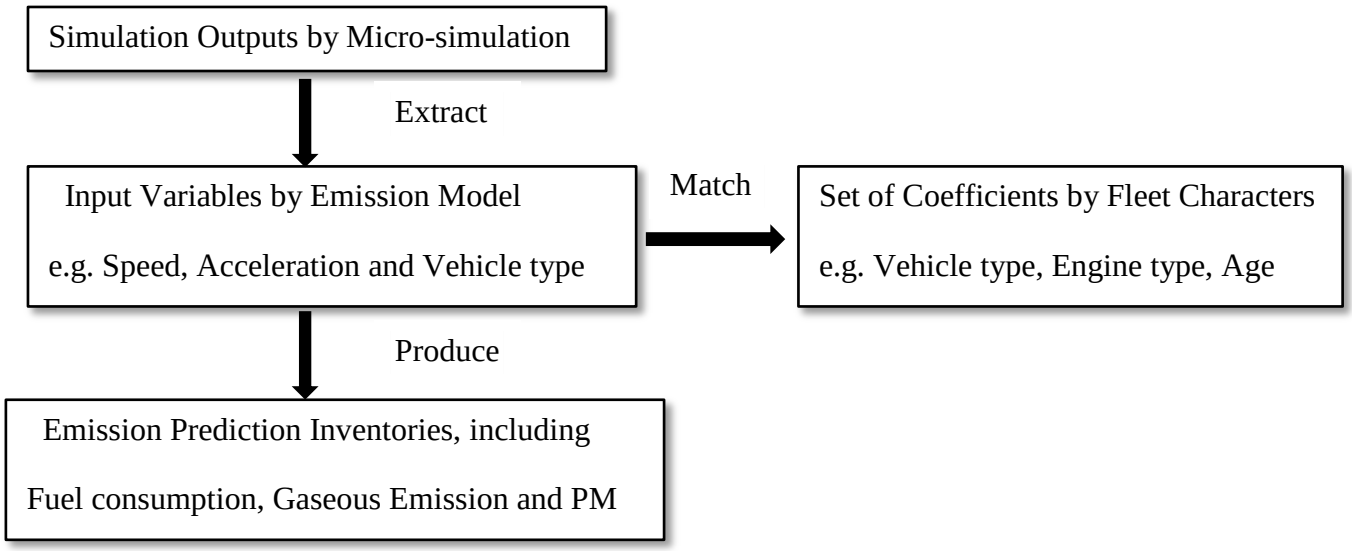

Figure 7.2 Framework for the micro-scale emission model application

7.3 Case-studies

The proposed new emissions models have been applied to two scenarios in Brisbane, namely, a section of motorway and a section of signalised arterial road. Significant amounts of emissions are generated at both locations. In addition, the dynamic nature of motorway traffic (Johnson and Ferreira, 2001) and the stop-start behaviour of traffic flow at intersections provide a series of challenges to modelling accuracy (Li et al., 2004). For the motorway simulation, the transition between congestion and free flow leads to a significant gap between simulated results and actual measurements (Zhu and Ferreira, 2012a). The new emission model can also be used to analyse traffic flow at signalised intersections. The deceleration and acceleration event behaviours at an intersection affect the emission intensity significantly (Minoura et al., 2009). Generally, the simulation of queues poses a number of challenges, namely: the acceleration profile of the leading vehicle in the queue and the headway of the following vehicles. Currently, constant acceleration is assumed by most simulation packages. However, Long (2000) has shown that linearly decreasing acceleration rates better represent both maximum vehicle acceleration capabilities and actual motorist behaviour. For the headway problem, Jin et al. (2009) have found that the distributions of the departure headways at each position in a queue are shown to approximately follow a log-normal distribution and the corresponding mean values level out gradually.

7.3.1 Motorway example

The section of motorway used for the study is part of the Pacific Motorway in Brisbane, selected from a large set of potential locations to avoid the merging and diverging effects on the mainstream motorway traffic flow (TRB, 2010). The chosen section consists of three lanes. Its distance to the CBD of Brisbane is shown in Figure 7.3. Figure 7.4 demonstrates

profiles of varied gaseous emissions by the instantaneous emission model and the proposed new model. Figure 7.5 illustrates the real-time vehicle counts and average speed on the motorway section. They show that the emissions are correlated with the traffic volume in the case of continuous traffic flow.

Figure 7.3 Pacific highway network diagram

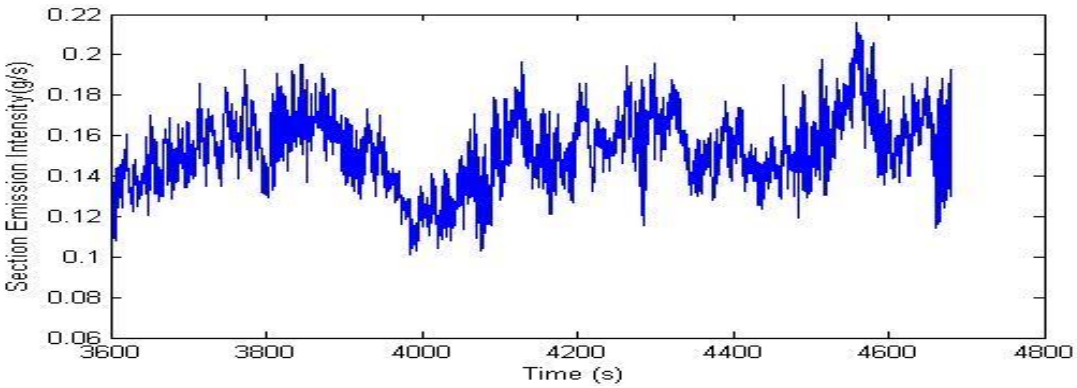

(a) HC emission profile by the instantaneous emission model (Int Panis et al., 2006b)

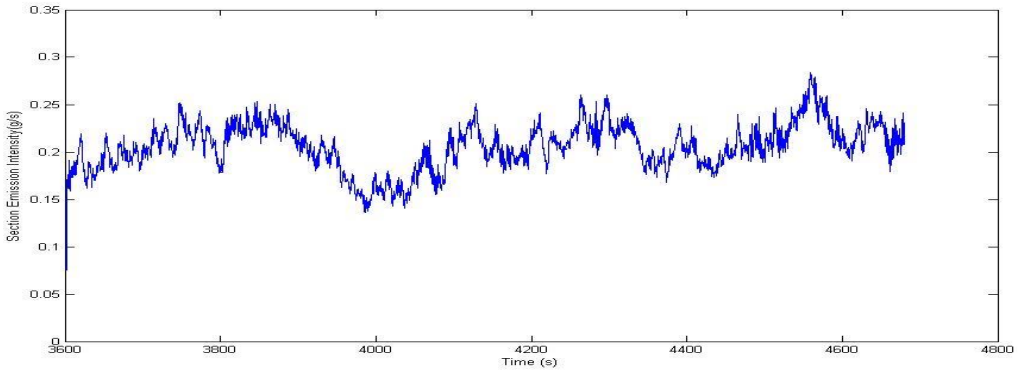

(b)HC emission profile using the proposed emission model (Zhu et al., 2013)

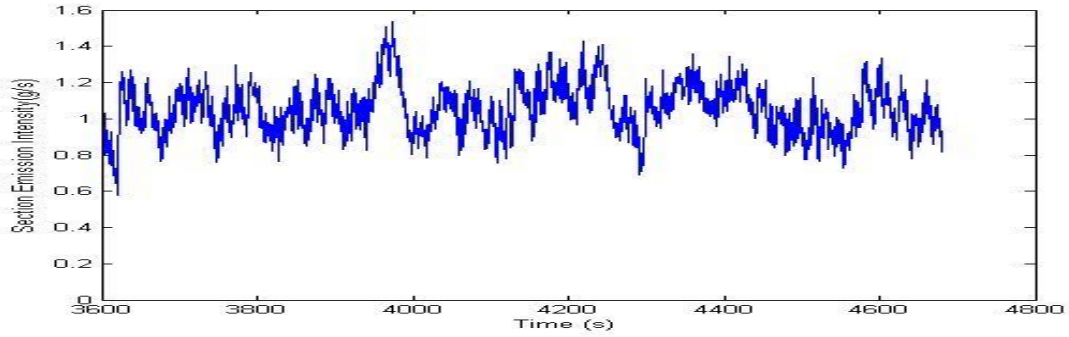

(c) CO emission profile using the proposed emission model (Zhu et al., 2013)

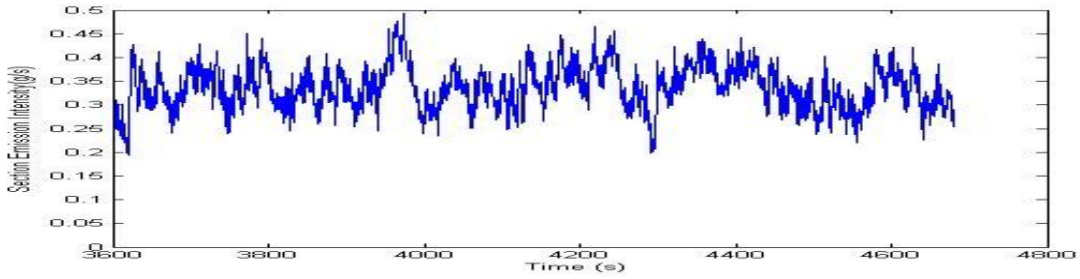

(d) NO_x emission profile using the proposed emission model (Zhu et al., 2013)

Figure 7.4 Emission profiles for the motorway

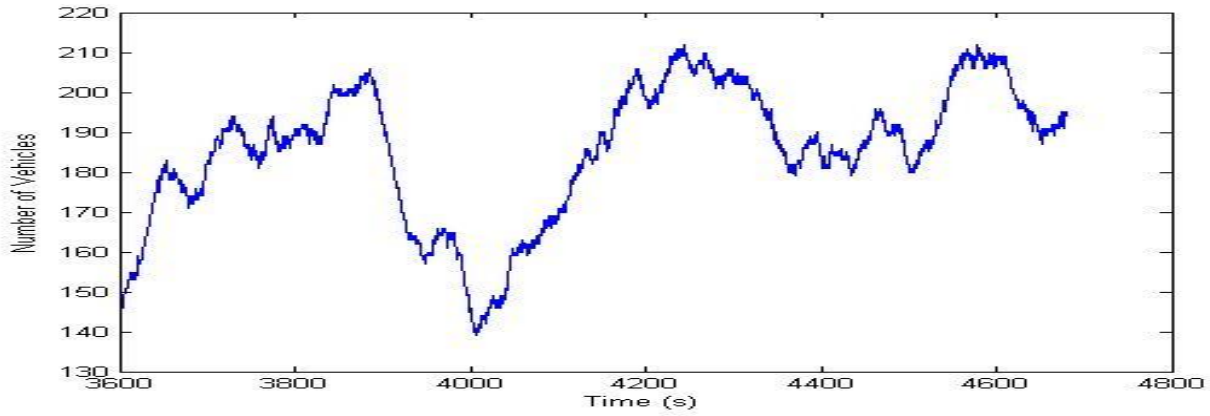

(a) Traffic flow on the motorway section (three lanes)

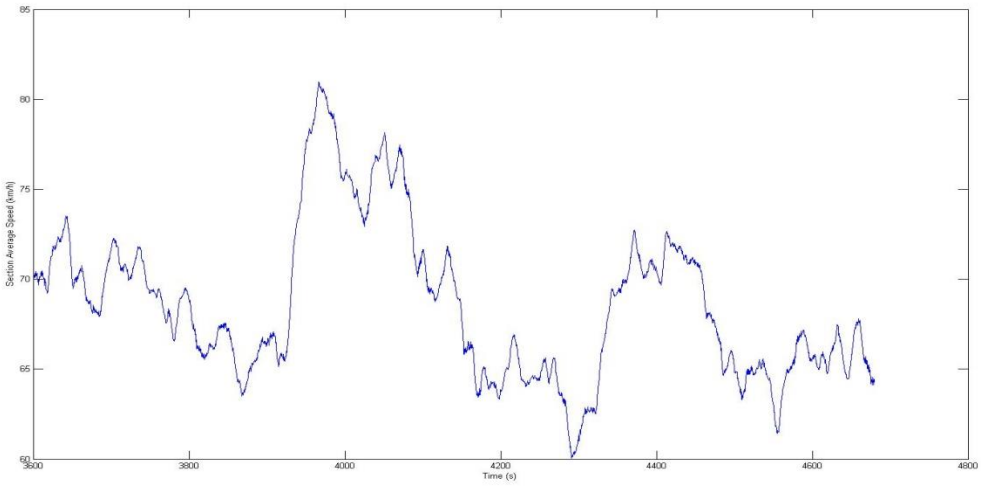

(b) Average speed on the motorway section (three lanes)

Figure 7.5 Motorway section vehicle counts and average speed

7.3.2 Intersection example

The signalled intersection of Cleveland-Redland Bay Rd and Benfer Rd has been previously modelled using the VISSIM package (Galiza and Tavassoli, 2009). One north-bound lane was selected here to be the test-bed site. A major proportion of vehicle emissions occur at the intersection approaches, due to the final acceleration to cruising speed and to the stop-and-go cycles (EPA, 2003). Figure 7.6 shows the location of the network under study. Figure 7.7 demonstrates varied simulated profiles of gaseous emissions by the instantaneous emission model and the proposed new model. Figure 7.8 illustrates the traffic queue at the intersection. In contrast to the motorway case, the emissions at the intersection vary dramatically. The acceleration (start-go) at the intersection accounts for a significant share of emissions.

Figure 7.6 Cleveland network map

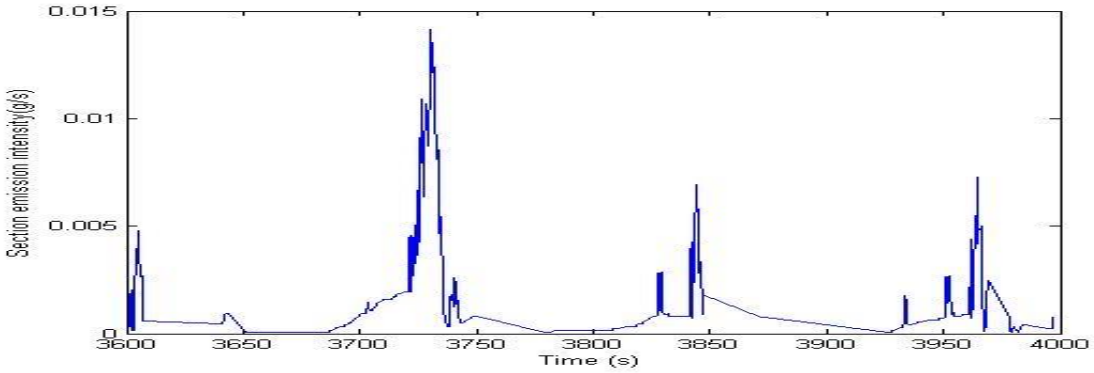

(a) HC emission profile using the instantaneous emission model (Int Panis et al., 2006b)

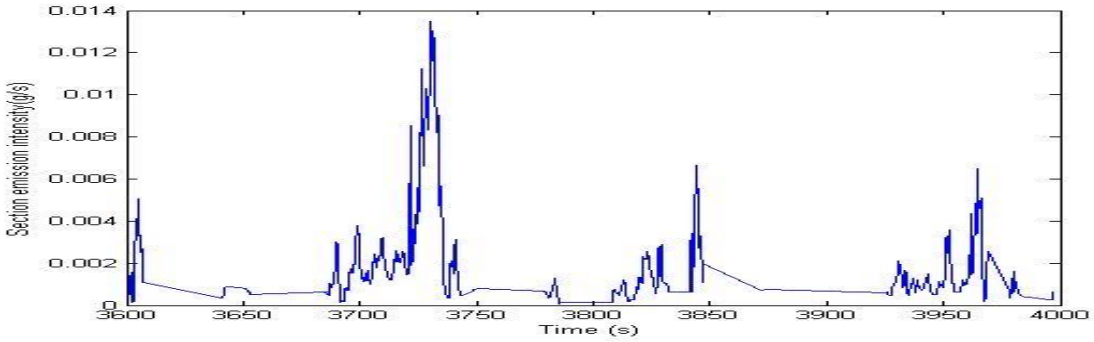

(b)HC emission profile using the proposed emission model (Zhu et al., 2013)

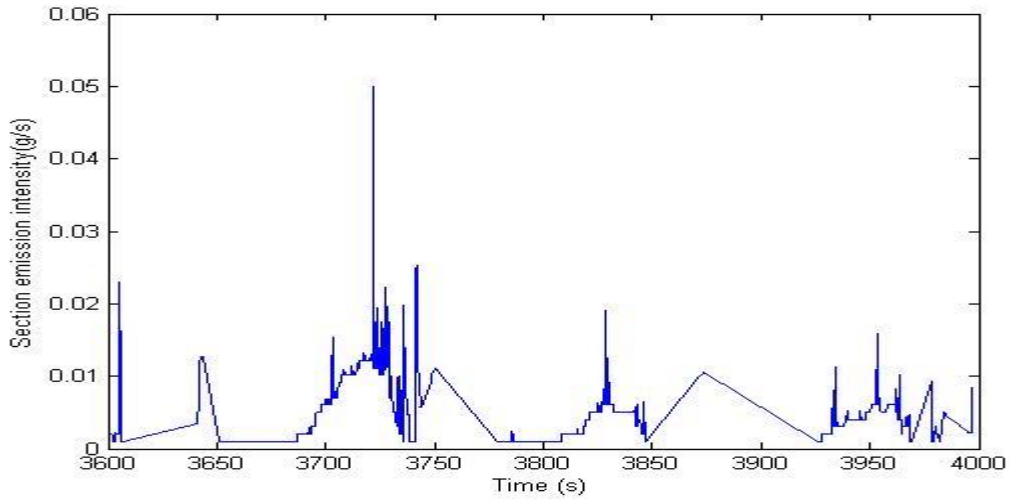

(c) CO emission profile using the proposed emission model (Zhu et al., 2013)

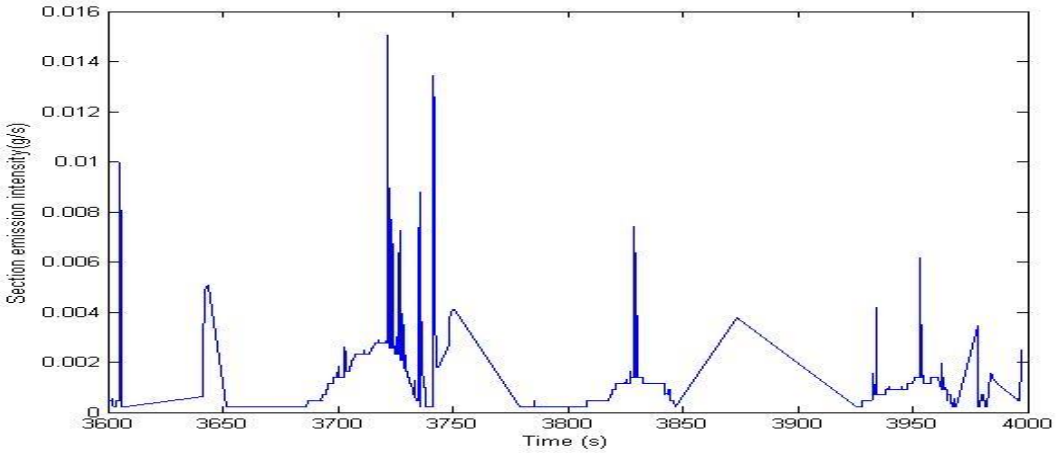

(d) NO_x emission profile using the proposed emission model (Zhu et al., 2013)

Figure 7.7 Simulated emission profiles for a signalised intersection

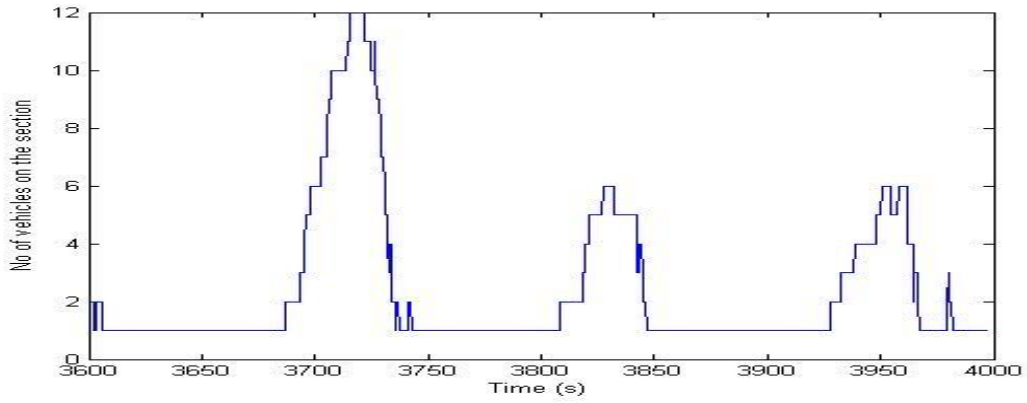

(a) Total traffic at the intersection (one lane)

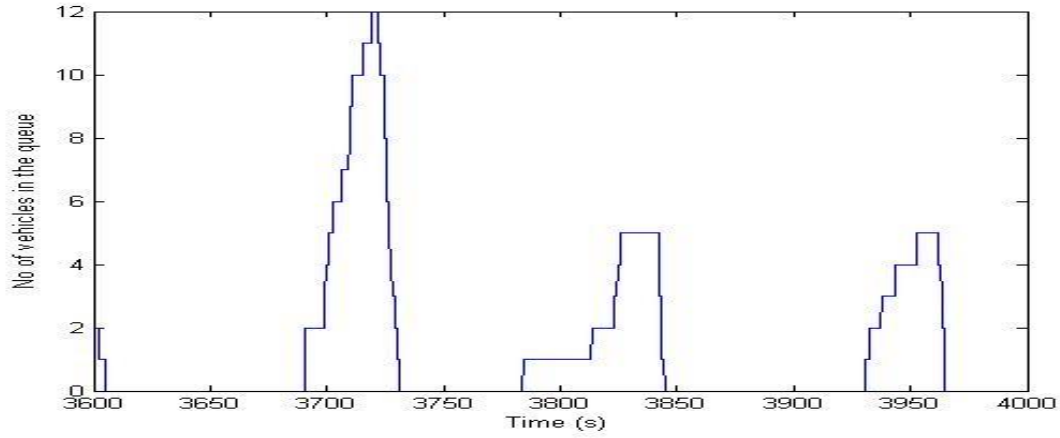

(b) Total queued traffic at the intersection (one lane)

Figure 7.8 Traffic at the intersection

7.4 Updating Aimsun equations to Australian conditions

The updating of 'default' parameters used in AIMSUN to represent the Australian vehicle fleet characteristics has been undertaken as part of the current research. The following two main steps were performed:

(1) The NISE2 dataset was used in conjunction with the CUEDC (1800 seconds) as described in Chapter 2. For each vehicle, the average speed, acceleration and emission rate were used for each second of time interval. Average values for these variables were derived by vehicle category. The NISE2 tested light-duty petrol vehicles were divided according to a matrix of vehicle categories, based mainly on engine capacity and the number of cylinders. The six vehicle categories used were:

Small passenger (PV-S)

Medium passenger (PV-M)

Large passenger (PV-L)

Compact sport utility (SUV-C)

Large sport utility (SUV-L)

Light Commercial (LCV)

For each category, non-linear multiple regression was used to estimate the best-fit parameters for the AIMSUN model (Equation 3.6).

(2) Having established new parameters for each pollutant, the resulting predictive models were validated with the NISE2 dataset vehicles that were not used in the calibration process.

The recalibrated NO_x emissions model was developed using all NISE2 vehicles with the exception of 10 vehicles in each category, which were used to validate the model. The results of using the improved model with these 'validation' vehicles are shown in Figure 7.9(a) for the LCV vehicle category. Figure 7.9(b) shows the corresponding results obtained when AIMSUN default parameters were used.

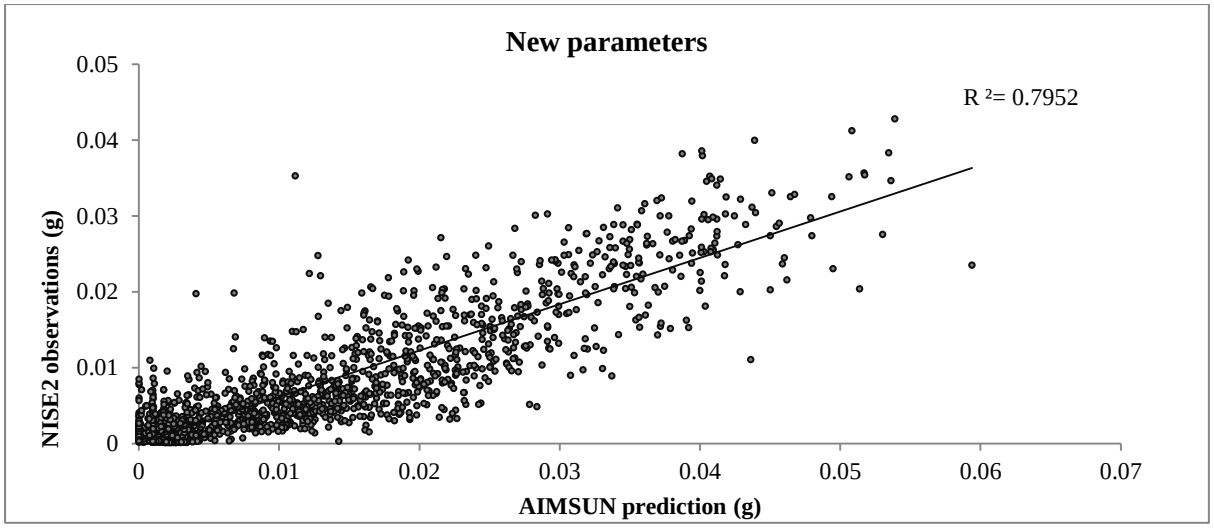

Figure 7.9(a): NO_x emission predictions for the same sample of LCV vehicles (using the new parameters)

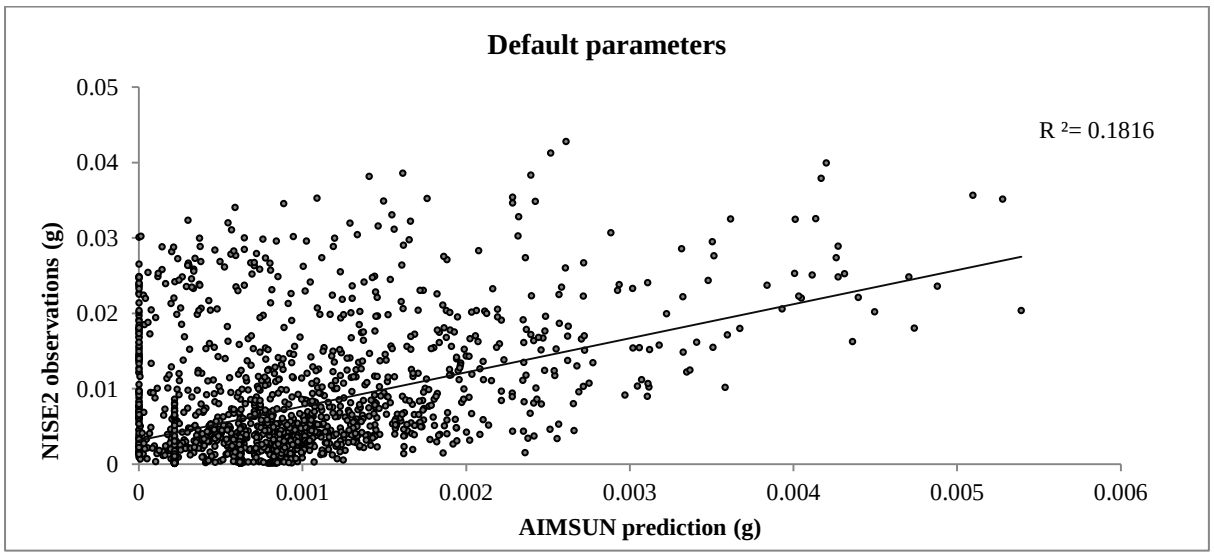

Figure 7.9(b): NO_x emission predictions for the same sample of LCV vehicles (using the AIMSUN default parameters)

Figure 7.9 NO_x emission predictions for the same sample of LCV vehicles

The summary results for all vehicle categories are shown in Table 7.2. There has been a significant improvement in the predictive ability of the recalibrated model, with the coefficient of determination (R^2) increasing to more than 0.6 for most vehicle categories.

Table 7.2 Evolution of the goodness of fit parameters

		R-Sq. (R^2)		Total cycle emissions (g)			Ratio	New Ratio
Pollutant	**Vehicle**	**Default**	**New**	**AIMSUN default**	**AIMSUN new**	**NISE2 Average**		
NO_x	PV-S	35%	63%	1.57	7.74	2.79	0.56	2.77
	PV-M	1%	26%		9.45	3.21	0.49	2.94
	PV-L	12%	52%		12.62	8.89	0.18	1.42
	SUV-C	12%	54%		8.85	4.35	0.36	2.03
	SUV-L	28%	67%		16.91	6.67	0.24	2.54
	LCV	18%	80%		20.75	12.73	0.12	1.63

To calibrate new parameters for the estimation of VOC and CO, the NISE2 dataset was used which included a total of 40 vehicles for validation purposes. Figure 7.10 and Figure 7.11 show the overall comparison of the model and observed results, when the new parameters are used. They also show the performance of the model for all vehicles combined and for LCVs separately. A significant improvement is seen when compared with the use of the original default parameters.

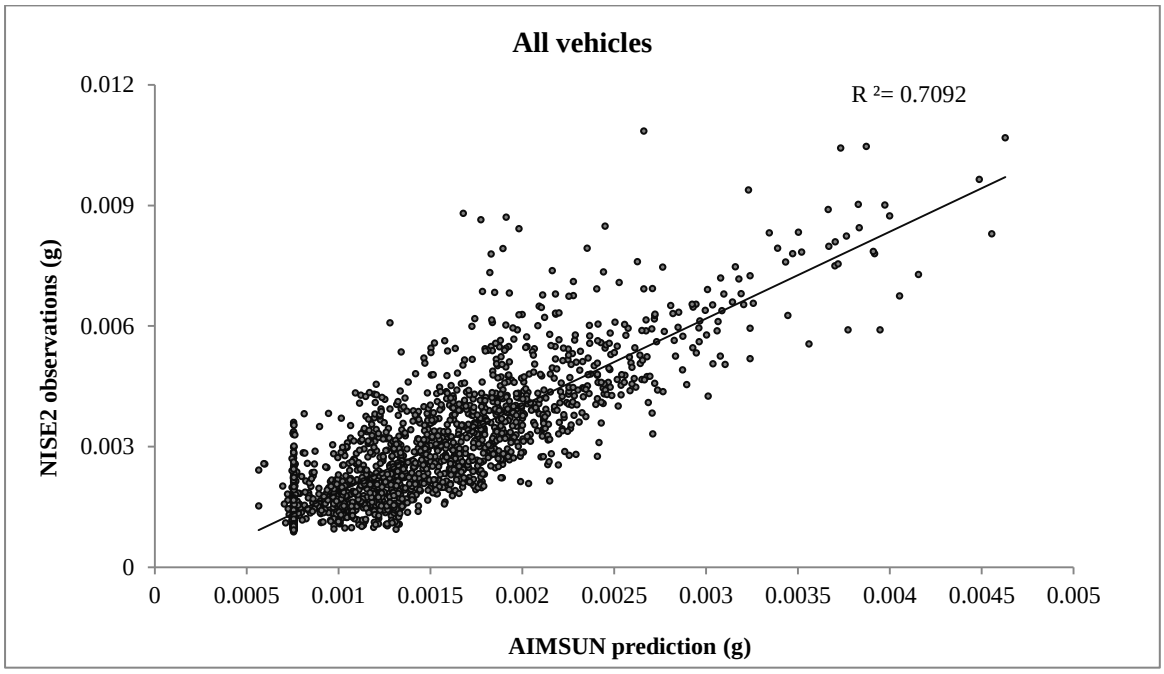

Figure 7.10 (a): VOC emission predictions for all vehicles

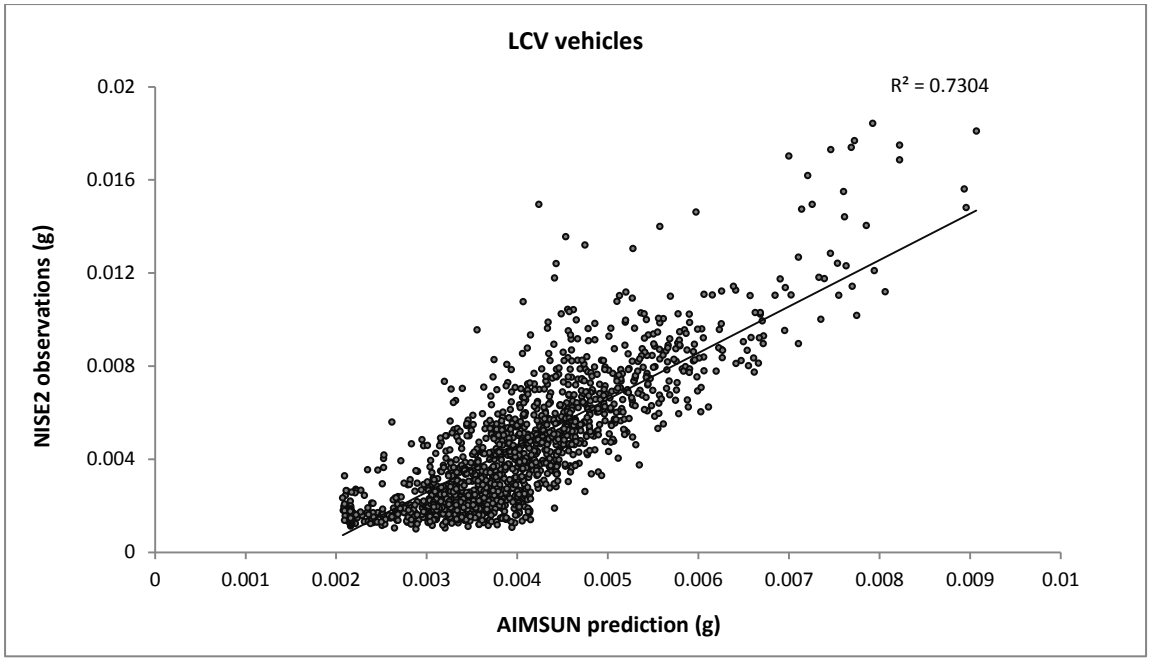

Figure 7.10(b): VOC emission predictions for LCVs

Figure 7.10 Performance of VOC emission predictions

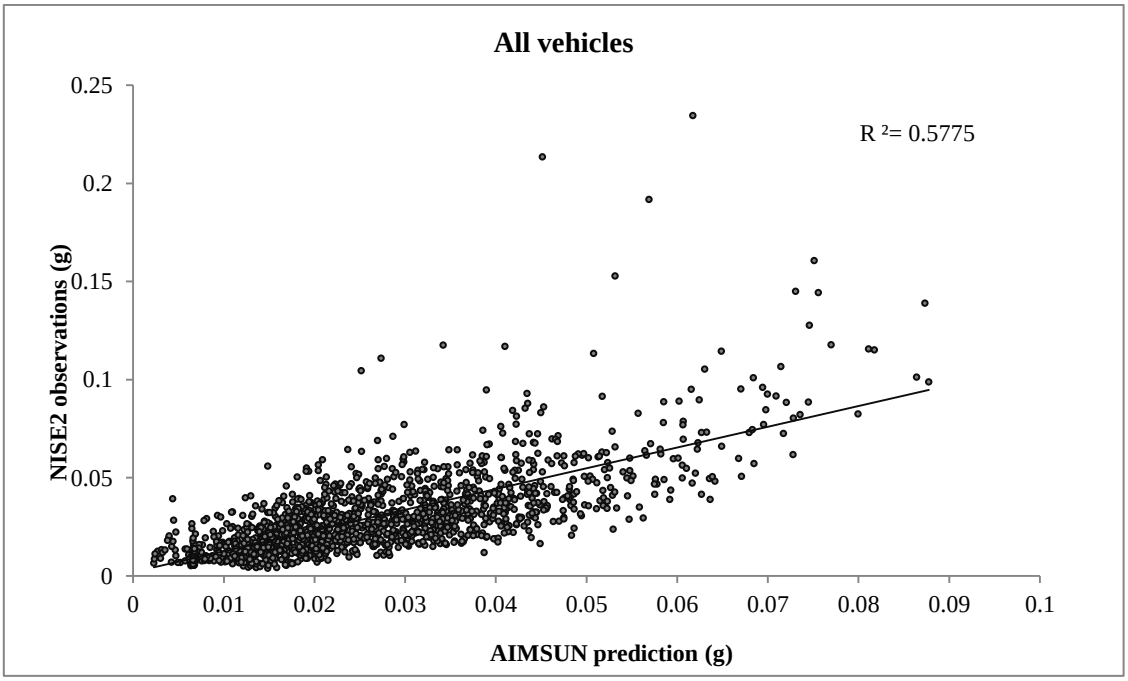

Figure 7.11(a): CO emission predictions for all vehicles

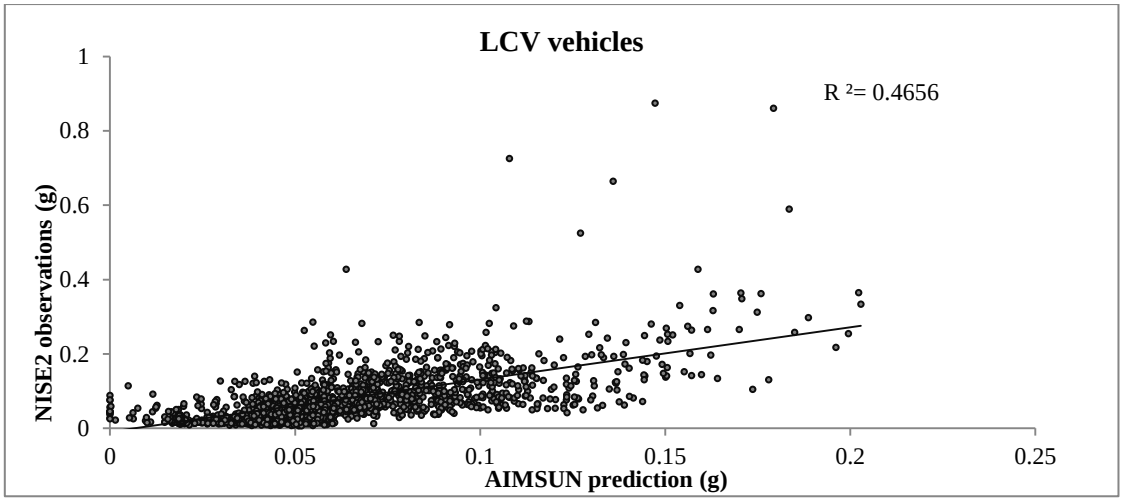

Figure 7.11(b): CO emission predictions for LCVs

Figure 7.11 Performance of CO emission predictions

Finally, Table 7.3 shows the new set of parameters that have been determined for each of the pollutants. For NO_x, every category has its own set of parameters, whereas for VOC and CO there are two set of parameters, namely, those representing the LCV category and those representing all other vehicle categories.

Table 7.3 New model parameters for Australian conditions

Pollutant	Vehicle category	Acceleration (a)	E0	f1	f2	f3	f4	f5	f6
NO_x	PV-S	(a≥-0.5 m/s^2)	0.001	1.00E-03	8.01E-05	9.35E-06	-3.00E-03	1.00E-03	1.00E-03
		(a<-0.5 m/s^2)	0.001	1.00E-03	2.77E-05	4.31E-06	1.00E-03	0.00E+00	2.36E-05
	PV-M	(a≥-0.5 m/s^2)	0.001	1.00E-03	9.03E-05	1.39E-05	-3.00E-03	1.00E-03	1.00E-03
		(a<-0.5 m/s^2)	0.001	1.00E-03	9.93E-05	4.80E-06	1.00E-03	1.00E-03	3.60E-05
	PV-L	(a≥-0.5 m/s^2)	0	1.00E-03	0.00E+00	3.35E-05	-1.00E-03	1.00E-03	0.00E+00
		(a<-0.5 m/s^2)	0.002	-5.00E-03	9.84E-05	4.24E-05	-3.00E-03	1.00E-03	1.00E-03
	SUV-C	(a≥-0.5 m/s^2)	0.001	1.00E-03	0.00E+00	1.73E-05	-2.00E-03	1.00E-03	1.00E-03
		(a<-0.5 m/s^2)	0	1.00E-03	-5.11E-05	7.50E-06	1.00E-03	0.00E+00	-2.71E-07
	SUV-L	(a≥-0.5 m/s^2)	0.002	2.00E-03	-9.22E-05	3.61E-05	-2.00E-03	1.00E-03	2.00E-03
		(a<-0.5 m/s^2)	0.001	2.00E-03	0.00E+00	1.08E-05	3.00E-03	1.00E-03	5.26E-05
	LCV	(a≥-0.5 m/s^2)	0	1.00E-03	-6.07E-05	5.13E-05	-2.00E-03	1.00E-03	2.00E-03
		(a<-0.5 m/s^2)	0.001	2.00E-03	3.75E-05	1.57E-05	1.00E-03	1.00E-03	9.41E-05
VOC	ALL	(a≥-0.5 m/s^2)	0	7.55E-04	8.92E-05	-2.04E-06	-2.05E-04	2.45E-04	1.21E-04
		(a<-0.5 m/s^2)	0	5.98E-04	1.13E-04	-3.92E-06	-2.30E-04	-8.23E-05	2.27E-05
	LCV	(a≥-0.5 m/s^2)	0	2.16E-03	2.12E-04	-5.13E-06	-6.87E-04	3.79E-04	2.32E-04
		(a<-0.5 m/s^2)	0	1.75E-03	3.86E-04	-1.35E-05	-7.98E-04	-1.99E-04	1.06E-04
CO	ALL	(a≥-0.5 m/s^2)	0	6.64E-03	1.46E-03	-5.69E-06	-1.37E-02	4.66E-03	3.36E-03
		(a<-0.5 m/s^2)	0	2.75E-03	2.23E-03	-6.45E-05	-6.97E-03	-2.49E-03	3.94E-04
	LCV	(a≥-0.5 m/s^2)	0	1.89E-02	3.00E-03	1.95E-06	-5.72E-02	1.70E-02	8.89E-03
		(a<-0.5 m/s^2)	0	4.13E-03	7.21E-03	-2.41E-04	-2.47E-02	-8.12E-03	1.11E-03

7.5 Summary

Because the lagged variables were unavailable at the beginning of simulation, the proposed new model underestimates the emission intensity for the un-signalised traffic condition. The two scenarios tested here show very different emission profiles. The acceleration component of the new model shows more sensitive reactions to vehicle acceleration, compared with the single-equation instantaneous model (the instantaneous emissions model).

Instead of the proposed new models, the coefficient localisation of the equation has resulted in a reduction of the measurement related error in the models, as the results have shown moderate improvements in the predictive ability of the models. However, the overall levels of accuracy present in such predictions remain poor, compared with the results in Table 5.3 -Table 5.5.

The profiles shown here for gaseous emission intensity demonstrate the advantage of emission micro-simulation modelling. The high-resolution predictions are more reliable due to the ability to deal with the dynamic nature of the vehicle trajectories. The emissions results for the motorway example depend on dynamic traffic conditions. On the other hand, the emissions results for the intersection example are mainly related to vehicle acceleration behaviour. The proposed new model is robust under varied traffic operations, despite the fact that the added model complexity means increased potential estimation forecasting errors. On the level of individual vehicle operation, there is a substantial gap between traffic simulation and traffic flow measurement for both signalised and non-signalised traffic. Therefore, the enhancement of emission predictions rests to a large extent on further improvements to traffic micro-simulation models.

Chapter 8. Conclusions

8.1 Main findings

General

Predictions of the pollution impacts of mode and route choice decisions need to be considered in conjunction with conventional travel demand modelling outputs. In order to evaluate the environmental impacts generated by the implementation of particular transportation management schemes over a period of time and make sound policy-related decisions based on such evaluations, environmental emissions models need to be developed as accurate and reliable assessment tools.

This thesis has reviewed macro and micro level emissions models which are integrated with corresponding traffic models. Strategic travel demand models tend to be large and regional in nature, whereas micro simulation models are used for detailed tactical or operational testing of options. Hence, microscopic traffic models should integrate real time emission prediction models, which are able to utilise high-resolution transportation modelling results, thereby generating potentially more precise emission estimates. The micro level models have been classified and evaluated here in terms of modelling approach, accuracy and robustness. The modelling approaches are classified into three types, namely: power based; speed based; and hybrid models. A review of microscopic emissions models has been undertaken using the results of Australian vehicle emissions measured in the field. It was found that the 'instantaneous traffic emissions' (model 5) produced the best overall result of modelling evaluations.

Development of emissions model

A comprehensive review of the relevant literature was undertaken (Chapter 3). It was found that the modelling of gaseous pollutants, namely CO, HC and NO_x continues to present significant challenges. Based on the reviews in Chapter 3, microscopic models use a combination of instantaneous velocity and acceleration to predict various gaseous pollutants including HC and CO. A range of variables for the instantaneous and lag velocity, acceleration and CO_2 emission rate were selected and tested. As a result, this thesis proposes a GA-based methodology to select the most appropriate explanatory variables, including lagging variables, to predict vehicle emissions. This method provides a new approach to the selection of a combination of variables among a large potential set. The new models deliver not only more accurate predictions but also robust performance for several types of vehicles. The approach is capable of solving combinatorial optimisation problems. To improve computational efficiency, distributed synchronous GA is based on distribution of workload among processors during the fitness function evaluation phase followed by a single central population regeneration. Hence, the massive fitness computations are assigned to workers in order to improve the computation efficiency.

Moreover, the proposed GA methodology provides a solution for a combinatorial optimisation problem, providing high modelling accuracy with statistically significant relationships between the selected predicting variables and the dependant variable.

Uncertainty analysis

To arrive at an optimal emissions modelling outcome, the interaction between two components namely, input data and model specification, needs to be taken into account. A more complex model may negate the overall modelling accuracy by increasing input data uncertainties. Hence, a compromise solution needs to be found. The two types of errors exhibit distinct characteristics for each stage of driving behaviour. Under free traffic flow conditions, the two types of errors are closely aligned and the overall accuracy of model outputs is close to its optimum level. However, the input data errors provide the main source of estimated uncertainty for traffic flow conditions of transition to congestion and very congested stages.

The micro-simulation modelling of congested and near congested traffic flow conditions yield significantly less robust estimates than is the case with free flow conditions. Model input data related to average vehicle speeds and accelerations at the micro-scale level, are critical to reduce overall emissions estimation errors. The profiles show more sensitive reactions to vehicle acceleration, compared with the single-equation instantaneous model.

This is particularly so for congested and near congested stages of the simulation. For applications of micro-simulation models dealing with urban congested conditions, the largest gain in terms of the likely accuracy of emissions estimates would seem to rest with improvement in input data reliability. Int Panis et al.'s (2006b) emission model has several advantages for CO_2 modelling, including good prediction accuracy and concise modelling structure. The complexity of emission modelling structures may not yield increased overall accuracy until the uncertainties attached to the input data can be significantly improved.

Emission modelling application

In Chapter 7, the new emission model was applied to a case study in Brisbane. Using different scenarios for different road configurations and traffic conditions, the results of applying the new approach were compared with those obtained by using default emissions parameters commonly found in a simulation package. The high-resolution profiles for gaseous emission intensity demonstrate the advantage of emission micro-simulation modelling. The high-resolution predictions are more reliable due to the ability to deal with the dynamic nature of vehicle trajectories. The proposed new model is robust under varied traffic operations, despite the fact that the added model complexity means increased potential estimation forecasting errors.

8.2 Research limitation and future research

Emissions model development

Despite the significant overall improvements for the modelling of gaseous pollutants, the models proposed here produce relatively low accuracy in predicting emissions for the deceleration mode. In addition, the accuracy of the new model may be compromised when driving with loads or in hilly terrain. Future research should focus on extending the modelling scope to include the full set of PM. Further investigations need to be put forward on the ageing effect of engines and catalytic converters along with emission modelling of emerging vehicle technologies, such as hybrid engine technology.

Modelling uncertainty

As was demonstrated in Chapter 6, Monte Carlo simulation is an effective methodology to address the quantification of modelling uncertainty. However, the uncertainties of input variables, such as vehicle speed and acceleration, need to be verified by high-resolution field data for the motorway scenario. For the signalised intersection scenario, the acceleration behaviour of the leading vehicles at intersections, as well as the following car headways are significant for queue simulation and emissions estimation. The assumption of constant acceleration was found to deviate substantially from observations collected by a driving simulator study. The latter also shows that the acceleration characteristics are significantly different between participants. In the case of signalised intersection flows, the emissions modelling is dependent on complex vehicle interactions, including queue discharging. Future enhancement of emission predictions rests to a large extent on further improvements to traffic micro-simulation models.

Modelling applications

The proposed emission model underestimates the emission intensity due to the absence of lag variables at the beginning of the simulation period. To overcome this problem, the emission model could be efficiently and effectively integrated with micro-simulation software.

The two scenarios based on different traffic conditions, show very different instantaneous emission profiles. At the level of individual vehicle operation, there is a substantial gap between traffic simulation and traffic flow measurement for both signalised and non-signalised traffic flow conditions. The emission results for the motorway example depend on dynamic traffic conditions. On the other hand, the emission results for the intersection example are mainly related to acceleration behaviour of the queued vehicles. In Appendix B, a new acceleration profile is proposed to simulate the leading vehicle in a queue. The resultant emission predictions are significantly different from the common constant-acceleration profile. Also, it could replace the constant-acceleration assumption. Moreover, a stochastic simulation approach, instead of a deterministic profile, may be adopted by traffic simulation packages to fit with the randomness of acceleration behaviours of the leading vehicle.

References

Abaza, K., Ashur, S., Al-Khatib, I., 2004. Integrated Pavement Management System with a Markovian Prediction Model. *Journal of Transportation Engineering* 130(1), 24-33.

ABS, 2009. Motor vehicle census, *In: 9309.0*. Australian Bureau of Statistics, Canberra.

Ahn, K., Rakha, H., Trani, A., Van Aerde, M., 2002. Estimating vehicle fuel consumption and emissions based on instantaneous speed and acceleration levels. *Journal of Transportation Engineering* 128(2), 182-190.

Ahrens, C.D., 2003. *Meteorology today: an introduction to weather, climate, and the environment*. Thomson/Brooks/Cole.

Akcelik, R., Besley, M., 2003. Operating cost, fuel consumption and emission models in aaSidra and aaMotion, *25th Conference of Australian Institutes of Transport Research (CAITR)*, University of South Australia, Adelaide, Australia.

André, M., 2004. The ARTEMIS European driving cycles for measuring car pollutant emissions. *Science of The Total Environment* 334–335(0), 73-84.

André, M., Rapone, M., 2009. Analysis and modelling of the pollutant emissions from European cars regarding the driving characteristics and test cycles. *Atmospheric Environment* 43(5), 986-995.

Barth, M., An, F., Norbeck, J., Ross, M., 1996. Modal emissions modeling: A physical approach. *Transportation Research Record*(1520), 81-88.

Barth, M., Scora, G., 2006. Comprehensive modal emissions model (CMEM), User's Guide, Version 3.01. University of California, Riverside.

BCC/QGEPA, 2004. Air Emissions inventory South-East Queensland Region, In: Agency, B.C.C.a.Q.G.E.P. (Ed.), Brisbane, Queensland.

Biggs, D.C., Akcelik, R., 1986. An energy related model of instantaneous fuel consumption. *Traffic Engineering & Control* 27(6), 320-325.

Biona, J.B.M., Culaba, A., 2006. Drive cycle development for tricycles. *Clean Technologies and Environmental Policy* 8(2), 131-137.

Bourrel, E., Lesort, J.-B., 2003. Mixing microscopic and macroscopic representations of traffic flow: Hybrid model based on Lighthill-Whitham-Richards theory. *Transportation Research Record: Journal of the Transportation Research Board* 1852(-1), 193-200.

Cantú-Paz, E., 1998. A survey of parallel genetic algorithms. *Calculateurs paralleles, reseaux et systems repartis* 10(2), 141-171.

Chatterjee, S., Laudato, M., Lynch, L.A., 1996. Genetic algorithms and their statistical applications: an introduction. *Computational Statistics & Data Analysis* 22(6), 633-651.

Chowdhury, D., Santen, L., Schadschneider, A., 2000. Statistical physics of vehicular traffic and some related systems. *Physics Report* 329(4-6), 199-329.

Chung, E., Rahman, M., Bevrani, K., Jiang, R., 2011. Evaluation of Queensland Department of Transport and Main Roads Managed Motorways. Smart Transport Research Centre, Queensland University of Technology, Brisbane

DTMR, 2010. Guidelines for the configuration and placement of vehicle detection sensors, *Traffic and Road Use Management Manual*. Department of Transport and Main Roads.Queensland Government, Brisbane , Australia.

DTMR, 2011. Pacific Motorway M1 Project location map. DTMR.

EPA, 1989. Federal Test Procedure.

EPA, 1997. Risk Assessment Forum, Guiding Principles for Monte Carlo Analysis. EPA/630/R-97/001.

EPA, 2003. User's Guide to MOBILE6.1 and MOBILE6.2; Mobile Source Emission Factor Model, *EPA420-R-03-010*. EPA, Washington, DC.

EPA, 2005. Clean Fuel Fleet Exhaust Emission Standards, In: Office of Transportation and Air Quality , E.P.A. (Ed.), United States
Favez, J.-Y., Weilenmann, M., Stilli, J., 2009. Cold start extra emissions as a function of engine stop time: Evolution over the last 10 years. *Atmospheric Environment* 43(5), 996-1007.
Fenger, J., 1999. Urban air quality. *Atmospheric Environment* 33(29), 4877-4900.
Ferreira, L., 2007. Using strategic transport models to predict energy, climate change and air quality impacts, *Portfolio Transport Modelling Team*. Queensland Transport, Brisbane.
Frey, H.C., Rouphail, N.M., Zhai, H., 2006. Speed-and facility-specific emission estimates for on-road light-duty vehicles on the basis of real-world speed profiles. *Transportation Research Record: Journal of the Transportation Research Board* 1987(-1), 128-137.
Galiza, R., Tavassoli, A., 2009. REDLAND BAY RD UPGRADE: MICRO-SIMULATION MODEL (VISSIM). ITS Research Laboratory, UQ Brisbane, QLD
Gentle, J.E., 2003. *Random Number Generation and Monte Carlo Methods*. Springer-Verlag,Inc. , New York.
Godley, S.T., Triggs, T.J., Fildes, B.N., 2002. Driving simulator validation for speed research. *Accident Analysis & Prevention* 34(5), 589-600.
Gordon, T., Bareket, Z., Kostyniuk, L., Barnes, M., Hagan, M., Kim, Z., Cody, D., Skabardonis, A., 2012. Site-Based Video System Design and Development.
Heywood, J.B., 1988. *Internal Combustion Engine Fundamentals* McGraw-Hill, New York.
Hidas, P., 2006. Evaluation and further development of car following models in microscopic traffic simulation, pp. 287-296.
Hourdakis, J., Michalopoulos, P.G., Kottommannil, J., 2003. Practical Procedure for Calibrating Microscopic Traffic Simulation Models, pp. 130-139.
Hung, W.T., Tong, H.Y., Lee, C.P., Ha, K., Pao, L.Y., 2007. Development of a practical driving cycle construction methodology: A case study in Hong Kong. *Transportation Research Part D: Transport and Environment* 12(2), 115-128.
Int Panis, L., Broekx, S., Liu, R., 2006a. Modelling instantaneous traffic emission and the influence of traffic speed limits. *Science of the Total Environment* 371(1-3), 270-285.
Int Panis, L., Broekx, S., Liu, R., 2006b. Modelling instantaneous traffic emission and the influence of traffic speed limits. *Science of The Total Environment* 371(1–3), 270-285.
Isaacson, D.L., Madsen, R.W., 1985. *Markov chains: theory and applications*. RE Krieger Publishing Company.
Jamriska, M., Morawska, L., 2001. A model for determination of motor vehicle emission factors from on-road measurements with a focus on submicrometer particles. *Science of The Total Environment* 264(3), 241-255.
Jin, X., Zhang, Y., Wang, F., Li, L., Yao, D., Su, Y., Wei, Z., 2009. Departure headways at signalized intersections: A log-normal distribution model approach. *Transportation Research Part C: Emerging Technologies* 17(3), 318-327.
Johnson, L., Ferreira, L., 2001. Modelling particle emissions from traffic flows at a freeway in Brisbane, Australia. *Transportation Research Part D: Transport and Environment* 6(5), 357-369.
Keogh, D.U., Kelly, J., Mengersen, K., Jayaratne, R., Ferreira, L., Morawska, L., 2010. Derivation of motor vehicle tailpipe particle emission factors suitable for modelling urban fleet emissions and air quality assessments. *Environmental Science and Pollution Research* 17(3), 724-739.
Kerner, B.S., 2004. Three-phase traffic theory and highway capacity. *Physica A: Statistical Mechanics and its Applications* 333(1-4), 379-440.

Kim, I., Ferreira, L, Tey, LS and Wallis, G, 2013. Integration of driving simulator and traffic simulation to analyse behavior at railway crossings, *Proceedings of the Institution of Mechanical Engineers, Part F: Journal of Rail and Rapid Transit*.
Klauer, B., Brown, J.D., 2004. Conceptualising imperfect knowledge in public decision making: ignorance, uncertainty, error and 'risk situations'. *Environmental Research, Engineering and Management* 27(1), 124-128.
Kousa, A., Kukkonen, J., Karppinen, A., Aarnio, P., Koskentalo, T., 2002. A model for evaluating the population exposure to ambient air pollution in an urban area. *Atmospheric Environment* 36(13), 2109-2119.
Kroese, D.P., Taimre, T., Botev, Z.I., 2011. *Handbook of Monte Carlo Methods*. John Wiley and Sons,Inc. , New Jersey.
Leung, D.Y.C., Williams, D.J., 2000. Modelling of motor vehicle fuel consumption and emissions using a power-based model. *Environmental Monitoring and Assessment* 65(1-2), 21-29.
Li, X., Li, G., Pang, S.-S., Yang, X., Tian, J., 2004. Signal timing of intersections using integrated optimization of traffic quality, emissions and fuel consumption: a note. *Transportation Research Part D: Transport and Environment* 9(5), 401-407.
Lin, J., Niemeier, D.A., 2003. Estimating regional air quality vehicle emission inventories: Constructing robust driving cycles. *Transportation Science* 37(3), 330-346.
Logothetis, N., 1988. Role of data transformation in taguchi analysis. *Quality and Reliability Engineering International* 4(1), 49-61.
Logothetis, N., Haigh, A., 1988. CHARACTERIZING AND OPTIMIZING MULTI-RESPONSE PROCESSES BY THE TAGUCHI METHOD. *Quality and Reliability Engineering International* 4(2), 159-169.
Long, G., 2000. Acceleration Characteristics of Starting Vehicles. *Transportation Research Record: Journal of the Transportation Research Board* 1737(-1), 58-70.
Luque, G., 2011. *Parallel genetic algorithms: theory and real world applications*. Springer-Verlag, Berlin.
MathWorks, 2012. MATLAB Documentation.
Minocha, V.K., 2005. Discussion of "Impact Stops on Vehicle Fuel Consumption and Emissions" by Hesham Rakha and Yonglian Ding. *Journal of Transportation Engineering* 131(7), 571-571.
Minoura, H., Takekawa, H., Terada, S., 2009. Roadside nanoparticles corresponding to vehicle emissions during one signal cycle. *Atmospheric Environment* 43(3), 546-556.
Mitchell, M., 1998. *An Introduction to Genetic Algorithms*. Mit Press, Cambridge, MA.
Morawska, L., Keogh, D.U., Thomas, S.B., Mengersen, K., 2008a. Modality in ambient particle size distributions and its potential as a basis for developing air quality regulation. *Atmospheric Environment* 42(7), 1617-1628.
Morawska, L., Ristovski, Z., Jayaratne, E.R., Keogh, D.U., Ling, X., 2008b. Ambient nano and ultrafine particles from motor vehicle emissions: Characteristics, ambient processing and implications on human exposure. *Atmospheric Environment* 42(35), 8113-8138.
Morawska, L., Thomas, S., Bofinger, N., Wainwright, D., Neale, D., 1998. Comprehensive characterization of aerosols in a subtropical urban atmosphere: Particle size distribution and correlation with gaseous pollutants. *Atmospheric Environment* 32(14-15), 2467-2478.
Muthén, L.K., Muthén, B.O., 2002. How to use a Monte Carlo study to decide on sample size and determine power. *Structural Equation Modeling* 9(4), 599-620.
Nishihata, Y., Mizuki, J., Akao, T., Tanaka, H., Uenishi, M., Kimura, M., Okamoto, T., Hamada, N., 2002. Self-regeneration of a Pd-perovskite catalyst for automotive emissions control. *Nature* 418(6894), 164-167.

North, R.J., Noland, R.B., Ochieng, W.Y., Polak, J.W., 2006. Modelling of particulate matter mass emissions from a light-duty diesel vehicle. *Transportation Research Part D: Transport and Environment* 11(5), 344-357.
Orbital, 2009. Second national in-service emissions study (NISE2): light duty petrol vehicle emissions testing. Road and Traffic Authority of New South Wales.
Pandian, S., Gokhale, S., Ghoshal, A.K., 2009. Evaluating effects of traffic and vehicle characteristics on vehicular emissions near traffic intersections. *Transportation Research Part D: Transport and Environment* 14(3), 180-196.
Panwai, S., Dia, H., 2005. Comparative evaluation of microscopic car-following behavior. *IEEE Transactions on Intelligent Transportation Systems* 6(3), 314-325.
PTV, A., 2005. VISUM User Manual Version 9.3. PTV AG
Qi, Y., Teng, H., Yu, L., 2004. Microscale Emission Models Incorporating Acceleration and Deceleration. *Journal of Transportation Engineering* 130(3), 348-359.
Rakha, H., Ahn, K., Trani, A., 2003. Comparison of MOBILE5a, MOBILE6, VT-MICRO, and CMEM models for estimating hot-stabilized light-duty gasoline vehicle emissions. *Canadian Journal of Civil Engineering* 30(6), 1010-1021.
Rakha, H.A., Ahn, K., Moran, K., Saerens, B., Bulck, E.V.d., 2011. Virginia Tech Comprehensive Power-Based Fuel Consumption Model: Model development and testing. *Transportation Research Part D: Transport and Environment* 16(7), 492-503.
Refsgaard, J.C., van der Sluijs, J.P., Højberg, A.L., Vanrolleghem, P.A., 2007. Uncertainty in the environmental modelling process - A framework and guidance. *Environmental Modelling and Software* 22(11), 1543-1556.
Samuel, S., Austin, L., Morrey, D., 2002. Automotive test drive cycles for emission measurement and real-world emission levels - A review. *Proceedings of the Institution of Mechanical Engineers, Part D: Journal of Automobile Engineering* 216(7), 555-564.
Smit, R., Dia, H., Morawska, L., 2009. *Road traffic emission and fuel consumption modelling: trends, new developments and future challenges, in: Traffic Related AirPollution*. Nova USA
Smit, R., McBroom, J., 2009. Use of microscopic simulation models to predict traffic emissions. *Road and Transport Research* 18(2), 49-54.
Toledo, T., 2007. Driving behaviour: Models and challenges. *Transport Reviews* 27(1), 65-84.
Toledo, T., Koutsopoulos, H.N., Davol, A., Ben-Akiva, M.E., Burghout, W., Andréasson, I., Johansson, T., Lundin, C., 2003. Calibration and Validation of Microscopic Traffic Simulation Tools: Stockholm Case Study, pp. 65-75.
Touran, A., Wiser, E.P., 1992. Monte Carlo technique with correlated random variables. *Journal of Construction Engineering and Management* 118(2), 258-272.
TRB, 2010. *Highway Capacity Manual 2010*. Transportation Research Board 500 Fifth St. NW, Washington, D.C. 20001.
TSS, 2010. Aimsun 6.1 manual. Transport Simulation System, Barcelona, Spain.
Unal, A., Rouphail, N., Frey, H., 2003. Effect of Arterial Signalization and Level of Service on Measured Vehicle Emissions. *Transportation Research Record: Journal of the Transportation Research Board* 1842(-1), 47-56.
Vladisavljevic, I., Martin, P.T., Stevanovic, A., 2007. Integration of mathematical and physical simulation to calibrate car-following behaviour of unimpaired and impaired drivers. *World Review of Intermodal Transportation Research* 1(4), 403-418.
Walker, W.E., Harremoe, S., P., Rotmans, J., Van der Sluijs, J.P., Van Asselt, M.B.A., Janssen, P., Krayer von Krauss, M.P., 2003. Defining uncertainty a conceptual basis for uncertainty management in model-based decision support. *Integrated Assessment* 4(1), 5-17.
Walsh, M.P., 2011. Automobiles and Climate Policy in the Rest of the OECD. *Cars and Carbon: Automobiles and European Climate Policy in a Global Context*, 355.

Wang, J., Dixon, K., Li, H., Ogle, J., 2004. Normal acceleration behavior of passenger vehicles starting from rest at all-way stop-controlled intersections. *Transportation Research Record: Journal of the Transportation Research Board* 1883(1), 158-166.
Weilenmann, M., Favez, J.-Y., Alvarez, R., 2009. Cold-start emissions of modern passenger cars at different low ambient temperatures and their evolution over vehicle legislation categories. *Atmospheric Environment* 43(15), 2419-2429.
Zhu, S., Ferreira, L., 2012a. Assessing the uncertainty in micro-simulation model outputs, *Australasian Transport Research Forum*, Perth.
Zhu, S., Ferreira, L., 2012b. Evaluation of vehicle emissions models for micro-simulation modelling: using CO2 as a case study. *Road and Transport Research* 21(3), 3-18.
Zhu, S., Tey, L.-S., Ferreira, L., 2013. Modelling Vehicle Gaseous Emissions Using a Genetic Algorithm Approach-Based on Australian emission data *Transportation Research Part C: Emerging Technologies*.
Zito, R., Primerano, F., 2005. NISE2 –Contract 2 Drive Cycle Development Methodology and Results. Orbital Engine Company and Department of the Environment and Heritage.

Appendix A. Assessing the uncertainty in micro-simulation model outputs (Zhu and Ferreira, 2012a)

A.1 Introduction

Micro simulation traffic models continue to be widely used as tools to analyse current and future road system performance. Such models tend to operate by concentrating on the movement of individual vehicles in the traffic stream on a second by second basis. The likely errors associated the outputs of such models are usually thought to be significantly lower than the 'coarser' models with deal with the movement of groups of vehicles over an average time period. The predicted vehicle speeds and the traffic volumes are the most important traffic indicators, and primary inputs of other models such as emission estimation. This appendix evaluates the uncertainty in the outputs of micro level models by comparing those outputs with field data obtained from loop detectors on disaggregated level.

A.2 Past works

Currently, limited research has been put forward on the validation of micro simulation outputs, in terms of the gap between prediction and measurement for vehicle speeds for each modelled time period. The performance of these types of models, with respect to their ability to predict average speeds and traffic volumes, is depended on several external and internal factors. This research focuses on uncertainty induced by internal factors in the form of the driver behaviour model used. Theoretically, micro simulation has two core algorithms, namely: car-following and lane-changing, which are the main drivers of overall model accuracy. Panwai and Dia (2005) undertook a comparative evaluation of car-following behaviour in a number of traffic simulation models to validate their reliability of the AIMSUN, PARAMICS, and VISSIM models). The results point to similar performance for the psychophysical spacing models used in VISSIM and PARAMICS with better performance reported for the Gipps-based models implemented. Hidas (2006) confirms the findings and points out that lane-changing behaviour is a challenge for prediction accuracy. In most models, lane-changing behaviour requires two stages, consideration of lane-changing and execution. The improvement of lane-changing may be facilitated in two major directions: an increase in the level of detail in the specification of models to better capture the complexity and sophistication of human decision-making processes; and an improvement in the quality of data used to calibrate such these models (Toledo, 2007).

A.3 Methodology

This research evaluates the uncertainty in the outputs of micro simulation models by comparing predicted results with field average speed data obtained from motorway loop detectors at the 1-minute disaggregated level. Currently, the Queensland based traffic operations system records real time data by using 1-minute average speed measurements and other road section performance indicators, such as flow count and density (DTMR, 2010). For major facilities, such as the Pacific motorway, this data is collected from a network of loop

detectors established by the Department of Transport and Main Roads (DTMR, 2011). A detailed Aimsun traffic micro-simulation model has recently been calibrated using data obtained from those loop detectors(Chung et al., 2011). Although loop detector data has its shortcomings, it is the only available extensive data set for model calibration purposes. This research assumes that detector measurement error can be neglected, after the more obvious instances of missing or spurious data has been omitted. An initial primary visual check indicates that the uncertainty in the model outputs is likely to be associated with traffic flow conditions, such as the level of congestion. Particularly, the fundamental traffic theory is qualitatively different from empirical traffic flow analysis on over-saturated conditions (Chowdhury et al., 2000).

Hence, a new traffic flow theory has been proposed, in which flow is classified into three conditions, namely: free flow; 'synchronised ' flow and queuing (Kerner, 2004). Synchronized flow refers to non-interrupted traffic flow without a long period of queuing. There is a tendency to a synchronization of vehicle speeds across different lanes on a multi-lane road in this flow.

To evaluate the uncertainty on different traffic conditions, the Taguchi method, an offline quality control technique, is introduced in this research (Logothetis and Haigh, 1988). This technique classifies the source of uncertainty into outer and inner noise. In this research, the former includes the external sources to micro simulation model outputs, such as in traffic conditions, driving behaviour variations and traffic management strategies. The current research has focused on the inner noise induced by the simulation algorithm itself. The performance of system output is evaluated using equation (1).

$$NSR=\frac{\sigma_i}{\mu_i} \quad \text{----------} \quad (1)$$

Where:
μ_i : Speed output expectation
σ_i : Absolute output error
NSR: Noise-to-signal ratio, percentage of error to prediction.

The model for the relationship between the output (μ_i) and its error (σ_i) is formulated as:

$$NSR=\emptyset(\mu_i)^k \quad \text{----------} \quad (2)$$

Where:
μ_i: Speed Output expectation
NSR: Noise-to-signal ratio
k and $\emptyset$: Coefficients

Equation 2 may have a Box-Cox transformation to produce an improved fitting (Logothetis, 1988).

$$\log(NSR)=\log(\emptyset) + klog(\mu_i) \quad \text{----------} \quad (3)$$

The speed prediction uncertainty is defined here as the difference between loop detector measurement and simulation model output. To have a meaningful simulation speed prediction, it is necessary to undertaken a calibration of the model parameters to minimize the internal noise. In engineering practise, calibration uses simulated and actual measurements including

traffic volumes, vehicle occupancies and speeds. The deviation between actual and measured values is minimised by adjusting the simulation parameters through trial-and-error. The simulation parameters are classified into two main categories, namely: global (those that affect the performance of the entire model) and local (those that affect only specific sections of the roadway). Hourdakis et al. (2003) suggest the global parameters are calibrated first followed by local parameter calibration. Examples of global parameters are the vehicle characteristics, such as desired speed, maximum acceleration/deceleration, simulation step; and driver reaction time). Link speed limits and capacities are local parameters. Toledo et al. (2003) point out the calibration process should begin with disaggregate data including information on detailed driver behaviour, such as vehicle trajectories of the subject and surrounding vehicles. Aggregate data (e.g. time headways, speeds, flows, etc.) are used to fine-tune parameters and estimate general parameters in the simulation. The application of the Aimsun model to a section of the Pacific Motorway studied here, follows established calibration methodology (Chung et al., 2011). To minimize the effects of external impacts on the uncertainty results, the measurement data was selected according to three main criteria, as shown below.

(1) Quality of instantaneous traffic flow simulated and measured outputs

The quality of simulated flow count was evaluated using Equation (4):

$$y = \frac{\sqrt{(o_i - e_i)^2}}{o_i} \qquad \text{----------} \qquad (4)$$

Where:

n : Number of observed values

o : Observed value

e : Simulated value

(2) Detector location

To avoid the merging and diverging effects on the mainstream motorway traffic flow, the selected detectors were around 460 metres away from on-ramp and off-ramp(TRB, 2010).

(3) Incidents affected data

Comparing with minute-by-minute traffic data on other days, the datasets with unusual and non-recurring traffic congested patterns were excluded to remove incident-induced results.

A.4 **Dataset description**

After detailed validation, three detector groups C/D/E satisfied all three criteria and were selected from a large set of potential locations. The location of all selected detectors are shown in Figure 1. The distance to the CBD of Brisbane is also shown in Figure 1. The selected datasets were used to investigate the relationship between the simulated speed output and its uncertainty as the flow moves from free flow to highly congested conditions.

Detectors A and B were used to investigate free flow and queuing status. The analysis was undertaken for each minute of both actual measured outputs and simulation model results.

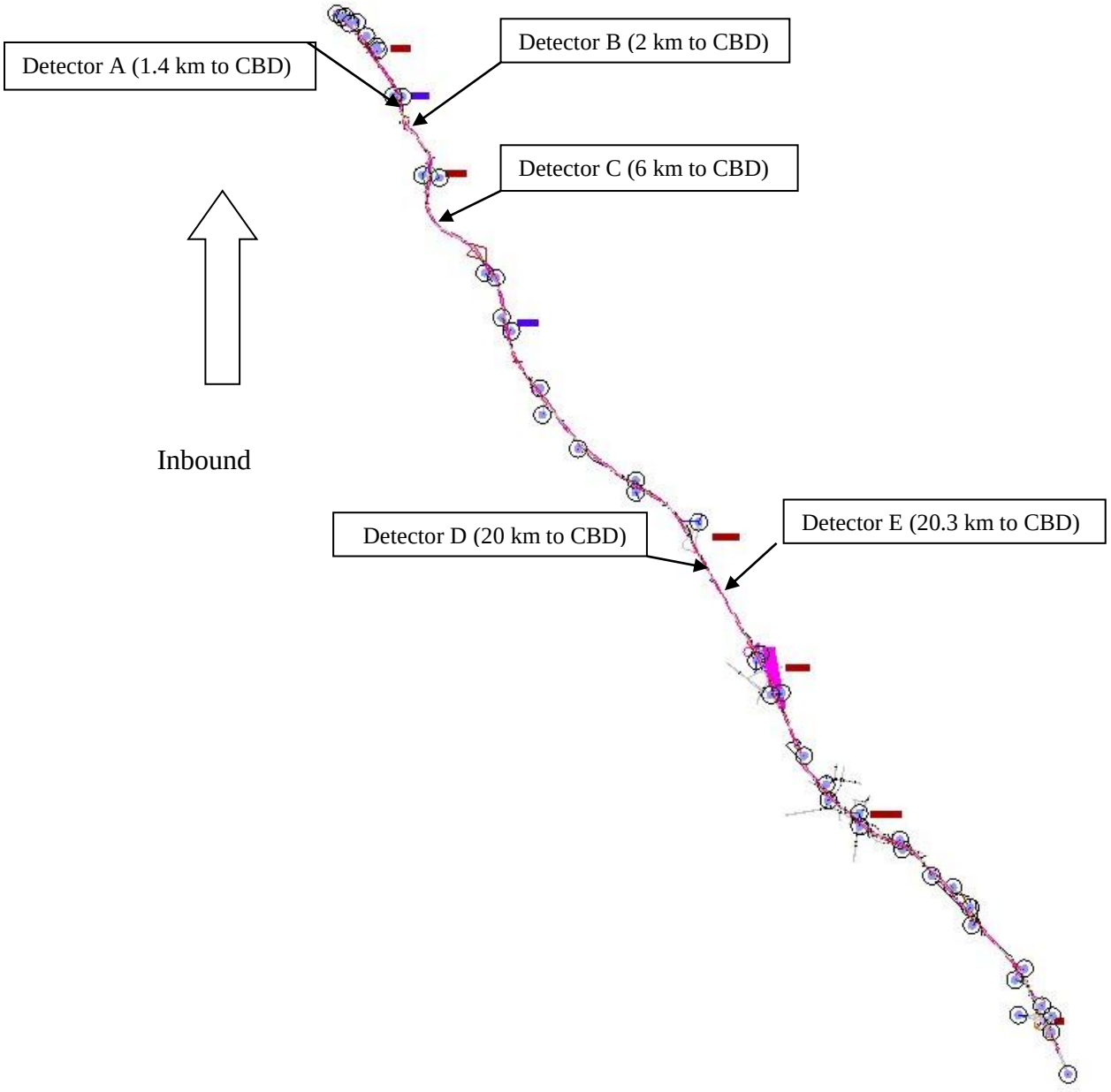

Figure 1: Pacific highway network map and selected detectors

A.5 **Uncertainty analysis**

Numerous datasets from different locations along the motorway indicate that the uncertainty in average speeds follows closely a normal distribution under off-peak time periods with free flow conditions, when tested using the Kolmogorov-Smirnov test. Using detector B as an example， Figure 2(a) and 2(b) demonstrate the flow and speed results for both the measured values and simulation outputs during an off-peak period. As a result, the coefficient k is 0 in Equation 2, showing non-correlation between speed prediction and uncertainty. The uncertainty expectation is a very low 1.9 km/h with a standard deviation of 4.7 km/h.

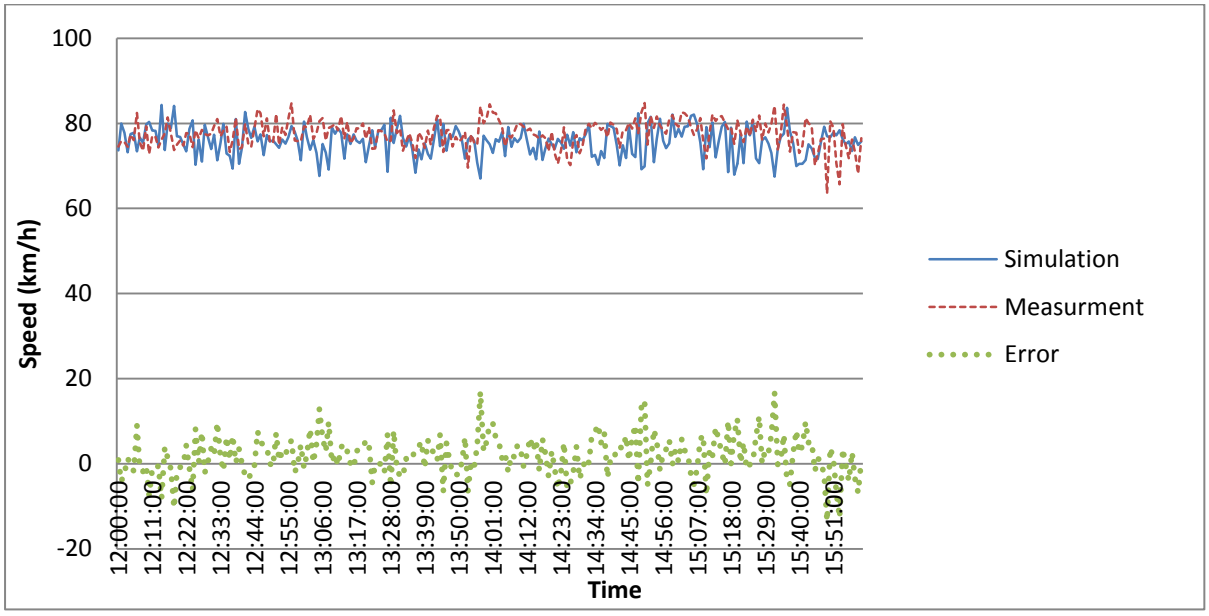

Figure 2(a): Simulation and measurement speed during non-peak period

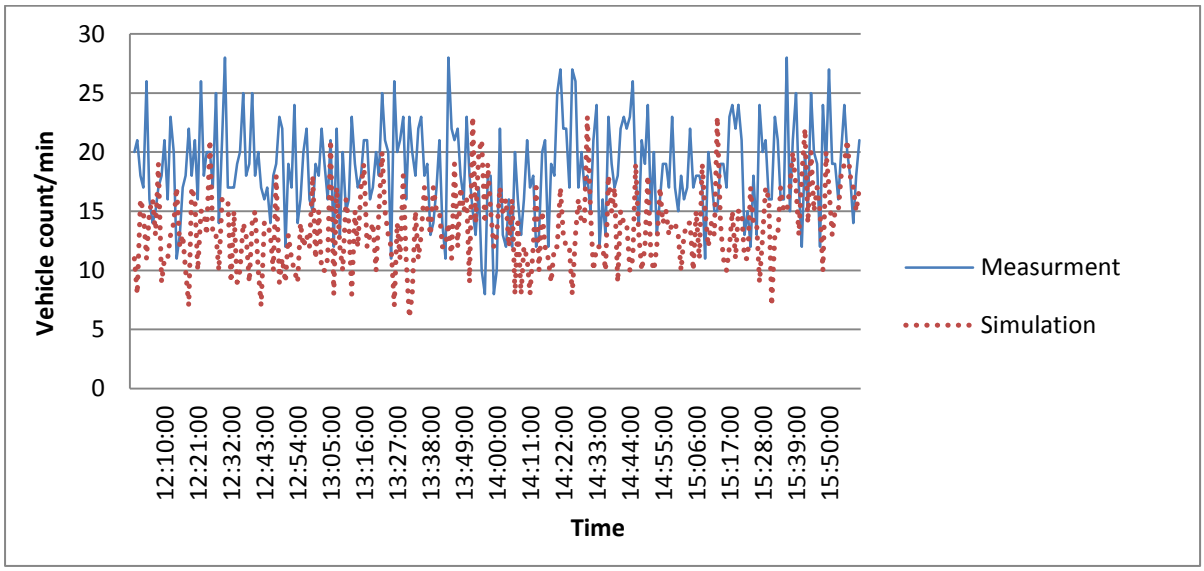

Figure 2(b): Simulation and measurement flow count during non-peak period

The vehicle speed related results obtained when measured data for one peak period is compared with simulation outputs are shown in Figure 3(a) and (b). In the latter, they present and sort the datasets in the descending order of vehicle speed. In the transitional stage between free flow and highly congested conditions at detector C, the relationship between uncertainty and average speed can be fitted using Equation 3. In this case the following results were obtained:

k= -4.29 and $\log(\emptyset) = 7.15$

Due to traffic speed fluctuations, linear regression analysis shows R^2 (Coefficient of determination) reaches 0.65, and the simulated speed, μ_i is statistical significant with NSR. Hence, minus exponential relationship between simulation speed and its NSR is established. Similarly, the negative correlations during the transitional stage have been replicated at other locations. Figure 3(b) demonstrates another example from detector E data.

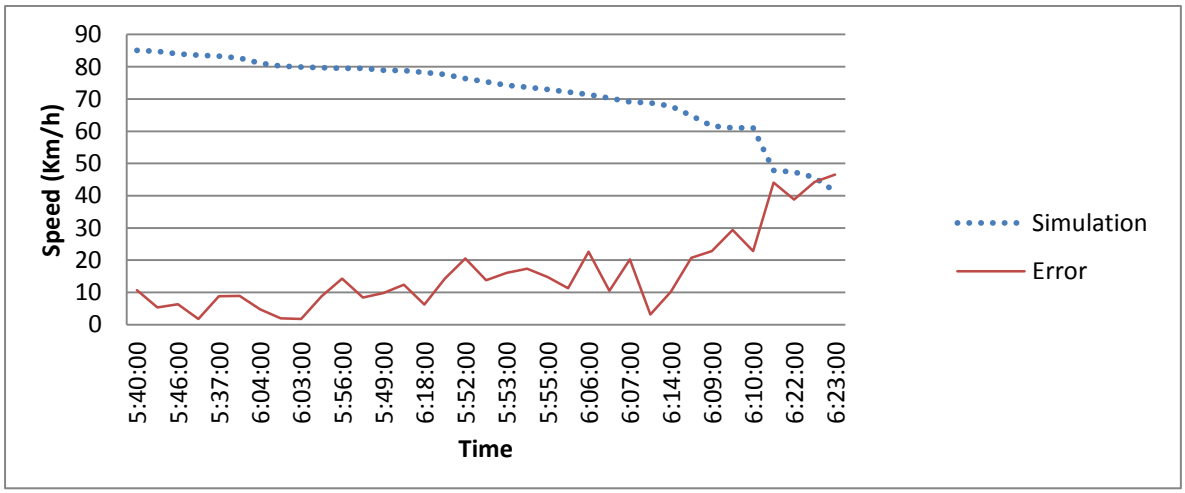

Figure 3(a): Simulation and measurement speed during transitional stage (detector C)

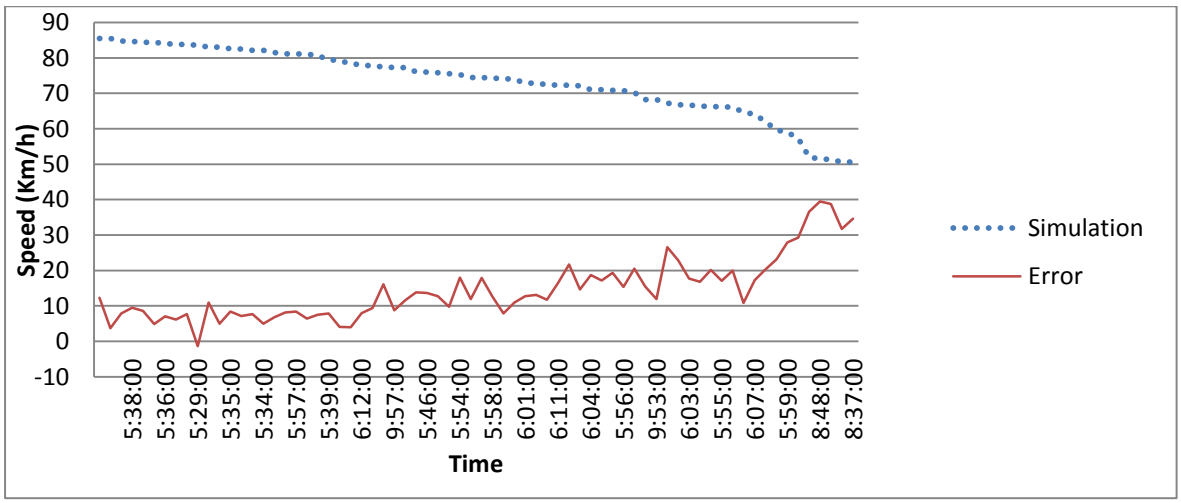

Figure 3(b): Simulation and measurement speed during transitional stage (detector E)

When traffic flow reaches capacity, unstable conditions prevail and simulation results appear to be much less reliable. For over-saturated conditions, both queuing and 'synchronized' flow conditions were found at different locations during periods. Figure 4 shows the speed measurements at detector C during the peak-hour. The results from the three inbound lanes at this detector show highly synchronized speeds across all lanes.

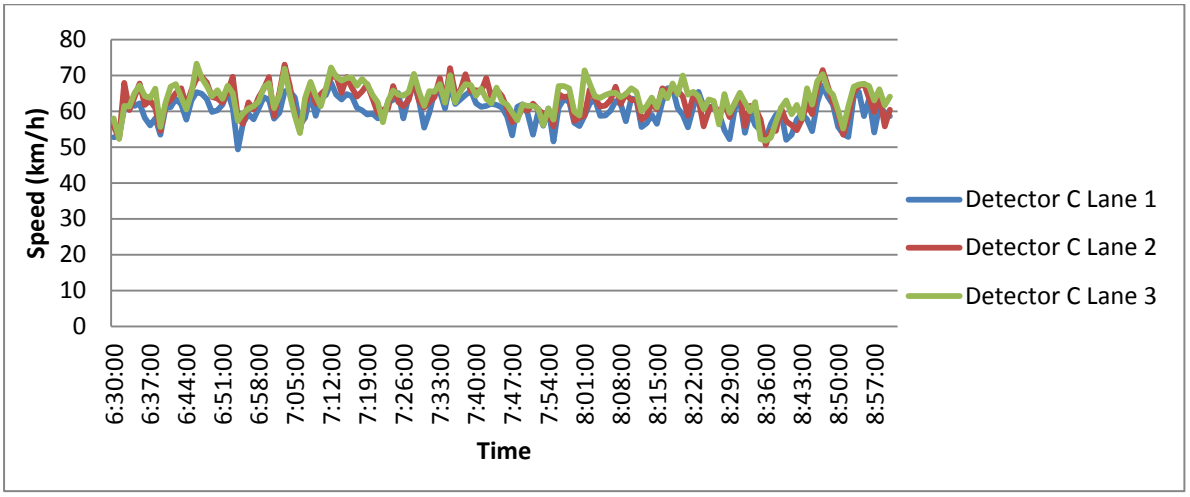

Figure 4: Detector C measured speeds in the morning peak hour

Figures 5(a) and 5(b) demonstrate modelled and measured vehicle speeds and volumes, respectively. The results related to detector C and a 3-hour morning peak period. The modelled traffic volume results show good agreement with measured values. The modelled vehicle speeds, when compared with measured values, follow a normal distribution. The uncertainty expectation is estimated at 23.2 km/h with a standard deviation is 10.4 km/h.

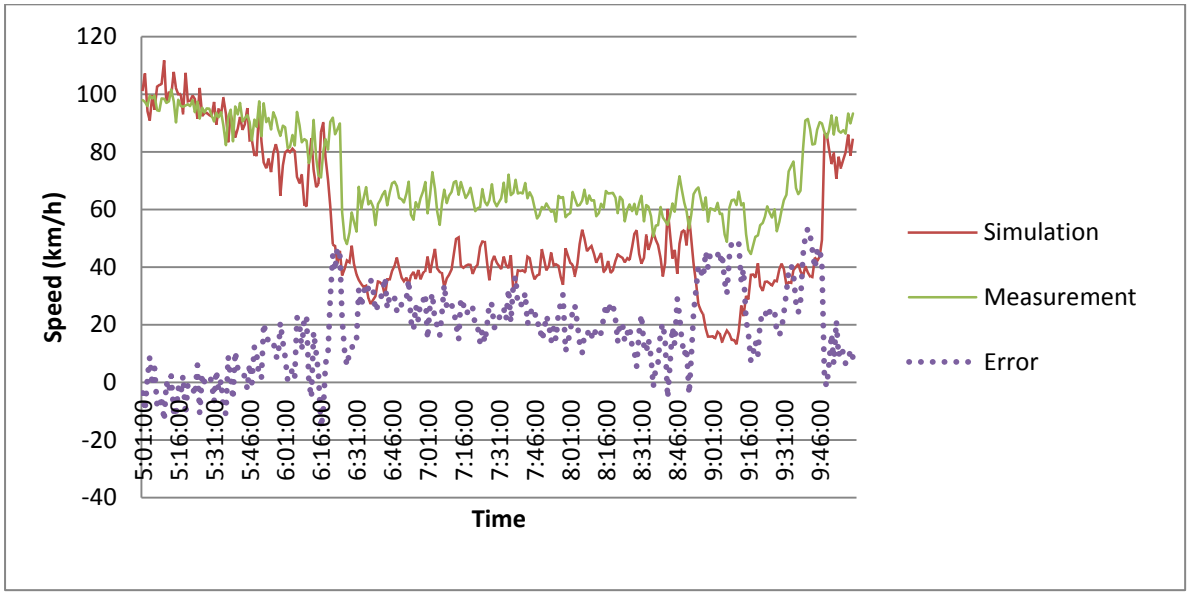

Figure 5(a): Simulated and measured average speeds: morning peak period (detector C)

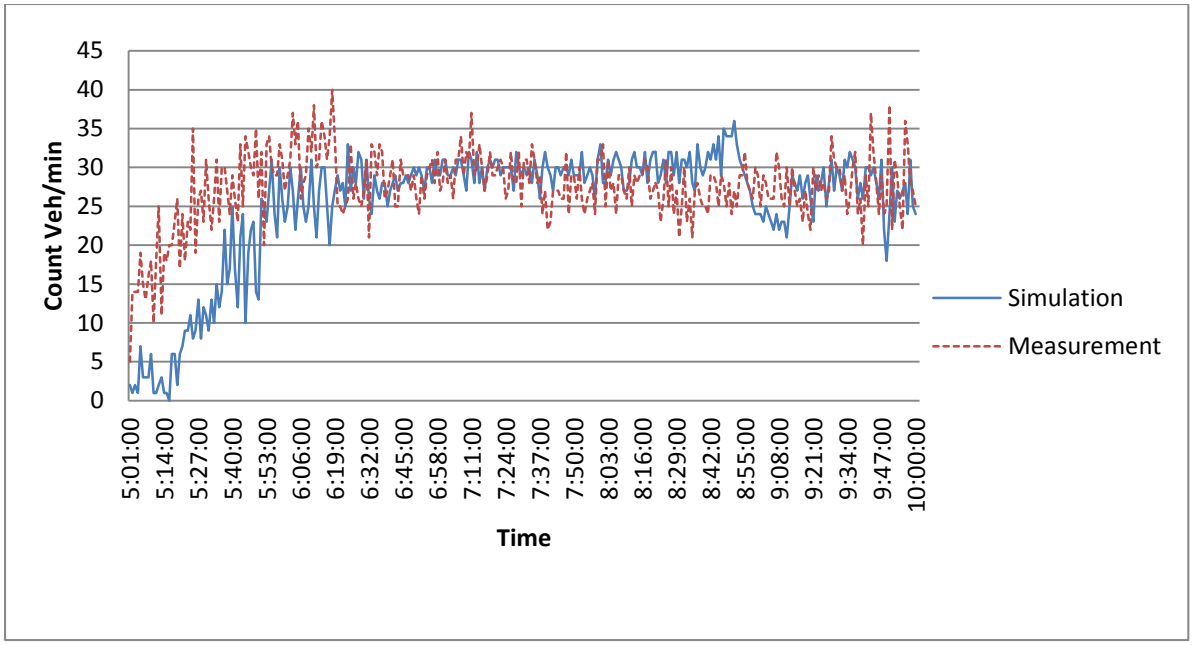

Figure 5(b): Simulated and measured traffic flow: morning peak period (detector C)

Similarly, Figures 6(a) and 6(b) demonstrate minute-by-minute traffic volumes and average speeds respectively. The data was collected at detector A in the morning peak direction. Traffic moves into queuing conditions for long periods, speed prediction uncertainty follows a normal distribution. The error expectation is 7.2 km/h with a standard deviation of 5.3 km/h, indicating the significant difference between queuing and 'synchronized' flow, as defined earlier.

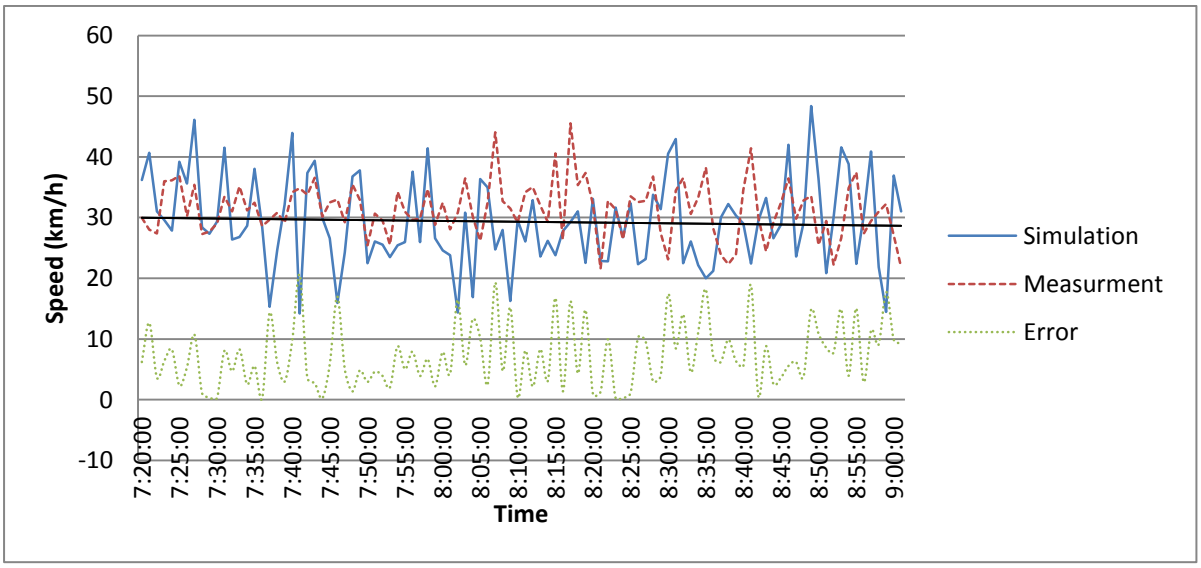

Figure 6(a): Simulated and measured average speed during peak hours (detector A)

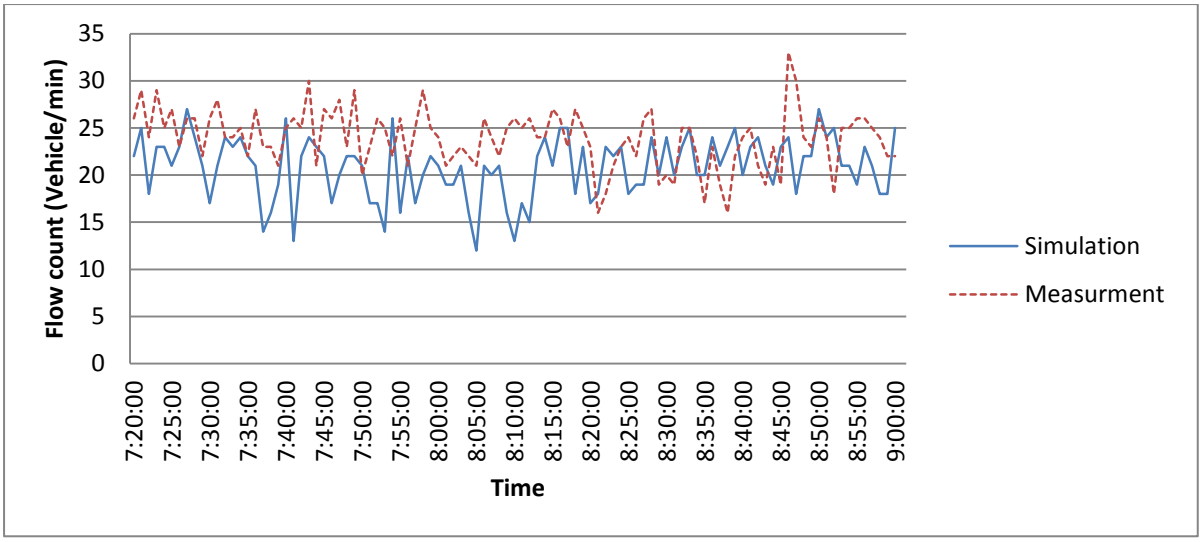

Figure 6(b): Simulated and measured flow count during peak hours (detector A)

A.6 **Summary**

The research concludes that model uncertainty shows very different characteristics for different traffic flow conditions. The Taguchi statistical method was applied to three traffic flow stages to establish the relationships between modelled vehicle speeds and measured speeds, on a minute-by-minute basis. Model output uncertainty shows very different characteristics for different traffic flow conditions. The Taguchi statistical method was applied to three traffic flow stages to establish the relationships between modelled vehicle speeds and measured speeds, on a minute-by-minute basis. The results show the close agreement between modelled and actual speeds under free flow conditions, the speed prediction uncertainties can be considered to follow zero-mean normal distribution (white noise).

In contrast, the transitional stage between free flow and queuing shows a higher level of discrepancy. As traffic volumes increase, the quality of model outputs shows statistically significant negative correlation with average speeds and a negative exponential equation has been fitted. When volumes reach saturation levels, the flow break-down phenomenon leads to large model errors.

For over-saturation traffic flow, the simulation algorithm follows the fundamental theory, therefore neglects the existence ‘synchronised’ flow condition. The simulation has an acceptable solution on queue condition prediction. Figure 7 gives a big picture for the relationship between uncertainty and simulated speed prediction.

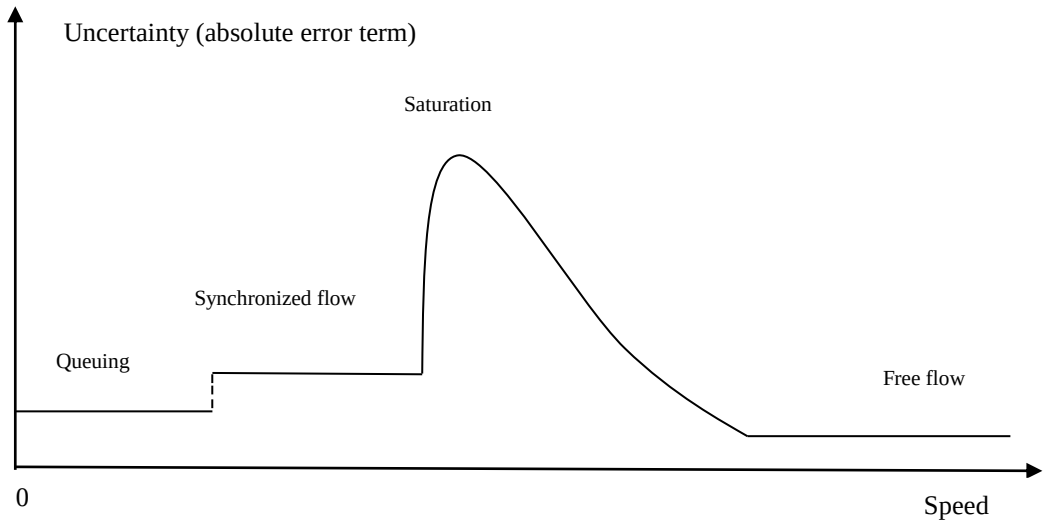

Figure 7: Relationship between speed prediction and uncertainty

Appendix B. Analysis of vehicle acceleration profiles for emissions modelling at signalised intersections (Zhu et al., 2014)

B.1 Introduction

Currently, very limited research has been done on leading vehicle acceleration behaviour at intersections. Generally, an assumption of constant acceleration is implemented by most micro-simulation packages. However, Wang et al. (2004) have assumed that drivers normally accelerate with a polynomial decreasing relationship with speed. Long (2000) has concluded that linearly decreasing acceleration rates better represent both maximum vehicle acceleration capabilities and actual motorist behaviour. The initial and primary challenge is data collection: high-resolution and accurately-positioned vehicle trajectory datasets are difficult to obtain in practice. Currently, there are two ways to collect trajectory datasets, namely, use of a vehicle-mounted GPS and a feature-capture camera (Gordon et al., 2012). The data accuracy of both methods is subject to surrounding environments, which downgrade the reliability of the leading vehicle acceleration behaviour. The issue is significant for both traffic simulation and modelling of vehicle fuel consumption and emissions, which rely on the acceleration characteristics of vehicles starting from idling. The major proportion of vehicle emissions occurs at intersection approaches, due to the final acceleration to cruising speed and to the stop-and-go cycles. The deceleration and acceleration behaviour at intersections affects the emission intensity significantly (Minoura et al., 2009). The challenges posed by the simulation of queues at a micro-scale level are the acceleration profile of the leading vehicle in the queue (Li et al., 2004) and the headway of the following vehicles (Jin et al., 2009).

This research focuses on using the outputs of a vehicle-simulator to establish an acceleration/speed cycle, which can deliver more precise vehicle trajectory predictions at an intersection. The research is organised as follows: Section 2 outlines the methodology used; Section 3 sets out the data used in the research and proposes a new speed/acceleration profile; and finally, the main conclusions are discussed in Section 4.

B.2 Methodology

B.2.1 Driving simulator experiment (Kim, 2013)

Participants

Forty male and female licensed drivers were selected to participate in the experiment ranging in age from 19 to 77 years. Participants completed four drives including one practice drive.

Apparatus and stimuli

Experimentation was conducted using a driving simulator composed of an automatic Holden Commodore vehicle. When seated in the simulator vehicle, the driver was immersed in a

virtual environment which included a 180 degree front field of view composed of three screens, simulated rear view mirror images on LCD screens, surround sound for engine and environmental noise, real car cabin and simulated vehicle motion. The road and environment were developed to create a sense of realistic traffic around the driven car.

Figure 1 Driving simulator at Carrs-Q

The simulator software also enabled the creation of realistic road networks with a combination of straight and curvy sections with intersections. The participant sat in the driver's seat of the car, and drove using two pedals (brake and accelerator only) and a steering wheel which provided force feedback.

B.2.2 The Markov process and estimation of the transition matrix

Given the randomness of driving acceleration behaviour, there are several successful Markov chain applications to establish representative speed cycles (Biona and Culaba, 2006; Lin and Niemeier, 2003). By definition, the *Markov process* is a discrete time stochastic process $\{Z_\gamma\}$, $\gamma = 1,2,\ldots$, T with state space S = (Abaza et al., 2004 . . . , K) ,such that for every step γ and all states $S_1, S_2,\ldots , S_\gamma$ (Isaacson and Madsen, 1985)

$$P\{ Z_\gamma = S_\gamma \mid Z_{\gamma-1} = S_{\gamma-1} \} \quad \text{-------} \quad \text{Equation} \quad 1$$

In other words, the probability of the current state being S_γ depends on the previous state only. The conditional probability, transferring from state 2 to state 1, $P\{Z_\gamma = 1|Z_{\gamma-1}=2\}$, is called transition probability and is typically denoted as P_{21}. A Markov chain with K states will have K^2 transition probabilities.

$$P = \begin{pmatrix} P_{11} & \cdots & P_{1k} \\ \vdots & \ddots & \vdots \\ P_{k1} & \cdots & P_{kk} \end{pmatrix}$$

Let N_{21} be the total number of repeated observations where the condition is $\{Z_\gamma = 1 | Z_{\gamma-1}=2\}$

$$P_{21} = \frac{N_{21}}{\sum N} \quad \text{-------} \quad \text{Equation 2}$$

Where

$\sum N$ is the total observations of all transitional conditions.

The flowchart in Figure 2 reconstructs the acceleration profile using the Markov process.

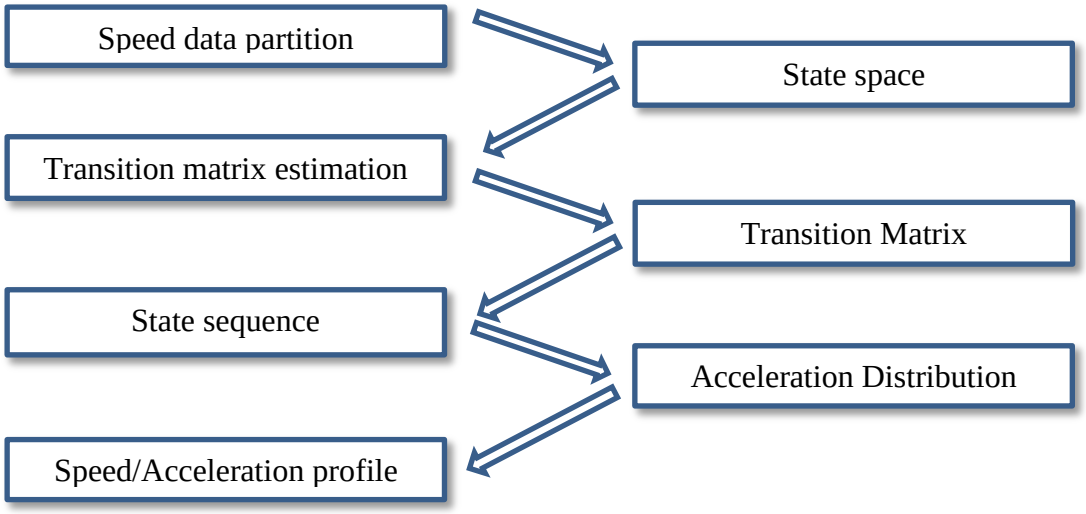

Figure 2 Methodology of acceleration profile establishment using the Markov process.

B.3 Acceleration behaviour analysis

B.3.1 Data collection and vehicle operation classification

An acceleration process is defined as the period starting with the idling condition and ending when speed reaches the maximum cruising speed. The leading vehicle trajectories were collected at an intersection in increments of 0.05 seconds. The dataset consisted of vehicle speed, acceleration, acceleration pedal movement and brake pedal movement. This dataset has been classified into 4 different states according to the criteria shown in Table 1.

Table 1. Vehicle operation classification

Operation state	Definition
1 Transition	Brake pedal movement =0; Acceleration pedal movement =0 and Speed>0
2 Acceleration	Brake pedal movement =0 and Acceleration pedal movement >0
3 Idling	Brake pedal movement =0; Acceleration pedal movement =0 and Speed=0
4 Brake	Brake pedal movement >0 and Acceleration pedal movement =0

Significant variation was observed between the driving behaviour of each participant. The dynamic speed profiles of three participants are illustrated in Figure 3. The results confirm the findings of Wang et al. (2004), that the constant acceleration assumption does not reflect realistic, actual driver behaviour. After analysing 40 different driver simulator runs, it was found that the process consists of only two main operational states, namely, transition (state 1) and acceleration (state 2). The acceleration dispersion does not result merely from how drivers accelerate but whether they accelerate, which does make the most significant contribution. Therefore, when facing a distinctly different speed profile due to acceleration behaviour, the statistical fitting is not able to generate any meaningful results.

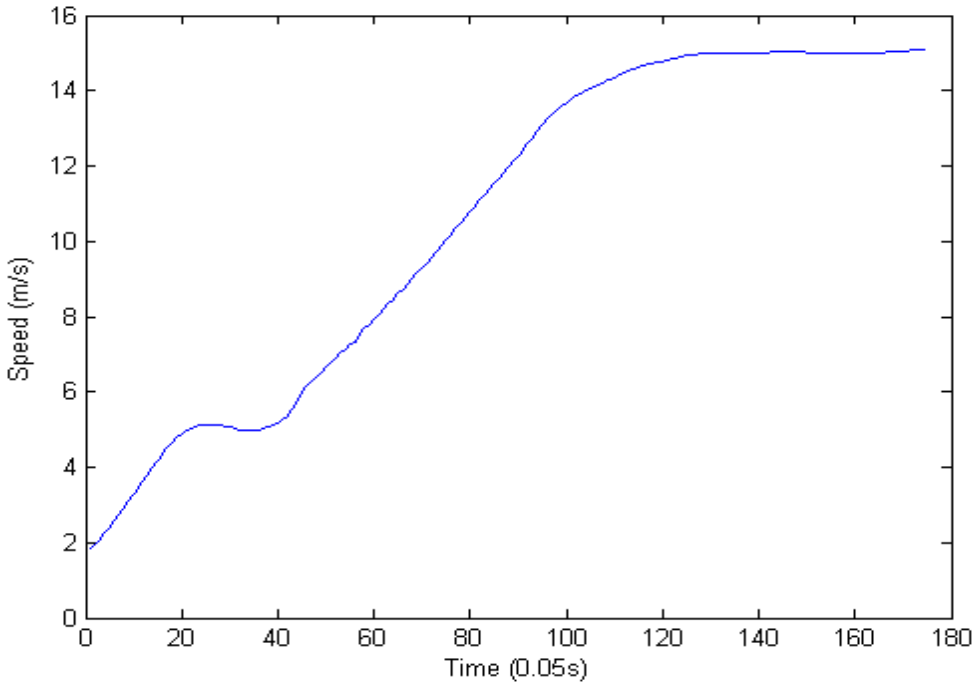

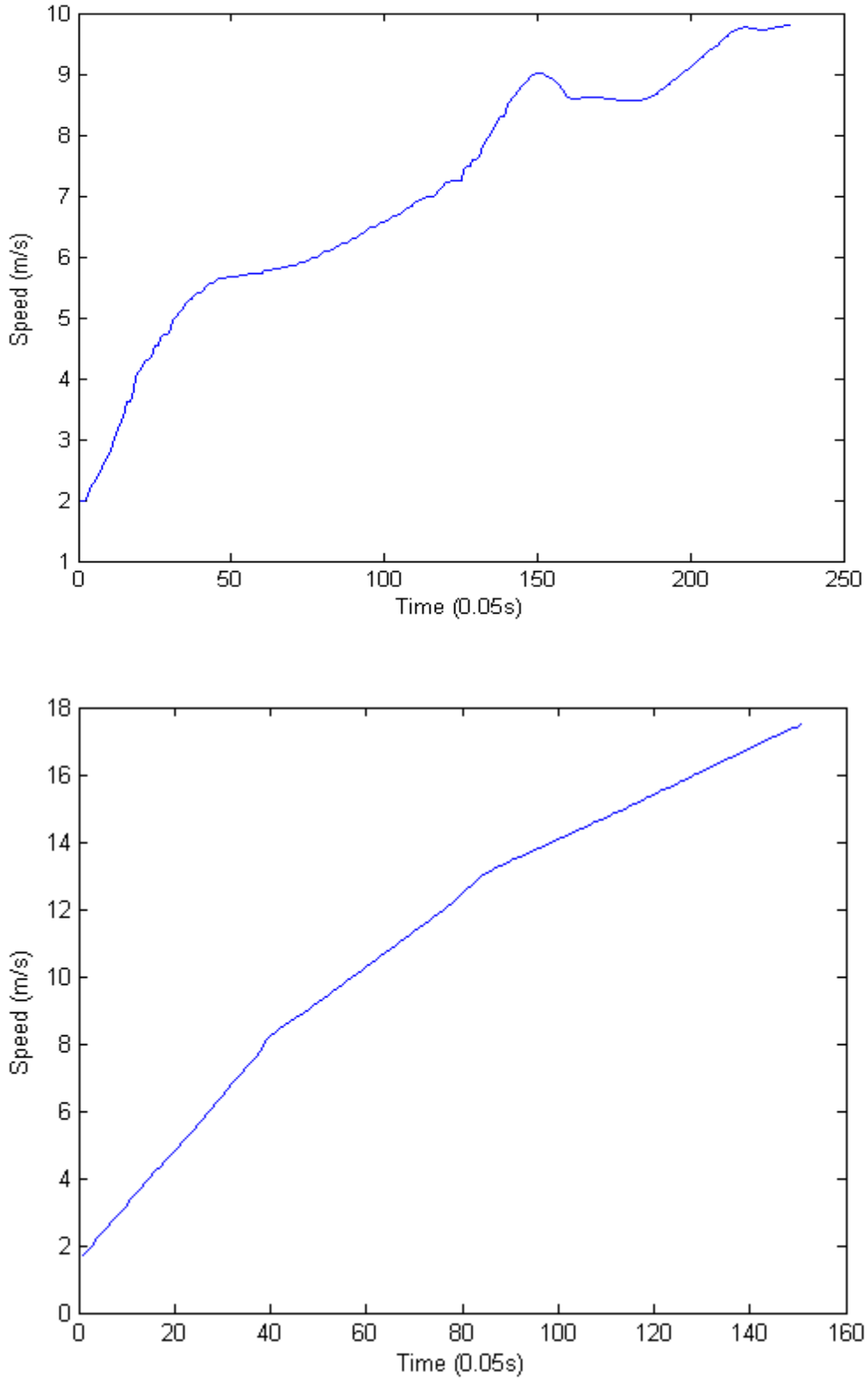

Figure 3 Selective speed profiles at an intersection

B.3.2 Transition matrix estimation

The probability of state-transition is estimated using Equation 2, by classification and analysing operational state sequences of all participants. The transition matrix consists of 4 state-transition probabilities as shown in Figure 4.

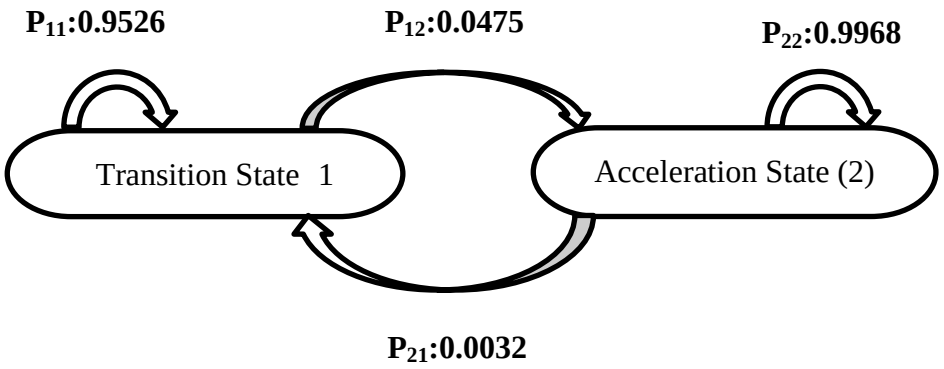

Figure 4. Transition matrix and state transitions by Markov process

$$P = \begin{pmatrix} 0.9526 & 0.0475 \\ 0.0032 & 0.9968 \end{pmatrix}$$

B.3.3 Acceleration profile reconstruction

The first step in reconstructing the acceleration profile is to re-establish state space using the transition matrix. The state space starts from state 1, and lasts for the average time of the acceleration processes defined in Section 3.1**.** Each step is 0.05 seconds.

{1 1 2 2 2 ……2 1 1 1 1 2……. 2 2 2}

Where:

1 is transition operation state

2 is acceleration operation state

Once the state space is established, the acceleration profile can be reconstructed by sampling the acceleration values from the two operational acceleration distributions. The sampling procedure is defined as following

Y= f (X) ------- Equation (3)

Where:

f(x) is cumulative distribution function of operational acceleration

Y is the probability

X is the acceleration

The acceleration distributions of both states, based on the datasets of all participants, are shown in Figure 5. For each part of the state space, the corresponding acceleration is calculated by generation of uniform-distribution random numbers as input of the reversed cumulative distribution function. Finally, the sample acceleration profile is generated from the sampling.

{0.369 0.366 1.303 3.576 0.987 2.721 2.257….1.09 0.054 0.388 0.005 2.036….0.004 0.989 0.420} (unit: m/s^2)

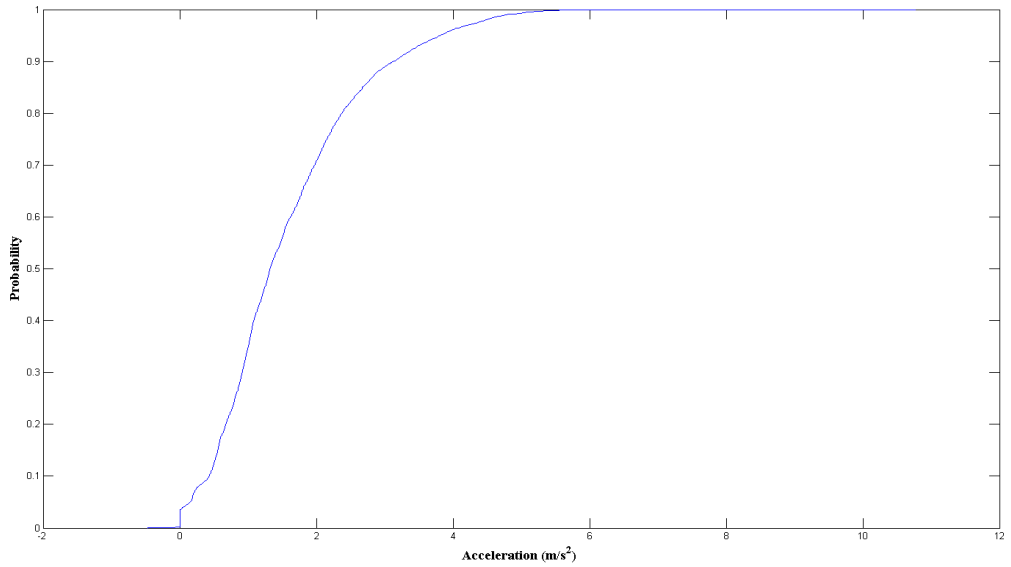

(a) Acceleration state acceleration distribution

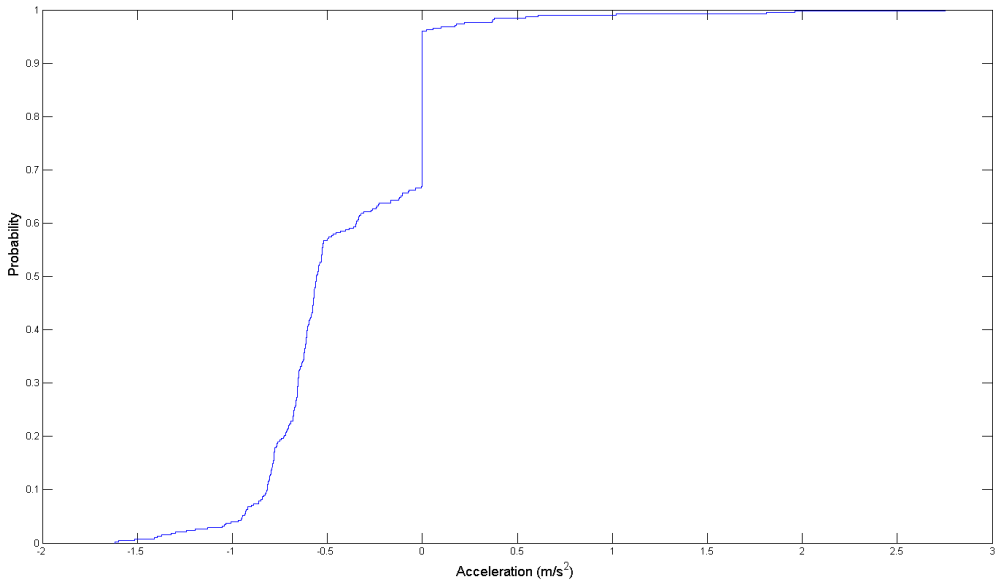

(b) Transition state acceleration distribution

Figure 5 Acceleration distributions (two operational states)

B.3.4 Acceleration/speed profile selection

A larger number of profile candidates can be produced by the Markov process. In order to select the most appropriate acceleration profile it is necessary to use a number of performance measures such as average acceleration, acceleration variation and transition time percentage. Selection criteria are put forward to evaluate performance measures, which are combined in Equation 4. The selected cycle is obtained through the process of minimising the differences between individual cycles and the overall average for all participants.

$$PM(i) = (\Delta CP(i))^2 + (\Delta AA(i))^2 + (\Delta AD(i))^2 \quad \text{-------} \quad \text{Equation (4)}$$

Where:

i=1 ,2 ,3……n^{th} candidate cycle . Δ is the differential operator .

PM: Overall performance measurement

CP: Cycle transition proportion

AA: Cycle average acceleration

AD: Cycle acceleration standard deviation

The proposed cycle is illustrated in Figure 6.

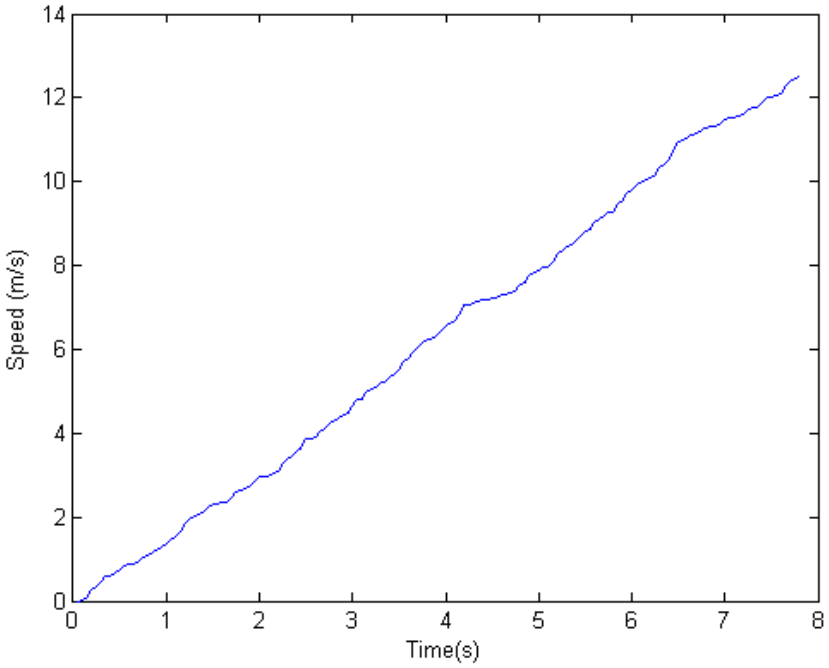

Figure 6 Proposed speed-time profile

B.4 Acceleration/speed profile application

The proposed speed profile can replace the constant-acceleration assumption at intersections. Furthermore, the stochastic Markov process can be applied using simulation software instead of the static constant-acceleration assumption. Besides the improvement of the vehicle trajectory prediction, it also affects calculations of fuel consumption and emissions significantly. An instantaneous traffic emissions model, developed by Int Panis et al. (Int Panis et al., 2006b), has been adopted by the AIMSUN traffic simulation model (TSS, 2010). This model integrates traffic simulation results with emission prediction equations. Thus, emission functions for each vehicle have been derived with instantaneous speed and acceleration as parameters using nonlinear multiple regression techniques. The model, shown in Equation 5, was calibrated using data from 25 vehicles (6 buses, 2 trucks and 17 cars) in Europe.

$$E_n(t) = \max\left[E_o,\ f_1 + f_2 v_n(t) + f_3 v_n(t)^2 + f_4 a_n(t) + f_5 a_n(t)^2 + f_6 v_n(t) a_n(t)\right] \quad \text{-------Equation 5}$$

Where:

$E_0\ (t)$ = a lower limit of emission (g/s) specified for each vehicle and pollutant type;

$V_n\ (t)$ = instantaneous speed of vehicle n at time t;

$a_n\ (t)$ = acceleration of vehicle n at time t;

f_1 *to* f_6 = emission constants specific for each vehicle and pollutant type determined by the regression analysis.

Two scenarios are generated using different speed profiles. One is the representative speed profile proposed in Section 3.4 while the other is based on the constant acceleration assumption. Figure 7 shows two CO_2 emission profiles calculated by Equation 5. The total emissions are 27.5g and 87.5g for the constant acceleration scenario and the Markov scenario, respectively. It also shows that the emission prediction is over-idealised under the constant acceleration assumption.

Figure 7 (a) CO2 emission profile using Markov process

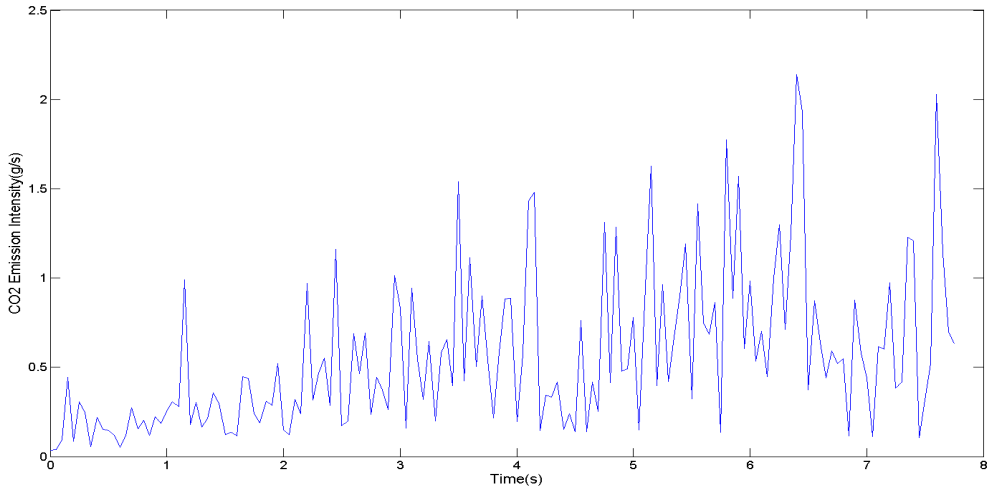

Figure 7 (b) CO2 emission profile using constant acceleration

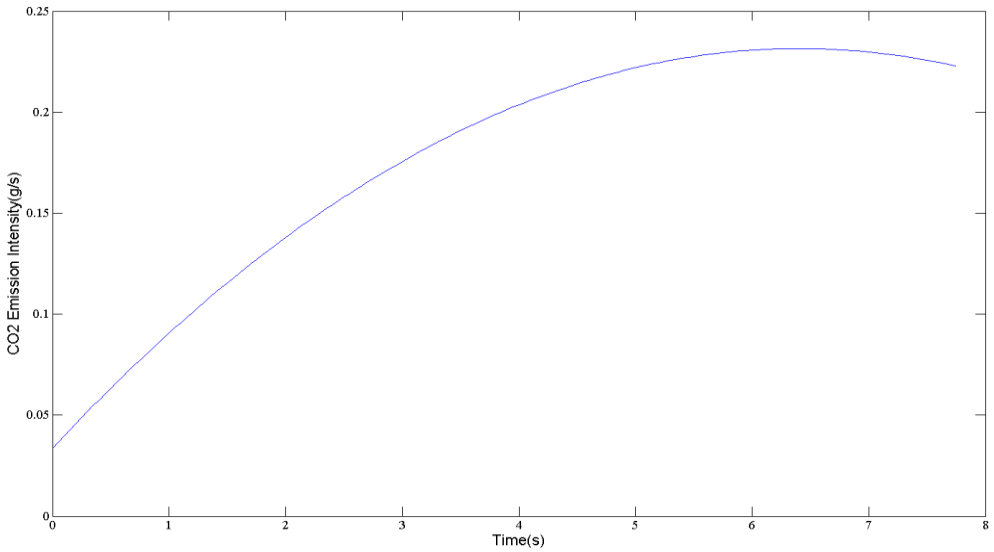

B.5 Summary

The common assumption in traffic simulation models is constant acceleration for the leading vehicle moving from a stationary position at an intersection. This research has shown that to be unrealistic using the results of 40 drivers in a driving simulator experiment. The high-resolution data from the driving simulator show significant differences for acceleration behaviour between participants. Hence, a typical acceleration profile is necessary to replace the current constant acceleration assumption for micro-simulation models. The randomness of acceleration behaviour can be simulated by the Markov process. Therefore, the acceleration profile can be reconstructed using a Markov process and the corresponding statistical features of the acceleration operation. Compared with other data collection methods used to establish the driving cycle (Lin and Niemeier, 2003), the high-resolution driving simulator data, including detailed acceleration/brake pedal movements, provides a more certain operational state classification.

However, the proposed speed/acceleration profile is based on simulator data, which may deviate from actual driving conditions (Godley et al., 2002). This research does not take turning manoeuvres and the influences of traffic management into consideration. The selection criteria of candidate driving cycles can be customised to improve the statistical fit using more realistic acceleration behaviour under various traffic conditions. The improvements to the methodology rely on the collection of vehicle trajectory data at a high level of resolution.